“Modulation of Ca^{2+} dependent inactivation of Ca^{2+} channels by intracellular signalling”

Dissertation
zur Erlangung des akademischen Grades

doctor rerum naturalium
(Dr. rer. nat.)

genehmigt durch die Fakultät für Naturwissenschaften
der Otto-von-Guericke-Universität Magdeburg

von

Dipl. Biol. Vladan Rankovic

geb.am

05.07.1975 in Smederevska Palanka, Serbia

Gutachter: **Prof. Dr. Oliver Stork**

Prof. Dr. Peter Lipp

eingericht am: 22.06.2009

vorteidigt am: 15.12.2009

To my parents and my family!

Vladan Rankovic

Acknowledgment

I would like to express all my gratitude to *Prof. Dr. Oliver Stork*, *Prof. Dr. Thomas Budde* and *Dr. Thomas Munsch* for supervising my work. They helped me to develop my scientific attitude through fruitful discussions and inspiring suggestions. Under their guidance I gained the knowledge and the confidence that enabled me to compile my PhD thesis successfully. During my PhD work they were my bosses but in the same time they were my very good friends. I am very thankful to them for being available whenever I needed help.

I am deeply grateful to *Dr. Peter Landgraf* for being a very good friend and for his excellent teaching in the field of molecular biology and protein biochemistry. His assistance and advices helped me in carrying out successfully many of the experiments presented in this study, and his support and friendliness always made our discussions both educational and enjoyable.

Moreover, I got valuable experience in protein biochemistry as well as help and support from *Dr. Michael R. Kreutz* and *Prof. Dr. Eckart D. Gundelfinger* which was also my supervisor in graduate school (GRK1167). To *Dr. Michael R. Kreutz* and *Marina Mikhaylova* I am also very thankful for kindly providing me with antibody and construct for caldendrin. Many thanks also to *Xenia Gorny* for giving me construct for AKAP 79.

During my PhD work I got help and support in molecular biology techniques, namely RT-PCR and quantitative Real-Time PCR, from *Dr. Tatyana Kanyshkova*. Moreover, I am very thankful to *Petra Ehling* for helping me with immunohistochemistry.

I am thankful to *Prof. Dr. Volkmar Lessmann* for supporting my work in Institute of Physiology as well as for inspiring discussions and helpful suggestions. My thanks also goes to *Dr. Tanja Brigadski* for helping me with German-English translations, and being available whenever I needed help.

I would also like to acknowledge the excellent technical assistance and constant support of *Regina Ziegler*, *Angela Jahn*, *Monika Marunde* and *Corinna Borutzki*. Their kind help allowed me to cross lot of difficulties.

The time I spent at the Institute of Physiology was a pleasant, eventful and exciting experience due to all my colleagues and co-workers.

Above all, this work was achieved thanks to the support, love and encouragement of my wife *Marija*, my family and all my friends, who were always present to help me to overcome difficult moments. Their support gave me the strength to look ahead.

Table of Contents:

English summary **1**

Zusammenfassung (German summary) **2**

1. Introduction **3**

1.1 Introduction of the thalamocortical system *3*

1.2 Voltage-gated Ca^{2+} channels and their classification *4*

1.3 Ca^{2+} signalling network in thalamus *6*

1.4 Calcium dependent inactivation (CDI) of VGCCs *7*

1.4.1 Identification of CDI *7*

1.4.2 Mechanisms of CDI *8*

1.4.2.1 Ca^{2+}- induced Ca^{2+} release (CICR) *8*

1.4.2.2 β-adrenergic signalling cascade *9*

1.4.2.2.1 cAMP-dependent PKA and A kinase anchoring protein member family (AKAPs) *11*

1.4.2.3 Cytoskeleton, calcium binding proteins and dephosphorylation processes in CDI modulation *13*

1.5 Aim of the project *13*

2. Materials **16**

2.1 Lab instruments and equipment *16*

2.2 Kits, enzymes and molecular biology reagents *16*

2.2.1 Molecular weight markers *17*

2.2.2 Plasmids *17*

2.2.3 Bacteria *17*

2.2.4 Mammalian cells *17*

2.2.5 Cell culture media and reagents for mammalian cells *18*

2.2.6 Culture medium and additives for bacteria *18*

2.3 Drugs *18*

2.4 Antibodies *20*

2.4.1 Primary antibodies for Western blot and immunostaining *20*

2.4.2 Secondary antibodies for Western blot and immunostaining *21*

2.5 Buffers and solvents used in biochemical or molecular biology work *21*

2.6 Animals *22*

3. Methods **23**

3.1 Tissue Preparation *23*

3.2 Patch clamp recordings *23*

3.3 Fluorimetric Ca^{2+} measurement (Ca^{2+} imaging) 24
3.4 Reverse transcription-polymerase chain reaction (RT-PCR) assays 24
3.5 Cell Type Specific RT - PCR 25
3.6 Quantitative Real - time PCR 26
3.7 Generation of recombinant fusion proteins 26
3.7.1 Polymerase chain reaction 26
3.7.2 DNA agarose gel electrophoresis 27
3.7.3 cDNA cloning into expression vectors 27
3.7.4 Electroporation 28
3.7.5 Mini DNA preparation 28
3.8 Isolation of recombinant fusion proteins 29
3.8.1 Induction of fusion protein synthesis (GST and MBP) 29
3.8.2 Purification of fusion proteins 29
3.9 Pull down assays 30
3.10 Sodium dodecyl sulphate polyacrylamide gel electrophoresis (SDS-PAGE) 31
3.10.1 Laemmli system 31
3.10.2 Coomassie staining of SDS-polyacrylamide gels 31
3.11 Western blot analysis 32
3.12 Immunoblot detection 32
3.13 Immunoprecipitation 32
3.14 Mammalian cell cultures 33
3.14.1 COS-7 cell culture 33
3.14.1.1 Materials and culturing of COS-7 cells 33
3.14.1.2 COS-7 cells transfection 33
3.14.2 Thalamic cultures 34
3.14.2.1 Preparation and culturing of dissociated cell cultures from the dorsal thalamus 34
3.14.3 Hippocampal cultures 34
3.15 Immunocytochemistry 34
3.16 Immunohistochemistry 35
3.17 Microscopy 35
3.18 Data analysis 35

4. Results 36
4.1 PCR expression patterns of the main components of the β-AR signalling cascade 36
4.1.1 $Ca_V1.2$ expression in whole brain and dLGN 36
4.1.2 Other components supposed to be involved in CDI modulation are also expressed in TC neurons 37
4.2 CDI is active in TC neurons in brain slices 39
4.2.1 The role of β-ARs in CDI modulation of L-type Ca^{2+} channels 41

4.2.2 β_2-ARs of dLGN are adrenergic receptors that mostly contribute to CDI modulation 42
4.2.3 Localization of β_2-ARs in cultured TC neurons 44
4.3 Modulators of RyR alter CDI in TC neurons 46
4.3.1 Control of HVA Ca^{2+} current amplitude by CICR during trains of mock action potentials 49
4.3.2 Control of basal level of Ca^{2+} in TC neurons 50
4.3.3 Localization of CDI and CICR relevant channels 52
4.4 Downstream β-AR signalling molecules supposed to be involved in CDI modulation of TC neurons 53
4.4.1 Blocking of PKA completely suppresses the modulation of CDI in TC neurons 53
4.4.2 AKAPs play a crucial role in the modulation of CDI in TC neurons 54
4.4.3 AKAPs assist in PKA translocation from somatic regions to the plasma membrane 55
4.4.4 Ternary complex formation by the main components of the β-AR signalling cascade in TC neurons 58
4.4.5 Protein-protein interactions between components of the ternary inactivation complex 60
4.5 Phosphorylation and dephosphorylation processes in modulation of CDI 62
4.6 Role of the cytoskeleton in modulation of CDI in TC neurons 63
4.7 Role of calcium binding proteins in CDI 65

5. Discussion 67
5.1 CDI in TC neurons 67
5.1.1 Interaction between CICR and CDI 68
5.1.1.1 Possible functional relevance of HVA Ca^{2+} channels and CICR-dependent CDI 69
5.1.2 β-AR stimulation and modulation of CDI of $Ca_V1.2$ via phosphorylation and dephosphorylation processes 69
5.1.2.1 Scaffold proteins like AKAPs specifically bind to the $Ca_V1.2$ and modulate channel after β-AR stimulation 71
5.1.2.2 Cytoskeleton, calcium binding proteins, and CDI upon activation of the β-AR signalling cascade 72
5.2 Functional significance of Ca^{2+} channel phosphorylation after β-AR stimulation 74

6. References 76
7. Abbreviations 84
8. Curriculum Vitae 87
9. Scientific publications 88
10. Erklärung 89

Figure and table index:

Table 1. *Classification of calcium channels according to the α subunit with their localization and sensitivity to specific substances* 4

Table 2. *Classification of calcium channels with amino acid sequence identity* 5

Figure 1. *Structure of calcium channel $Ca_V1.2$* 5

Figure 2. *U shaped inactivation curve as an electrophysiological hallmark of the CDI of VGCCs* .. 8

Figure 3. *Regulation of L-type Ca^{2+} channels by Ca^{2+} and phosphorylation – dephosphorylation reactions* 10

Figure 4. *Organization of PKA holoenzyme and binding with AKAP* 11

Figure 5. *Simplified β-AR signalling cascade with downstream signalling molecules and the final effector calcium channel $Ca_V1.2$* 12

Figure 6. *Expression patterns of mRNAs of main components of β-AR signalling cascade in the dLGN of Long Evans rats* 36

Figure 7. *Expression pattern of HVA Ca^{2+} channels in extracts from whole brain and the VB region of thalamus of LE rats* 37

Figure 8. *Single cell expression profiles of AKAP5, AKAP7 and the Gs subunit of G proteins (Gnas)* 38

Figure 9. *Expression profiles of AKAP5 and AKAP7 obtained by qRT-PCR from LE rat brain tissue* 38

Figure 10. *Identification of CDI in TC neurons in the slice preparation* 40

Figure 11. *From receptors to CDI modulation of calcium channels $Ca_V1.2$* 41

Figure 12. *Modulation of β-AR influences properties of CDI inactivation in TC neurons* 42

Figure 13. *Type specific activation of β-ARs and effects on CDI modulation in TC neurons* 43

Figure 14. *β_2-AR specifically modulates CDI in TC neurons of dLGN* 44

Figure 15. *Localization of β_2-AR in cultured TC neurons* 45

Figure 16. *Effect of Caffeine on CDI* 46

Figure 17. *Influence of different types of intracellular Ca^{2+} release channels on CDI* 47

Figure 18. *Influence of store-operated Ca^{2+} influx on CDI* 48

Figure 19. *Interaction between CDI and intracellular Ca^{2+} stores during trains of action potential-like stimuli* 50

Figure 20. *Calcium imaging of TC neurons after Caffeine stimulation* 51

Figure 21. *Localization of RyR2 and $Ca_V1.2$ in cultured TC neurons* 52

Figure 22. *Inhibition of PKA completely suppresses the effect of β-AR stimulation on CDI in TC neurons* 54

Figure 23. *Inhibition of PKA binding to AKAPs suppresses the effect of β-AR stimulation in TC neurons* 55

Figure 24. *Translocation of PKA after β-AR stimulation in 10 days old cultured hippocampal neurons* 56

Figure 25. *PKA translocation after β-AR stimulation is dependent on AKAPs in hippocampal neurons* 57

Figure 26. *Localization of $Ca_V1.2$, AKAP 150 and PKARIIβ in cultured TC neurons 58*
Figure 27. *Localization of $Ca_V1.2$ and PKARIIβ in brain tissues 59*
Figure 28. *Expression of $Ca_V3.3$ and $Ca_V2.1$ in thalamus 60*
Figure 29. *Interaction partners important for CDI modulation in TC neurons 61*
Figure 30. *The role of dephosphorylation processes in CDI modulation of TC neurons 62*
Figure 31. *Localization of $Ca_V1.2$ and PP2A in cultured TC neurons 63*
Figure 32. *Involvement of the cytoskeleton in CDI of TC neurons 64*
Figure 33. *Localization of $Ca_V1.2$ and caldendrin in cultured TC neurons 65*
Figure 34*. Interaction between AKAPs and CDD 66*

Summary

Voltage-dependent Ca^{2+} channels are the one of the main routes of cellular Ca^{2+} entry. Intracellular Ca^{2+} ions control processes as diverse as cell proliferation, neuronal development and transmitter release. All of these functions have to be accomplished within a narrow range of Ca^{2+} concentrations, as this cation can be toxic if its level is not tightly controlled. The Ca^{2+}-dependent inactivation (CDI) of voltage-dependent Ca^{2+} channels is an auto-inhibitory feedback mechanism controlling the Ca^{2+}-influx. In thalamocortical relay neurons this is a very prominent mechanism, but its modulation is not well understood. Recent studies in hippocampal cells have shown a functional link between beta-adrenergic receptors (β-AR) and L-type Ca^{2+} channels ($Ca_V1.2$) via protein kinase A (PKA) and A kinase anchoring proteins (AKAPs). Therefore, we here combined electrophysiological, immunological and molecular biological techniques to investigate a possible role of β-AR stimulation, PKA and AKAPs in the modulation of CDI of $Ca_V1.2$ in thalamocortical relay neurons. Our data show that under whole cell patch clamp conditions using double-pulse protocols, β-AR stimulation contributes to modulation of CDI in thalamocortical relay neurons. These effects could be blocked by inhibition of PKA with a cell-permeable inhibitor (myristoylated protein kinase inhibitor-(14-22)-amide) or AKAP St-Ht31 inhibitory peptide, suggesting a critical role of these molecules downstream of the receptor. Blocking of dephosphorylation processes by Okadaic acid revealed an additional contribution of protein phosphatases to the modulation of CDI after β-AR stimulation. Furthermore, we demonstrated that stimulation of β-AR with Isoproterenol caused the translocation of PKA from cytoplasmatic regions to sites close to the plasma membrane and calcium channels in primary hippocampal neurons. Also, the translocation of PKA was reduced by application of AKAP St-Ht31 inhibitory peptide. These data suggest that AKAPs mediate targeting of PKA to L-type Ca^{2+} channels allowing their phosphorylation and modulation of CDI. Finally, we provide evidence for a new interaction between AKAPs and calcium-binding protein caldendrin which may be of specific interest for modulation of CDI in TC neurons. Together with immunocytochemistry and pull down experiments, our data shed light on the existence of a possible inactivation complex for CDI in thalamocortical relay neurons consisting of $Ca_V1.2$, PKA and proteins from the AKAP family. The present study will contribute to our current knowledge of the physiology of thalamocortical neurons in general and to the modulation of CDI of calcium channels in particular.

Zusammenfassung

Spannungsabhängige Ca^{2+}-Kanäle stellen einen wichtigen Mechanismus des Ca^{2+}-Einstromes in Zellen dar. Intrazelluläre Ca^{2+}-Ionen regulieren so unterschiedliche Prozesse wie Proliferation und Entwicklung von Neuronen oder die Freisetzung von Neurotransmittern. Die intrazelluläre Ca^{2+}-Konzentration muß dazu innerhalb enger Grenzen kontrolliert werden, da hohe Konzentrationen zellschädigend wirken. Einen bedeutenden Rückkopplung-Mechanismus zur Kontrolle des Ca^{2+}-Einstromes stellt die Ca^{2+}-abhängige Inaktivierung von spannungs-abhängigen Ca^{2+}-Kanälen (CDI) dar. In thalamocortikalen Schaltneuronen ist dieser Mechanismus zur Kontrolle des Ca^{2+}-Einstromes noch wenig verstanden. Studien an hippokampalen Neuronen legen eine Modulation der CDI durch funktionelle Interaktionen zwischen β-adrenergen Rezeptoren (β-ARs) und L-Typ Ca^{2+}-Kanälen ($Ca_v1.2$) über die Proteinkinase A (PKA) und A-Kinase Ankerproteine (AKAPs) nahe. Eine solche Modulation der CDI von $Ca_v1.2$-Kanälen thalamocortikaler Schaltneurone nach Stimulation β-adrenerger Rezeptoren wurde in der vorliegenden Arbeit mithilfe von elektrophysiologischen, immunohistochemischen und molekularbiologischen Ansätzen untersucht. Mit Hilfe der Ganzzell „patch-clamp“ Technik konnte eine Modulation der CDI thalamocortikaler Neurone in Hirnscnitt-Präparaten nach Stimulation β-adrenerger Rezeptoren gezeigt werden. Die Effekte β-adrenerger Stimulation konnten durch spezifische Inhibitoren von PKA und AKAPs mittels eines membrangängigen Inhibitors (myristoylierter Protein Kinase Inhibitor-(14-22)-amid) bzw. AKAP St-Ht31 Peptid vollständig blockiert werden, was auf deren Rolle in der Signalkette zwischen Rezeptor und Effektor hindeutet. Blockierung von Phosphatasen durch Okadeinsäure hatte dagegen eine Verstärkung der CDI nach β-adrenerger Stimulation zur Folge. An Primärkulturen hippokampaler Neurone konnte darüberhinaus eine Translokation von cytoplasmatischer PKA zur Plasmamembran und zu Ca^{2+}-Kanälen beobachtet werden, die sich durch AKAP St-Ht31 Peptid blockieren ließ. Diese Daten legen eine durch AKAPs vermittelte Phosphorylierung von Ca^{2+}-Kanälen durch PKA nahe. Auf einen möglichen Beitrag Ca^{2+}-bindender Proteine wie Caldendrin zur Modulation der CDI in thalamocortikalen Neuronen weist eine erstmals gezeigte Protein-Protein Interaktion zwischen AKAPs und Caldendrin hin. Zusammen mit den Daten weiterer immuncytochemischer und „pull-down“ Experimente legen die Ergebnisse der vorgelegten Arbeit die Existenz eines Proteinkomplexes zur Regulation der CDI in thalamocortikalen Schaltneuronen, bestehend aus $Ca_v1.2$-Kanälen, PKA und AKAPs, nahe. Die vorgelegte Arbeit erweitert das Verständnis der Regulation Ca^{2+}-abhängiger Mechanismen thalamocorticaler Neurone.

1. Introduction

The thalamocortical system is the neuronal substrate of rhythmic oscillatory and tonic single spike activity during the behavioural states of sleep and wakefulness. Calcium (Ca^{2+}) channels play an essential role during these activity states. Low voltage-activated (LVA) channels exert important functions during sleep oscillations and high voltage-activated (HVA) channels are mainly active during tonic activity associated with awaked states. While much is known about the role of LVA channels, the functional impact of HVA channels is still puzzling. Furthermore, the role of Ca^{2+} beyond being a charge carrier only begins to evolve in recent thalamic studies. In this respect the existence of ON mechanisms, leading to an increase in the intracellular Ca^{2+} concentration (e.g. Ca^{2+} influx via plasmamembrane channels and Ca^{2+} release from intracellular stores), and OFF mechanisms, leading to the restriction of Ca^{2+} influx and restoring basal Ca^{2+} concentrations (e.g. inhibition of plasmamembrane Ca^{2+} channels), have been demonstrated in thalamic neurons. The present study has been undertaken to further unravel the function of HVA Ca^{2+} channels and the interaction between ON and OFF mechanisms as well as their modulation by neurotransmitters in the thalamus.

1.1 Introduction of the thalamocortical system

The cerebral cortex receives nearly all sensory information through the thalamus. The thalamus is a paired structure joined at the midline and sitting very near the centre of the brain. There are two major components. The first one is the **dorsal thalamus**, which is comprised of roughly 15 nuclei with relay cells that project to the cerebral cortex. One of them is the dorsal lateral geniculate nucleus (dLGN), the main relay station of the visual pathway in primates. The second one is the **ventral thalamus**, to which the *nucleus reticularis thalami* (NRT) belongs. NRT cells are GABAergic and project to the dorsal thalamus to inhibit thalamocortical relay neurons (TC). The other cellular components of the thalamus, in addition to TC and NRT cells, are local interneurons (IN), which are also GABAergic, sit amongst the relay cells, and inhibit them. TC neurons collect inputs from the sensory periphery, process and modulate them together with NRT and IN and transmit the processed information to the cortex.

The reliability and faithfulness with which synaptic inputs from the periphery are transmitted to the cortex by TC neurons varies with the behavioural state of an animal (sleep or wakefulness). TC neurons display two typical modes of action potential generation: burst firing with between two to six Na^{+}/K^{+} action potentials riding on top of a low threshold Ca^{2+} spike during periods of slow-wave sleep and tonic, single-spike activity with trains of action potentials during states of wakefulness *(Pape et al., 2004)*. Voltage-gated Ca^{2+} channels (VGCCs) play an important role in these two activity modes of the thalamus.

1.2 Voltage-gated Ca^{2+} channels and their classification

Voltage-gated Ca^{2+} channels are a large family of integral membrane proteins. They control the selective flow of Ca^{2+} ions down their electrochemical gradient in response to changes in membrane potential. Most neurons express multiple types of Ca^{2+} channels, which differ in their functional properties such as their rates and voltage dependence of inactivation. There are two types of VGCCs: low voltage-activated Ca^{2+} channels (LVA) and high voltage-activated Ca^{2+} channels (HVA). The T-type Ca^{2+} channels belong to the former group and are characterized by their small conductance, negative activation range and rapid inactivation kinetics. By contrast, HVA channels are activated at more depolarized potentials and are divided based on their pharmacological and biophysical profiles into N-, P-, Q-, L- and R-types *(Budde et al., 2002)*.

The application of molecular biological techniques have helped to refine this classification and have permitted the identification of the subunit composition of VGCCs. High voltage activated Ca^{2+} channels consist of a α_1 subunit that forms the core of the channel and β, α_2-δ, and possibly γ subunits that modulate the functional properties of the α_1 subunit. By contrast, the α_1 subunit of low voltage-activated channels does not appear to associate with any of the known ancillary Ca^{2+} channel subunits. Table 1. shows classification of calcium channels according to the α subunit *(Catteral et al., 2005)*.

Calcium Channel	α1 Subunit	Type	Localization	Specific Blocker
$Ca_V1.1$ $Ca_V1.2$ $Ca_V1.3$ $Ca_V1.4$	α1S α1C α1D α1F	L	Skeletal muscle Cardiac muscle, endocrine cells, neurons Endocrine cells, neurons Retina	DHPs, PAAs, BZPs
$Ca_V2.1$ $Ca_V2.2$ $Ca_V2.3$	α1A α1B α1E	P/Q N R	Neurons	ω-Agatoxin IVA ω-Conotoxin GVIA SNX 4182
$Ca_V3.1$ $Ca_V3.2$ $Ca_V3.3$	α1G α1H α1I	T	Skeletal muscle, cardiac muscle, neurons	Kurtoxin

DHPs = Dihydropyridines, PAAs = phenylalkylamines, BZTs = Benzothiazepines

Table 1. Classification of calcium channels according to the α subunit with their localization and sensitivity to specific substances.

Electrophysiological, immunocytochemical and *in situ* hybridization studies have shown that thalamic relay neurons express low voltage-activated ($Ca_V3.1$–3.3 or T-type calcium currents) and high voltage-activated ($Ca_V1.2$–1.3 or L-type currents, $Ca_V2.1$–2.3 or P/Q-, N-, and R-type currents)

Ca^{2+} channel subtypes. While $Ca_V3.1$ is the main T-type isoform in the dorsal thalamus, all HVA subtypes seem to be expressed in TC neurons and CDI exists only in two of these, namely P/Q- and L-type *(Meuth et al., 2001)*.

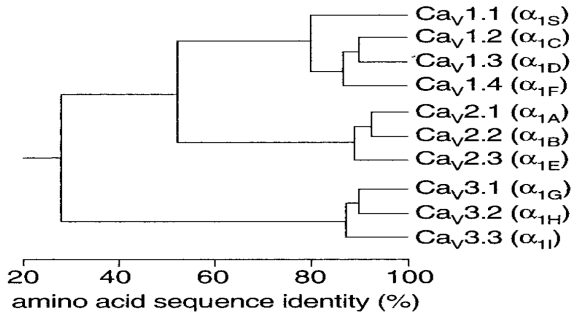

Table 2. Classification of calcium channels with amino acid sequence identity (*Catterall et al, 2003)*

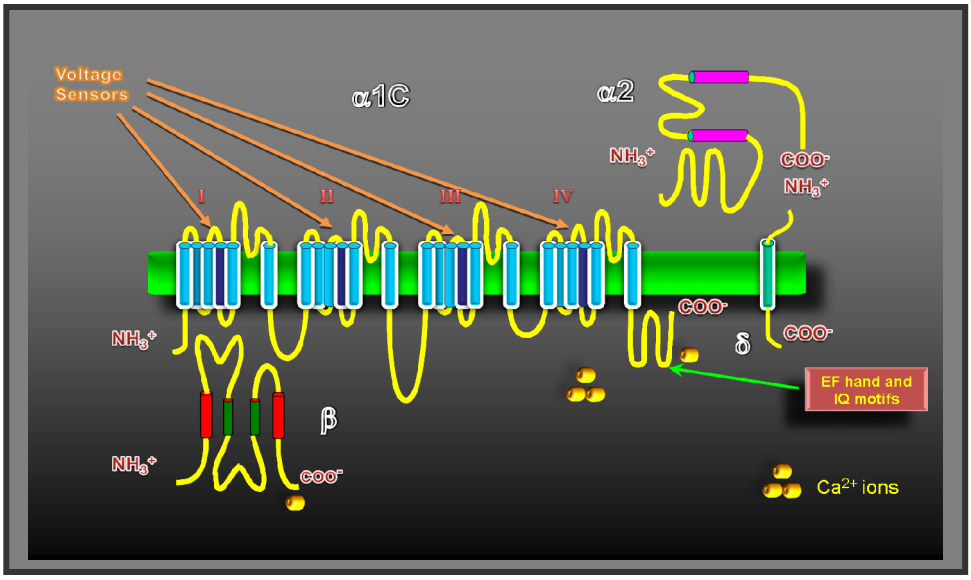

Figure 1. Structure of calcium channel $Ca_V1.2$. It consists from pore forming transmembrane α1C, intracellular β, δ and extracellular α2 subunits. I-IV represents the four repeats of the pore forming subunit, each consisting of 6 segments (S1-S6). The location of the voltage sensors, EF hands (Ca^{2+} binding domain) and IQ motifs (mediate interactions with calmodulin) on C-terminus of α1C subunit are indicated.

As mentioned above, voltage-dependent activation of LVA channels in the plasma membrane of thalamic neurons results in an influx of Ca^{2+} triggering the generation of rhythmic burst discharges, as typically occurs during slow-wave sleep and certain forms of generalized epilepsies. Furthermore, different types of voltage-operated Ca^{2+} channels, mainly HVA channels, are recruited during tonic

firing in these neurons, and are thought to contribute to the faithful transfer of sensory signals to the cortex during wakefulness. While much is known about T-type (LVA) Ca^{2+} channels and sleep oscillations, much less is described about HVA channels and their functional role. However, they seem to be more relevant for wake activity and sensory information processing. Transmitters of the ascending brainstem (ARAS) are thought to induce the switch from sleep to wakefulness, for instance, noradrenaline (NA). This neurotransmitter increases the amplitude and rate of activation of I_h (hyperpolarization-activated cation current), which may allow NA to selectively limit the amplitude and duration of membrane hyperpolarization. This selectively suppresses rhythmic burst activity in thalamocortical relay neurons during rhythmic burst activity *(Pape & McCormick, 1989)*.

1.3 Ca^{2+} signalling network in thalamus

In the thalamus, the role of Ca^{2+} has traditionally been viewed as that of an electrical charge carrier. However, Ca^{2+} ions have been shown to control processes as diverse as cell proliferation, neuronal development and transmitter release *(Berridge et al., 2003)*. All of these functions have to be accomplished within a narrow range of Ca^{2+} concentrations, since calcium can be toxic if its concentration is not tightly controlled. Effective mechanisms, such as pumps and exchangers, remove Ca^{2+} ions from cytoplasm restoring the resting concentration once the ions have fulfilled their signalling role. In addition to pumps and exchangers, several mechanisms of channel inactivation have appeared during evolution to control Ca^{2+} entry: fast and slow voltage-dependent inactivation (VDI) *(Stotz & Zamponi, 2001)* as well as Ca^{2+}-dependent inactivation (CDI) which will be discussed in more details later.

More recently, evidence is accumulating that thalamic neurons, like other types of cells, also use the intracellular pool of Ca^{2+}. The release of intracellular Ca^{2+} stored within the endoplasmic reticulum is mediated via inositol 1,4,5-trisphosphate ($InsP_3$) and ryanodine receptors (RyRs). It was demonstrated in cardiac excitation contraction coupling that Ca^{2+}-induced Ca^{2+} release (CICR) from RyRs, triggered by Ca^{2+} entry through the nearby L-type Ca^{2+} channel, induces CDI of the Ca^{2+} channel *(Takamatsu et al., 2003)*. Inactivation of Ca^{2+} channels is an important component of this complex signalling system. These data indicate a fine tuning of Ca^{2+}-dependent mechanisms that will help to control intracellular Ca^{2+} transients and associated Ca^{2+}-signalling processes. Thus, it can be suggested that there is a complex Ca^{2+} signalling network in thalamic cells connecting HVA/L-type Ca^{2+} channels, CICR and CDI processes. However, the functional relevance of these mechanisms, their interplay and their modulation by transmitters are not well understood.

1.4 Calcium dependent inactivation (CDI) of VGCCs

1.4.1 Identification of CDI

CDI is a regulatory mechanism in which Ca^{2+} ions restrict their own entry into the cell by one of the main routes of Ca^{2+} influx, the VGCCs. Therefore, CDI as an important autoinhibitory mechanism provides crucial negative feedback in numerous neuronal and non-neuronal settings. The mechanisms that underlie this feedback inhibition have been under investigation for more than twenty years, but still are not clearly understood. Various mechanisms can mediate CDI, including the cytoskeleton, phosphorylation-dephosphorylation processes, ryanodine-sensitive intracellular Ca^{2+} stores and Ca^{2+}-binding proteins, and distinct channels are involved in this process.

Among the first who studied the role of CDI in control of Ca^{2+}-influx through VGCCs, Brehm and Eckert could demonstrate in *Paramecium* that inactivation was faster in solution containing Ca^{2+} as the charge carrier, as compared to Ba^{2+} containing solution *(Brehm & Eckert, 1978)*. Similarly, they found that Ca^{2+} buffers reduced inactivation and that the inactivation curve obtained with a double-pulse protocol was U-shaped. Because of these findings, they proposed the existence of a Ca^{2+}-dependent mechanism for inactivation of *Paramecium* Ca^{2+} channels. Similar results were obtained subsequently in molluscan and mammalian neurons. Very recently, the major mechanisms of CDI could be elucidated for thalamocortical relay neurons *(Meuth et al., 2001, 2002 and 2005)*.

CDI can be detected based on several hallmarks (Fig. 2). First, CDI tends to be fast. Channel inactivation is evidenced as a decay of current during prolonged depolarization. The current amplitude at the end of a depolarizing test pulse is divided by the peak current amplitude to define an inactivation ratio, providing a measure of the degree of inactivation. Second, CDI normally results in a U-shaped inactivation curve. The approach of choice to measure this inactivation curve is a double-pulse protocol in which a conditioning voltage step to varying potentials is followed by a brief gap and a test pulse to a fixed voltage. The voltage of the test pulse is set to evoke maximal current amplitude, and serves to reveal the number of channels that can be activated. Conditioning steps to very positive or negative voltages evoke minimal Ca^{2+} currents, and yield near maximal Ca^{2+} current in response to the test pulse (Fig. 2b green trace and blue trace). By contrast, a conditioning step to the maximum of Ca^{2+} current activation evokes maximal Ca^{2+} entry and results in a minimal current on the test pulse (Fig. 2b red trace). This reduction occurs as a result of CDI. Consequently, the amplitude of the current evoked by the test pulse typically shows a U-shaped dependency on the conditioning-pulse potential in current-voltage (I-V) plots (Fig. 2d blue line), and the maximal rate of inactivation occurs near the peak of the I-V relationship.

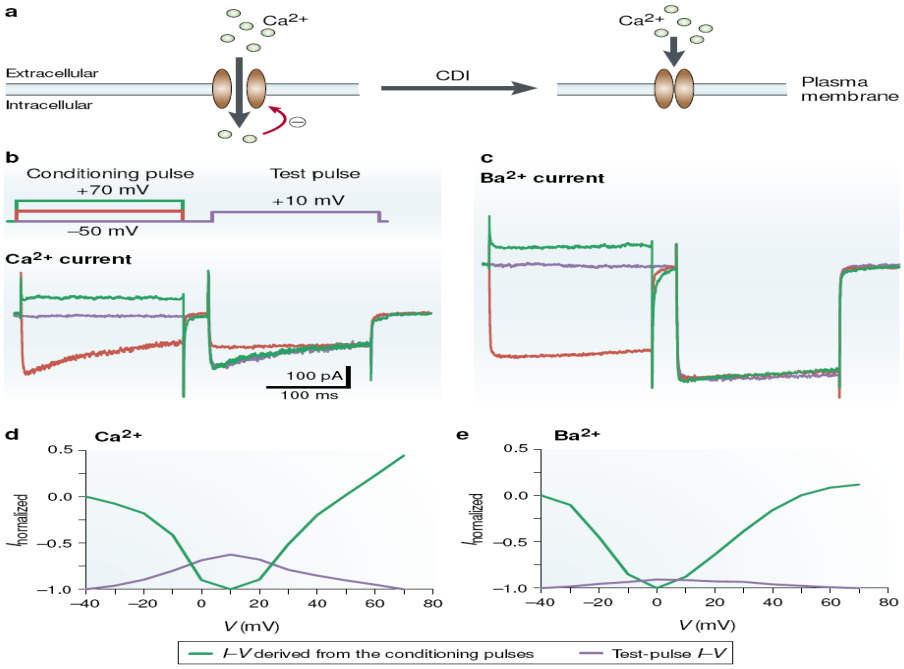

Figure 2. **U shaped inactivation curve as an electrophysiological hallmark of the CDI of VGCCs** (from *Budde et al., 2002*)

Another hallmark of CDI is the effect of Ba^{2+} as a charge carrier. Since Ba^{2+} is typically less effective than Ca^{2+} in inactivating the channels, the use of Ba^{2+} as the principal charge carrier results in a reduction of the rate of inactivation, a decrease in the inactivation ratio and in the U-shape of the inactivation curve (Fig. 2c-e). Last but not the least, in addition to macroscopic currents, single channel recordings can be used to confirm the occurrence of CDI. When compared with Ba^{2+} currents, unitary L-type Ca^{2+} currents are smaller in amplitude and the unitary channel openings are less frequent, with only rare openings after several minutes.

Since L-type Ca^{2+} channels have been demonstrated to be controlled by neurotransmitters in cardiac myocytes *(Findlay, 2003)*, such mechanisms may also modulate CDI in thalamocortical relay neurons via activation of G protein coupled neurotransmitter systems, like NA.

1.4.2 Mechanisms of CDI

1.4.2.1 Ca^{2+}-induced Ca^{2+} release (CICR)

It is known that in cardiac muscle cells, there is a close functional coupling between L-type Ca^{2+} channels in the plasma membrane and intracellular Ca^{2+}- release channels of the ryanodine receptor type in the membrane of the sarcoplasmic reticulum (SR) *(Sham et al., 1995)*. This highly localized interaction leads to the release of Ca^{2+} from intracellular Ca^{2+} stores in a process known as CICR *(Fabiato, 1983)*, which is followed by cellular contraction. Because of this close coupling, it is

not surprising that L-type Ca^{2+} channels are inactivated by Ca^{2+} release from the SR *(Sham et al., 1995)*. Furthermore, it is possible to distinguish two phases in the CDI of cardiac Ca^{2+} channels: an early fast phase that depends on Ca^{2+} released from the SR, and a late slow phase that depends on Ca^{2+} flow through VGCCs *(Sun et al., 1997)*. In neurons, there is also a close functional coupling between L-type Ca^{2+} channels and RyRs *(Chavis et al., 1996)*. Although a contribution of CICR to CDI has not been tested in neurons yet, CICR has important functional roles in these cells *(Berridge, 1998)*. Therefore, CICR might be at least partially involved in the CDI of neuronal Ca^{2+} channels.

Recent studies have begun to unravel a complex Ca^{2+}-signalling network with interacting extra- and intracellular Ca^{2+} sources *(Budde et al., 2002; Pape et al., 2004)*. Tonic patterns of Na+/K+ spikes are known to mediate the transfer of sensory information from the periphery to the primary sensory cortex. This pattern is supported by activation of HVA Ca^{2+} currents, CICR from intracellular stores via RyR and a repolarizing mechanism involving Ca^{2+}-dependent K+ channels *(Budde et al., 2000; Meuth et al., 2002)*. Furthermore, tonic activity is accompanied by transient increases in the intracellular Ca^{2+} concentration ($[Ca^{2+}]_i$) *(Munsch et al., 1997; Zhou et al., 1997)* and is coupled to CDI, thereby limiting the amount of Ca^{2+} entering the cell *(Meuth et al., 2001; Meuth et al., 2002)*. These data indicate a fine tuning of Ca^{2+}-dependent mechanisms that will help to control intracellular Ca^{2+} transients and associated Ca^{2+}-signalling processes.

Inactivation of Ca^{2+} channels is an important component of this complex signalling system. However, the rate and extent of inactivation varies dramatically between Ca^{2+} channel subtypes and neuronal cell types *(Jones, 2003)*. In general, as was previously described, Ca^{2+} channels can be inactivated by either VDI or Ca^{2+}- dependent processes, namely CDI, which represents a classical feedback mechanism between Ca^{2+} entry and $[Ca^{2+}]_i$ *(Eckert & Tillotson, 1981; Hering et al., 2000; Stotz & Zamponi, 2001; Budde et al., 2002)*.

1.4.2.2 β-adrenergic signalling cascade

Another prominent mechanism of CDI of neuronal Ca^{2+} channels might be via phosphorylation and dephosphorylation processes, especially after stimulation of β-adrenergic receptors (β-ARs). The β-ARs belong to the family of G-protein coupled receptors (GPCRs). They consist of seven transmembrane domains, three intra- and three extracellular loops, one extracellular N-terminal domain and one intracellular C-terminal tail. Three subtypes of adrenergic receptors have been distinguished: β_1-, β_2-, and β_3-adrenoceptors. Signalling cascade starts after stimulation of receptor with NA or another agonist, leading to activation of G proteins and adenylate cyclase (AC). Subsequent cyclic adenosine monophosphate (cAMP) production activates various downstream effectors (Fig. 3; see further text for details).

It has been already shown that a subpopulation of L-type Ca^{2+} channels is localized in myocytes as part of a macromolecular signalling complex necessary for the β-adrenergic receptor regulation of L-type calcium currents *(Hulme et al., 2003)*. In this system, as well as in hippocampal cells, β-adrenergic receptor is directly linked to one of its final effectors, namely L-type Ca^{2+} channel, $Ca_V1.2$ *(Davare et al., 2001)*. This receptor-channel complex also contains a G protein, an adenylat cyclase, cAMP–dependent protein kinase (PKA), and a counteracting phosphatase, PP2A. It is thought that PKA is kept in close proximity to a variety of its substrates by A kinase anchoring proteins (AKAPs). In neurons, this function can be accomplished by microtubule-associated protein MAP2b or AKAP 7 (15/18) and AKAP 5 (79/150) that can recruit PKA to $Ca_V1.2$. Other AKAPs, for instance gravin, are involved in β-AR regulation and desensitization *(Wong et al., 2004)*. Activated PKA together with AKAPs might phosphorylate calcium channels and keep them in an open state. After phosphorylation, the channel is no longer sensitive to CDI. Therefore, an intriguing possibility exists that there is a β-AR-related signalling complex that modulates CDI of L-type Ca^{2+} channels in the thalamus in a state-dependent manner.

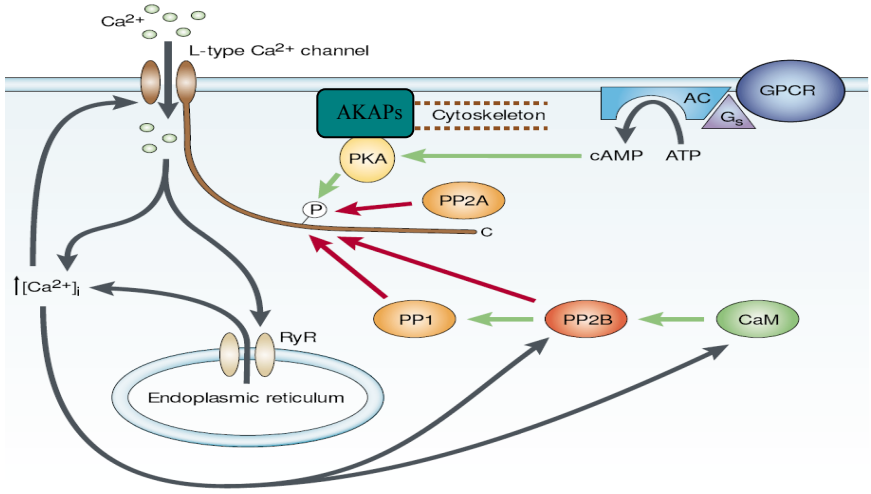

Figure 3. Regulation of L-type Ca^{2+} channels by Ca^{2+} and phosphorylation – dephosphorylation reactions. See text for details. Black arrows indicate the movement of Ca^{2+} and cellular metabolites. Green and red arrows indicate activation and inhibition, respectively (modified from *Budde et al., 2002*).

Ca^{2+} entering the cell through an L-type Ca^{2+} channel might induce CDI by interfering directly with the channel complex. As shown for cardiac L-type channels, the Ca^{2+} responsible for inducing CDI might be released from the endoplasmic reticulum (ER) through RyRs in a process called CICR *(Sun et al., 1997)*. In addition, CDI might be induced by dephosphorylation of the channel at Ser1928 *(Hell et al., 1993)*. This reaction is mediated by the protein phosphatase calcineurin (PP2B) *(Armstrong, 1989)*, an enzyme that is activated by Ca^{2+} and calmodulin (CaM)

(Guerini, 1997). The effect of calcineurin might be exerted by protein phosphatase 1 (PP1), which is disinhibited by calcineurin *(Guerini, 1997)*. In mammalian neurons, $Ca_V1.2$ channels are also dephosphorylated by PP2A, which is closely associated with the channel *(Davare et al., 2000)*. To effectively control channel activity by phosphorylation–dephosphorylation, the counteracting cAMP-dependent PKA is also closely targeted to the channel through microtubule-associated protein 2 *(Davare et al., 2000)*. As has been shown in thalamocortical relay neurons, the phosphorylation of L-type Ca^{2+} channels by PKA blocks CDI *(Meuth et al., 2002)*. PKA might be stimulated through different GPCR cascades. For example, the stimulation of β-adrenoceptors leads to Gs-mediated activation of AC, increased cAMP production and, finally, stimulation of PKA.

In the thalamocortical relay neurons cAMP is known to positively shift the voltage dependence of I_h *(Pape & McCormick., 1989)* and to reduce CDI *(Meuth et al., 2002)*. Thus, CDI and cAMP cascade are prominent mechanisms to modulate the firing properties of TC neurons. Experimental data suggest a state-dependent modulation of CDI by NA during wakefulness. However, the interaction between Ca^{2+} and cAMP-dependent pathways has not been analyzed yet and the role of β-adrenergic modulation of Ca^{2+}-influx and CDI in thalamocortical neurons is still elusive.

1.4.2.2.1 cAMP-dependent PKA and A kinase anchoring protein member family (AKAPs)

PKA is a heterotetramer that consists of two catalytic (C) subunits held in an inactive conformation by a regulatory (R) subunit dimer. The type-I PKA holoenzyme contains RI subunits (RIa or RIb) and is primarily cytoplasmic, whereas the type-II holoenzyme contains RII subunits (RIIa or RIIb) and is associated with particulate subcellular fractions. Binding of cAMP to PKA R subunits releases the active C subunit (Cα, Cβ or Cγ) to phosphorylate nearby substrates *(Dell'Acqua & Scott, 1997)*.

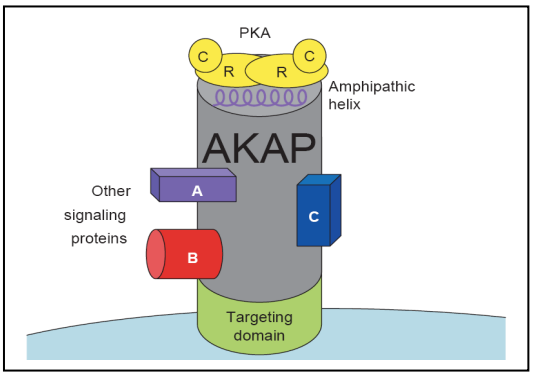

Figure 4. Organization of PKA holoenzyme and binding with AKAP

AKAPs are a family of >50 anchoring proteins that, although being structurally diverse, have in common the ability to bind to and target PKA *(Tasken et al., 2004; Wong & Scott, 2004)* (Fig. 4). Anchoring of PKA to an AKAP is achieved by the interaction of the R-subunit dimer with a 14–18 amino acid amphipathic α-helix region of AKAP *(Newlon et al., 2001)*. Disruption of PKA anchoring has been demonstrated experimentally using Ht31, a peptide that encompasses this amphipathic helical region from an AKAP, AKAP-Lbc, which has a high affinity for the RII subunits of PKA. Although most AKAPs that have been characterized bind to RII subunits with high affinity, several AKAPs have been reported to interact specifically with RI *(Angelo & Rubin, 1998)*.

D-AKAP1 and D-AKAP2 are examples of dual-specificity AKAPs that can anchor both types of R subunit *(Huang et al., 1997; Wang et al., 2001)*. AKAPs also have unique protein–lipid or protein–protein targeting domains that tether the PKA–AKAP complex to distinct subcellular locations to respond to local cAMP gradients *(Wong & Scott, 2004; Dell'Acqua & Scott, 1997; Trotter et al., 1999)*.

Recent studies demonstrated that $Ca_V1.2$ Ca^{2+} channels could physically associate with either AKAP79/150 (AKAP5) or AKAP15/18 (AKAP7) through a modified leucine zipper interaction *(Oliveria et al., 2007; Hulme et al., 2003)*. Thus, AKAPs are interesting potential candidates for modulation of CDI process in TC neurons.

According to our hypothesis, stimulation of β-ARs leads to activation of adenylate cyclase via G proteins and subsequent generation of cAMP, which then activates PKA. Mediated by AKAPs, PKA finally targets it´s effector, $Ca_V1.2$ channels, and phosphorylates them (Fig. 5). However, the precise role these molecules play in a presumed inactivation complex in TC neurons is still not clear and therefore was investigated in this study. Also, the role of calcium binding proteins in the modulation of CDI in TC neurons is still under debate, especially the role of caldendrin. Therefore, we also addressed the possible role of this protein in modulation of CDI.

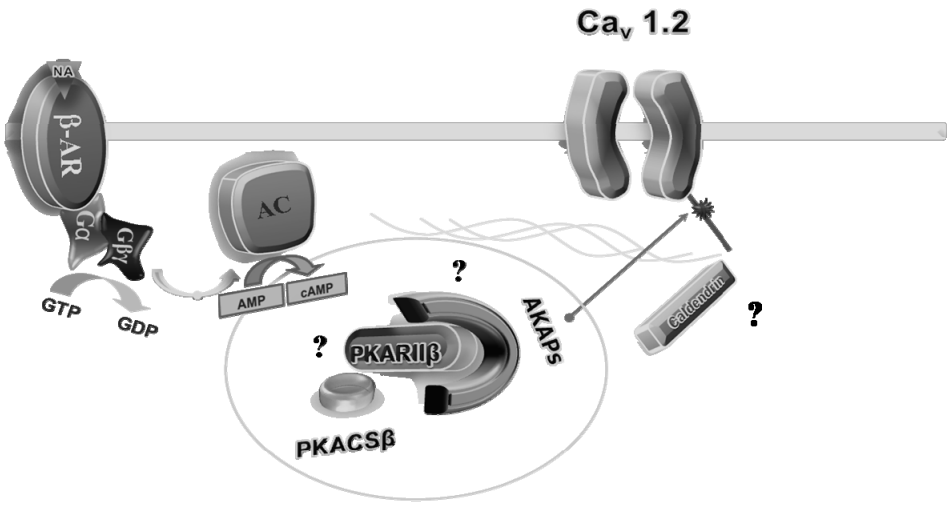

Figure 5. Simplified β-AR signalling cascade with downstream signalling molecules and the final effector calcium channel $Ca_V1.2$. Oval circle marks molecules included in the following study (PKARIIβ and AKAPs). Question marks stand for PKA, AKAPs and caldendrin and represent their possible role in CDI modulation of Ca^{2+} channel $Ca_V1.2$ in TC neurons. See text for details.

1.4.2.3 Cytoskeleton, calcium binding proteins and dephosphorylation processes in CDI modulation

Experiments in various types of cells have revealed a range of other mechanisms mediating CDI. For instance, involvement of the cytoskeleton has been found in cardiac myocytes *(Lader et al., 1999)*, hippocampal cells *(Beck et al., 1999; Johnson & Byerly, 1994),* and snail neurons *(Gera & Byerly, 1999; Johnson & Byerly, 1993)*. Moreover, calmodulin has been identified as the Ca^{2+} sensor for CDI of L-type and P/Q-type Ca^{2+} channels in expression systems *(Lee et al., 2000; Peterson et al., 1999; Qin et al., 1999; Zühlke et al., 1999)*, whereby these channels are regulated by calmodulin in a lobe specific manner *(Liang et al., 2003)*. To fulfil this function, Ca^{2+}-free calmodulin and L-type Ca^{2+} channels are preassociated as has been shown by fluorescence resonance energy transfer (FRET) two-hybrid mapping *(Erickson et al., 2003)*. Furthermore, other Ca^{2+}-binding proteins like NCS 1 (neuronal Ca^{2+} sensor protein 1), CaBP1 (neuronal Ca^{2+}-binding protein 1) or caldendrin (CDD) modulate HVA Ca^{2+} channels in a manner that is markedly different from modulation by calmodulin *(Lee et al., 2002; Rousset et al., 2003)*. In thalamocortical relay neurons CDI is modulated by counterbalancing phosphorylation/dephosphorylation processes involving different kinases [PKA, calcium-calmodulin (CaM) kinase] and protein phosphatases (PP1, PP2A, calcineurin) *(Meuth et al., 2002)*. However, more research is needed to further gain our knowledge of HVA Ca^{2+} channel function in the thalamus by probing the influence of Ca^{2+}-binding proteins and the cytoskeleton on CDI in thalamocortical relay neurons.

1.5 Aim of the project

The main aim of the presented project is to determine how CDI in thalamocortical relay neurons can be modulated. Previous results from our group have suggested that the cytoskeleton is involved in CDI. Namely, cytoskeletal stabilizers (taxol, phalloidin) reduced CDI in relay neurons *(Meuth et al., 2005)*. This led to a model in which microtubules stabilize a microfilament lattice, with the latter probably binding directly to the Ca^{2+} channel complex. The model suggests that the Ca^{2+} sensitivity of Ca^{2+} channels could be mediated by cytoskeletal depolymerization, since both microtubule and microfilament components of the cytoskeleton are disrupted by increases in the $[Ca^{2+}]_i$. It was also shown that there is a close connection between intracellular calcium stores and thalamocortical activity states *(Budde et al., 2000)*. On the other hand, recent evidence hints that β-adrenergic cascade can be involved in CDI regulation in thalamocortical neurons, since it has been shown to be one of the important regulatory mechanisms of CDI in heart physiology. However, the role of CDI and its regulation by brainstem transmitters is still elusive.

Therefore, the working hypothesis of this work assumes a membrane associated signalling complex involved in Ca^{2+}-dependent inactivation of Ca^{2+} channel. The proposed complex is organized by the cytoskeleton and includes the transmitter receptor and the effector, namely the Ca^{2+} channel, as well as other components of the β-adrenergic signalling cascade stimulating protein kinase A. However, the organisation of this complex as well as the roles of the molecules involved is not well understood. Therefore, the cellular localisation (somatodendritic distribution) and arrangement of single components of the proposed complex at the cell membrane as well as their role in modulation of CDI in TC neurons is investigated in this study. Moreover, the cellular localisation of specific components of the β-adrenergic cascade in TC neurons in comparison to local-circuit interneurons is addressed.

To address these issues, this study combines different methodological approaches. These range from functional electrophysiological studies where we used classical double pulse protocol to evoke Ca^{2+} currents to molecular biological techniques and protein biochemistry methods for identifying expression and interactions of components supposed to be involved in CDI modulation in TC neurons.

- Considering the working hypothesis described above, the experimental strategy of this project can be defined as follows:

- **<u>Obtaining RT-PCR expression profiles</u>** for:
  - *Ca^{2+} channels,*
  - *β-adrenergic receptors,*
  - *G proteins,*
  - *Adenylate cyclase,*
  - *AKAPs.*

- **<u>Identification of mechanisms for modulation of CDI</u>**:
  - *Involvement of cytoskeleton and intracellular Ca^{2+} stores*

    Using specific substances for cytoskeletal rearrangement like phalloidin, cytohalasin or taxol in electrophysiological experiments, the role of cytoskeleton in modulation of CDI will be investigated. Blockers and inducers of Ca^{2+} release from intracellular Ca^{2+} stores like Caffeine or ryanodine will be used in a similar way.
  - *Connection with Ca^{2+} binding proteins (parvalbumin, calbindin, ...)*

    Previous results in our group demonstrated that application of parvalbumin and calbindin reduced CDI significantly *(Meuth et al., 2005)*. However, further investigations are needed to determine the influence of other calcium binding proteins (e.g. caldendrin).

- *Involvement of enzymatic mechanisms (PP1, PP2A, PP2B, PKA)*

  Using inhibitors of PKA or Okadaic acid to inhibit phosphatases, the influence of these enzymes on modulation of CDI will be determined.

- *Direct interactions of potential modulators with L type Ca^{2+} channel*
- *Stimulation/inhibition of β-adrenergic receptors with agonist/ antagonists*

➢ **<u>Determination of cellular localization</u>** of:

- *$Ca_V1.2$ and comparison with some other types ($Ca_V2.1$ or $Ca_V3.3$)*
- *β-adrenergic receptors*
- *Localisation of other very important players of signalling cascade like PKA, AKAPs, protein phosphatases and their colocalization with $Ca_V1.2$.*

Through investigation of mechanisms involved in regulation of CDI, the present study will contribute to current knowledge of the physiology of thalamocortical neurons and the function of HVA channels. While role of LVA channels during sleep oscillations has been extensively analysed, much less is known about the role of HVA channels during tonic firing which is typically related to wakefulness. Resolving the questions addressed in this study will be the basis to understand β-adrenergic signalling, Ca^{2+} signalling and the autoprotective CDI mechanism in relay neurons thereby increasing current understanding of the general physiology of the thalamocortical system.

2. Materials

2.1 Lab instruments and equipment

Item	**Company**
Spectrophotometer SmartSpec™ Plus	Bio Rad, Germany
Vibratome Series 1000	Pelco®101
EPC-9/2 amplifier	HEKA double patch clamp, Germany
Cryostat Leica CM3050	Leica, Germany
Gene Pulser II and Pulse Controller Plus	Bio-Rad, Germany
Leica microscope	Leica Microsystems, Germany
Electrophoresis power supply	Hoefer Scientific Instruments, Germany
Gel electrophoresis system	Hoefer Scientific Instruments, Germany
Western blot system	Hoefer Scientific Instruments, Germany
Borosilicate glass pipettes (GC150TF-10)	Clark Electromedical Instruments, UK
Axioskop microscope	Zeiss, Germany

2.2 Kits, enzymes and molecular biology reagents

Product	**Company**
Endonucleases (Restriction enzymes)	New England Biolabs, UK
Taq DNA polymerase	Roche, Germany
T4 DNA ligase	New England Biolabs, UK
Pfu Turbo-DNA-Polymerase	Fermentas, Germany
Oligonucleotides (Primer)	Invitrogen, Germany
Nucleospin PCR cleanup gel extraction Kit	Macherey-Nagel, Germany
EndoFree Plasmid Maxi Kit	Macherey-Nagel, Germany
RNeasy Kit	Qiagen, Germany
Plasmid Mini Kit	Qiagen, Germany
µMACS™ Epitope Tag Protein Isolation Kit	Miltenyi Biotec, Germany

2.2.1 Molecular weight markers

DNA molecular weight markers	**Company**
1kb DNA ladder	Fermentas
100bp DNA ladder	Fermentas
Protein molecular weight markers	**Company**
PageRuler™ Prestained Protein Ladder	Fermentas
BenchMarker™ Protein Ladder	Invitrogen

2.2.2 Plasmids

Plasmid	**Company**
pGEX4T2	GE Healthcare, Uppsala, Sweden
pMALc2x	New England BioLabs, Hertfortshire, UK
pEGFP-N3	Clontech, USA
pcDNA 3.1 A(+)	Invitrogen, Germany
pGEM-T easy vector	Promega, Medison, USA

2.2.3 Bacteria

Bacterial Cells	**Company**
E.coli BL21-CodonPlus®DE3-RIPL	Stratagene
E.coli XL10 XL1 Blue MRF'	Stratagene

2.2.4 Mammalian cells

Mammalian cell line	**Company**
Kidney Fibroblast Cells from African green monkey (COS-7 cells)	Clontech

2.2.5 Cell culture media and reagents for mammalian cells

Item	Composition
DMEM+	Dulbecco's Modified Eagle Medium (Invitrogen), 10% fetal calf serum, 2 mM L-glutamine, penicillin, streptomycin, 100 µg/ml each
Trypsin	0.5% Stock solution, diluted 1:10 in HBSS (Invitrogen)
Poly-D-lysin	100 mg/l poly-D-lysin in 100 mM boric acid, pH 8.5, sterile filtered
HBSS	Hank´s balanced salt solution, Ca^{2+} and Mg^{2+} free (Invitrogen)
Optimem I	Modified Eagle's Minimum Essential Medium
Neurobasal	Invitrogen

2.2.6 Culture medium and additives for bacteria

Culture medium	Composition
LB-medium	20 g LB Broth Base (Invitrogen) / 1000 ml H_2O
LB-Agar	15 g Select Agar (Invitrogen) / 1000 ml LB-medium
SOC-medium	20 g/l peptone 140 (Gibco); 5 g/l yeast extract (Gibco); 10 mM NaCl; 2.5 mM KCl; 10 mM $MgSO_4$; 20 mM Glucose

All media were autoclavated at 121°C for 15 minutes. The additives were filtered with a 0.2 µm filter-unit (Schleicher & Schuell) and stored at –20°C.

2.3 Drugs

The drugs used in this work were purchased from following companies:

Substance	Concentration	Diluted in	Company
Caffeine	5, 10, 20 mM	water	Sigma, Germany
Ascorbic acid	1 mM	water	Sigma, Germany
Heparin	10 µM	water	Sigma, Germany
2-APB	100 µM	DMSO	Sigma, Germany

Cyclopiazonic acid	10 µM	DMSO	Sigma, Germany
InCellect AKAP St-Ht31 inhibitor	50 µM	water	Promega, UK
InCellect AKAP St-Ht31 control peptide	50 µM	water	Promega, UK
CGP 20712A dihydrochloride	10 µM	water	Tocris, USA
ICI 118,551 hydrochloride	10 µM	water	Tocris, USA
SR 59230A hydrochloride	10 µM	water	Tocris, USA
Salmeterol	10 µM	Ethanol	Tocris, USA
Isoproterenol hydrochloride	10 µM	water	Tocris, USA
Procaterol hydrochloride	10 µM	water	Tocris, USA
BRL 37344 sodium salt	10 µM	water	Tocris, USA
Formoterol hemifumarate	10 µM	DMSO	Tocris, USA
Ryanodine	10, 20 µM	Water, DMSO	Tocris, USA
Thapsigargin	10 µM	DMSO	Tocris, USA
Calcineurin autoinhibitory peptide	10 µM	DMSO	Tocris, USA
Cypermethrin	10µM	Ethanol	Tocris, USA
Cantharidin	10 µM	DMSO	Tocris, USA
Okadaic acid	10 µM	DMSO	Tocris, USA
PKI 14-22 myristoylated amide	10 µM	water	Tocris, USA
Forskolin	50 µM	DMSO	Tocris, USA
Tetrodotoxin (TTX)	100 µM	ACSF	Tocris, USA
4-aminopyridine (4-AP)	4 mM	ACSF	Tocris, USA

2.4 Antibodies

2.4.1 Primary antibodies for Western blot and immunostaining

The antibodies were purchased from following companies or kindly provided by:

Antibodies	**Species**	**WB dilution**	**IF dilution**	**Company**
Anti - RyR (C3-33)	rabbit	1:500	1:500	Abcam, UK
Anti - $Ca_V1.2$	rabbit	1:200	1:200	Alomone Labs, Israel
Anti - $Ca_V2.1$	rabbit		1:200	Alomone Labs, Israel
Anti - $Ca_V3.3$	rabbit	1:200	1:200	Alomone Labs, Israel
Anti - AKAP150 (C-20)	goat		1:200	Santa Cruz Biotechnology, USA
Anti - AKAP150 (N-19)	goat		1:200	Santa Cruz Biotechnology, USA
Anti - PKARIIβ	mouse	1:500	1:500	BD Biosciences, USA
Anti - β2 (H-73)	rabbit		1:400	Santa Cruz Biotechnology, USA
Anti - MAP2 (HM-2)	mouse		1:1000	Sigma, Germany
Anti - MAP2b	mouse		1:1000	BD Biosciences, USA
Anti - parvalbumin	rabbit		1:500	SWant, Switzerland
Anti - PP2A	sheep		1:500	Acris, Germany
Anti - calmodulin (2D1+1F11+6G4)	mouse		1:200	Sigma, USA
Anti - caldendrin	mouse		1:500	Dr. Michael R. Kreutz (1)
Anti-GFP	mouse	1:5000		Bapco
Anti – GST G7781	rabbit	1:750		Sigma, Germany
Anti MBP	rabbit	1:1000		Sigma, Germany
Anti – c-myc (9E10)	mouse	1:500		Santa Cruz Biotechnology, USA
Anti – PSD95	mouse		1:1000	BD Biosciences, USA
Anti - MBP	mouse	1:1000		NEB, UK
Anti – c-myc	rabbit	1:500		Clontech

Anti-GFP	rabbit	1:7500		Abcam, UK
Anti-GFP	rabbit	1:5000		Sigma, Germany

(1) Institute for Neurobiology, Centre for Learning and memory, Department of Neurochemistry, Brenneckestrasse 6, D-39118, Magdeburg, Germany.

2.4.2 Secondary antibodies for Western blot and immunostaining

The antibodies were purchased from following companies:

Antibodies	**Species**	**Dilution**	**Company**
Anti-mouse IgG, Alexa Fluor™ 488, 568 or 647 conjugated	goat	1:1000	Molecular Probes, Invitrogen
Anti-rabbit IgG, Alexa Fluor™ 488, 568 or 647 conjugated	goat	1:1000	Molecular Probes, Invitrogen
Anti-mouse IgG, peroxidase-conjugated	goat	1:5000	Dako
Anti-rabbit IgG (H&L) HRP-linked	goat	1:5000	Cell Signalling
Anti-mouse, cy-3	rabbit	1:750	Dako
Anti-rabbit, cy-3	goat	1:750	Dako
Anti-mouse IgG, Alexa Fluor™ 488, 568 or 647 conjugated	donkey	1:1000	Molecular Probes, Invitrogen

2.5 Buffers and solvents used in biochemical or molecular biology work

PBS	137 mM NaCl, 2.6 mM KCl, 8.1 mM Na_2HPO_4, 1.4 mM KH_2PO_4, pH 7.4
TBS	20 mM Tris, 150 mM NaCl, pH 8.0
TBST	20 mM Tris, 150 mM NaCl, pH 8.0, 0.1% Tween 20
TBSTA	20 mM Tris, 150 mM NaCl, pH 8.0, 0.1% Tween20, 0.02% NaN_3
TBE	89 mM Tris, 89 mM Boric acid, 2 mM EDTA, pH 8.0
TAE	40 mM Tris, 0.2 mM acetic acid, 1 mM EDTA, pH 7.6
6 x DNA sample buffer	30% (v/v) Glycerine, 50 mM EDTA, 0.25% Bromophenol-blue, 0.25% Xylene Cyanol

SDS-sample buffer	62.5 mM Tris-HCl, pH 6.8, 2% glycerol, 0.005% bromphenol blue, 100 mM DL-dithiotreitol
PFA	4% parafolmaldehyde

2.6 Animals

In this work, Long Evans rats *(Rattus norvegicus familiaris)* were used. The rats were bred at the Institute of Physiology, Magdeburg. Handling with the animals was according to the rules of the Otto-von-Guericke University and federal rules of the state Sachsen-Anhalt.

3. Methods

3.1 Tissue Preparation

Thalamic slices were prepared from juvenile postnatal day (P) 12–P24 Long–Evans rats. After anaesthesia with isofluran, animals were decapitated and a block of tissue containing the dorsal lateral geniculate nucleus (dLGN) was rapidly removed and placed in chilled (2–4°C), oxygenated slicing solution (pH 7.35, with NaOH) containing the following (in mM): sucrose, 195; glucose, 11; Pipes, 20; KCl, 2.5; $MgSO_4$, 10; and $CaCl_2$, 0.5. Coronal slices of the thalamus were cut at 300 µm on a vibratome and kept submerged in artificial cerebrospinal fluid (ACSF; pH 7.35, with 95% O_2-5% CO_2) containing the following (in mM): NaCl, 125; KCl, 2.5; NaH_2PO_4, 1.25; $NaHCO_3$, 22–26; $MgSO_4$, 2; $CaCl_2$, 2; and glucose, 10. Slices were heated for 20 min to 34°C before being cooled to room temperature, and allowed to rest for 60 to 90 min.

3.2 Patch clamp recordings

Whole-cell recordings under voltage clamp condition were performed on visually identified TC neurons of the dLGN at room temperature (21–23°C) using borosilicate glass pipettes (GC150TF-10, Clark Electromedical Instruments, Pangbourne, UK) connected to an EPC-9/2 amplifier (HEKA double patch clamp, Germany). The typical electrode resistance was 2–4 MΩ, while access resistance was 5–15 MΩ. Series resistance compensation was routinely used (30%). With a holding potential of -40 mV, voltage-clamp experiments were governed by Pulse software (HEKA Electronics). For standard recordings the following solutions were used: (i) extracellular solution (in mM): NaCl, 125; KCl, 2.5; NaH_2PO_4, 1.25; $NaHCO_3$, 22–26; $MgSO_4$, 2; $CaCl_2$, 2; and glucose, 10; TTX, 0.001; 4-AP, 4; pH 7.35 with NaOH. (ii) intracellular solution: Cs-gluconate, 85; Cs_3-citrate, 10; NaCl, 10; KCl, 1; EGTA. 1.1; $CaCl_2$, 0.1; $MgCl_2$, 0.25; HEPES, 10; TEA-Cl, 15; Mg-ATP, 3; Na_2-GTP, 0.5; pH 7.25 with CsOH. For measurements with trains of action potential-like stimuli the following intracellular solution was used (in mM): NaCl, 10; $CsMeSO_4$, 95; EGTA, 1.1; HEPES, 10; KCl, 1; TEA-Cl, 15; 4-AP, 5; QX-314-Cl, 3.35; phosphocreatin, 15; $MgCl_2$, 0.25; $CaCl_2$, 0.1; Mg-ATP, 3; Na-GTP, 0.5.

HVA Ca^{2+} currents were evoked from a holding potential of -40 mV and conditioning pulses to varying potentials (-40 to +60 mV, 200 ms duration) were followed by a brief gap (-40 mV, 50 ms) and a subsequent analyzing test pulse to a fixed potential of +10 mV (200 ms). For standard recordings Ca^{2+} was used as a charge carrier and 1.1 mM EGTA was included to the intracellular solution. In one set of experiments, Ba^{2+} was used as a charge carrier and 11 mM BAPTA was

included to the intracellular solution. Currents were evoked by double-pulse protocol where pre-pulse was varied between -40 and +60 mV (200 ms) and post-pulse fixed at +10 mV (200 ms). The degree of inactivation was determined by dividing the test pulse amplitude with a conditioning pulse to +10 mV by the test pulse amplitude elicited from the holding potential of -40 mV. Bar charts typically show the normalized amplitude of the remaining current. All values are presented as mean ± SEM. Statistical significance was evaluated by the Student's t test. Values of $p \leq 0.05$ were considered statistically significant. GraphPad Prism 5.0 and Microcal Origin 6.0 software was used for data analysis and figure plotting.

3.3 Fluorimetric Ca^{2+} measurement (Ca^{2+} imaging)

Isolated thalamic slices were placed under an upright microscope (Axioskop, Zeiss) and whole-cell recordings were performed at 24°C using borosilicate glass pipettes connected to an EPC-9 (HEKA) amplifier. Typical electrode resistance was 2-5 MΩ with access resistance in the range of 5-20 MΩ. Series resistance compensation >20% was routinely used. The internal pipette solution was (in mM): Cs-gluconat, 85; Cs-citrat, 10; NaCl, 10; HEPES, 10; $CaCl_2$, 0.1; $MgCl_2$, 0.25; KCl, 1; TEA-Cl, 15. Fluorimetric Ca^{2+} measurements were performed with bis-fura-2 (Molecular Probes, Invitrogen) added to the pipette solution at a concentration of 100 µM. Cells were illuminated with a monochromator, and images were captured at 1 Hz with 12 bit resolution on a CCD camera (PentaMAX, Princeton Inc., NJ, USA). Consecutive paired exposures to 350 and 380 nm were used to achieve digital fluorescence images. The 350/380 nm ration was calculated offline.

3.4 Reverse transcription-polymerase chain reaction (RT-PCR) assays

Poly A^+ mRNA was prepared from freshly dissected tissue by extraction with Trizol reagent according to the manufacturer's instruction (Oligotex, Qiagen, Hilden, Germany). First-strand cDNA synthesis was primed with oligo (dT) from 0.5-1 µg of mRNA, using the SuperScript II enzyme (Invitrogen Life Technologies). The following primers were used (for calcium channels α1C-α1E, G-proteins, adenylat cyclase, and β-receptors):

Nucleotides	PubMed accession number
Alpha1S (nucleotides 445-828)	*accession No. L04684*
Alpha1C (nucleotides 2624-3033)	*accession No. NM_012517*
Alpha1D (nucleotides 3691-4200)	*accession No. NM_017298*
Alpha1F (nucleotides 3196-3608)	*accession No. NM_0053701*
Alpha1A (nucleotides 5115-5387)	*accession No. NM_012918*
Alpha1B (nucleotides 1742-2051)	*accession No. NM_147141*
Alpha1E (nucleotides 5831-6377)	*accession No. NM_019294*
Galpha q (nucleotides188 -560)	*accession No. AF_234260*
Galpha11 (nucleotides 139-554)	*accession No. AF239674*
Galpha i-1 (nucleotides 669-1198)	*accession No. NM_013145*
Galpha i-2 (nucleotides 1125-1520)	*accession No. NM_031035*
Galpha i-3 (nucleotides 1993-2367)	*accession No. NM_013106*
β1-AR (nucleotides 742-1104)	*accession No. NM_012701*
β2-AR (nucleotides 676-964)	*accession No. NM_012492*
β3-AR (nucleotides 398-797)	*accession No. NM_013108*
AC1 (nucleotides 1361-1863)	*accession No. NM_001107239*
AC6 (nucleotides 1581-1940)	*accession No. NM_012812*
AC8 (nucleotides 3001-3480)	*accession No. NM_017142*

3.5 Cell Type Specific RT - PCR

Brain tissue from P14-P24 Long Evans rats consisting of dLGN was sliced using vibratome on 500 μM thick slices. The cells content was sucked into the pipette and transferred into 3 ml carrier RNA buffer (RNeasy Micro Kit, QIAGEN) by breaking the tip of the pipette and expelling 3 ml of solution with positive pressure. The pipette solution (6 ml) was supplemented with a recombinant ribonuclease inhibitor (0.24 U/ml; RNasin; Promega, Madison, WI, USA). Cytoplasm from single, identified cells were pooled (interneurons and TC neurons, respectively), and the RNA was isolated without DNase treatment using an RNA isolation kit (RNeasy Micro Kit, QIAGEN). Reverse transcription (RT) protocol was used for cDNA preparation from isolated RNA. Integrity of all obtained cDNAs was checked using primers for house keeping gene GAPDH. After confirmation of integrity, same cDNAs were used for standard RT-PCRs with specific primers for each gene of interest. PCR products were separated by size on 1% agarose gels and visualised using Eagle eye system after ethidium bromide staining. By this method were analysed AKAP 5, AKAP 7, and stimulatory subunit of G-proteins (Gnas).

3.6 Quantitative Real - time PCR

Real-time PCR was performed using the Real PCR Master Mix 2.5X (Eppendorf) and the ABI Prism 7000 Sequence Detection System (Applied Biosystems); PCR program was: 2 min at 50°C, 10 min at 95°C, 50 cycles: 15 s at 95°C and 1 min at 60°C. Analysed probes were AKAP 5, AKAP 7, Gnas and β-2 microglobulin like standard (used for normalisation). Results were analysed with the ABI Prism 7000 SDS software. The efficiency of real-time primer/probes was nearly identical. Quantification was done using the comparative CT method as described earlier *(Budde et al., 2005)*. GAPDH expression was checked as a positive control. The PCR protocol for GAPDH amplification was: 3 min 94°C; 50 cycles (30 s 94°C, 1 min 61°C, 1 min 72°C); 7 min 72°C; ∞ 4°C. Primer sequences for GAPDH (nucleotides 789–1028, accession No. NM017008) were:
forward, 5′- TGATGACATCAAGAAGGTGGTGAA-3′;
reverse, 5′ TCCTTGGAGGCCATGTAGGCCAT- 3′.

3.7 Generation of recombinant fusion proteins

3.7.1 Polymerase chain reaction

Cloning procedure started using rat cDNA and performing standard PCRs with appropriate primers for specific target genes. If cDNA constructs were generated by PCR specific primers were resuspended at a concentration of 0.5 µM and used in the amplification reaction at a final concentration of 10 pmol/µl (Invitrogen). The concentration of the deoxyribonucleotide triphosphates was 200 µM plus 2.5 U of thermo stable Pfu-Turbo-DNA-polymerase (Fermentas). The temperature profile used for PCR was as follows:

Cycles	**Process**	**Time and temperature**
1x	Initial denaturation	2.5 minute at 94°C
30x	Denaturation Annealing Extension	1 minute at 94°C 1 minute at 55-65°C (primer pair dependent) 1 minute at 72°C/1000 base pairs (bp)
1x	Final extension	7 minutes at 72°C

Annealing temperature is primer dependent and was specifically adjusted to the required conditions for each pair of primers that were used.

Primers used for PCR:

AKAP 5	Bam HI for. CGG GAT CCA TGG AGA CCA GCG TTT CTG AG Sal rev. GCG TCG ACT CAC TGG AAC AGC GTA TTT AT
AKAP 7 (I)	EcoRI HI for. GGA ATT CAT GGA GCG CCC CGC CGC GGG AG Sal I rev. GCG TCG ACT CAC TTC CGG TTG TTA TCA CT
AKAP 7 (II)	Bam HI for. CGG GAT CCA TGG AGC GCC CCG CC Sal I rev. GCG TCG ACT CAC TTC CGG TTG TTA TCA CT
PKA csβ	Xho I for. CCC TCG AGA TGG GGA ACA CGG CGA TCG CCA AG Bam HI rev. CGG GAT CCA TGG AGC GCC CCG CC
PKARIIβ	EcoRI for. GGA ATT CAT GAG GAC AGT GCT GAC TGT ATG T Xho I rev. CCC TCG AGT GCA GTG GGC TCA ACA ATA TCC AT

PCRs products were purified via extraction from 1% agarose gels using kits for purification (PCR cleanup gel extraction kit Macherey-Nagel). After purification products were digested overnight with appropriate restriction enzymes (BioLabs, UK).

3.7.2 DNA agarose gel electrophoresis

DNA fragments obtained after PCR or after restriction digestion were separated according to their size by one-dimensional agarose gel electrophoresis using TAE as a running buffer. Agarose gels (0.8-2.0% w/v) were prepared by melting the agarose (UltraPure, Gibco) in the same buffer. To visualize the DNA under UV light, 5 - 10 µl Ethidium bromide solution (10 mg/ml in H_2O) was added before gel polymerization. The DNA samples were prepared in 6x loading buffer and were loaded onto the gel. Gels were run at 80V in 1x TBE or 1x TAE buffer. The DNA fragments were visualized under UV-light and photographed with an Eagle eye (Stratagene) using the gel documentation system Gel Doc (Biorad, München, Germany).

3.7.3 cDNA cloning into expression vectors

DNA fragments of interest were amplified by PCR as described above. Following agarose gel electrophoresis in TAE buffer to confirm the right molecular weight of the products, the fragments were purified by the PCR cleanup gel extraction kit (Macherey-Nagel). The fragments were then subjected to enzymatic digestion, purified again and ligated with T4 ligase to the pre-digested vector. The ligations were performed at 16°C overnight. The used DNA fragment/vector ratio was 4:1.

	Company
Insert (DNA) 7µl	
Vector (DNA) 1 µl	
10xbuffer ligase 1µl	Promega
T4DNA ligase (Promega) 1µl	Promega

To select for positive clones, the ligated fragment-vectors were transformed by electroporation into *E. coli* XL-1 Blue competent cells for subsequent DNA mini-prep isolation.

3.7.4 Electroporation

Electrocompetent *E. coli* XL-1 Blue MRF' cells were thawed on ice, 1 µl (1 µg) of plasmid DNA was added to each tube containing competent cells, and the cells were transferred to pre-cooled 0.2 cm cuvette. Electroporator parameter setting was as the following: voltage, 2.4 kV; capacitor, 25 F; resistor, 200 Ohme; time constant, 5.0 ms.

1 ml prewarmed SOC medium was added to the cells and agitated for 1h at 1200 rpm and 37°C. Subsequently the cells were centrifuged for 5 minutes at 200 rpm and the pellet was resuspended in 100 µl of the SOC medium. 80 µl or 20 µl of the mixture was plated on LB/Ampicillin (Amp) or Kanamycin (Kan) agar plate, depending on the resistance gene present in the expression vector that was used. Thereafter, the plates were incubated at 37°C overnight.

3.7.5 Mini DNA preparation

Buffer	**Composition**
P1 Buffer	50 mM Tris/HCl pH 8.0, 10 mM EDTA, 100 µg/ml RNase A (4°C)
P2 Buffer	200 mM NaOH, 1% (w/v) SDS
P3 Buffer	3 M potassium acetate, pH 5.5

Single colonies from agar plates were picked into 2 ml of LB medium containing the respective antibiotic and grown overnight at 37°C in bacterial shaker. DNA plasmids were purified (from a 2 ml LB overnight culture) by alkaline lysis using Plasmid Mini Kit (Qiagen, Gemany) according to manufacturer's instructions. Briefly, the cells were pelleted, resuspended in 300 µl of P1 buffer and lysed with 300 µl of P2 buffer. In this step proteins and DNA were denatured and RNA hydrolyzed. With 300 µl of P3 buffer the mixture was neutralized, which leads to the precipitation of denatured proteins and chromosomal DNA. The debris was removed by centrifugation of the lysate at

6000 x g for 10 minutes. The supernatant was transferred to a new tube and 630 µl of isopropanol were added and mixed. The plasmid DNA was precipitated by centrifugation at 13000 x g for 10 minutes at 4°C. The precipitated DNA was washed with 500 µl of ice-cold 70% (v/v) ethanol and centrifuged for 10 minutes at top speed. The pellet was dried, redissolved in 50 µl of dH_2O or appropriate buffer and stored at -20°C. The DNA from isolated clones was incubated with restriction enzymes and the positive clones showing the insert with the expected molecular weight were identified by agarose gel electrophoresis. The identity of these clones was subsequently confirmed by sequence analysis (Seqlab, Göttingen).

For mammalian cell transfection, DNA with high concentration and purity was prepared using the Plasmid Midi Kit (Qiagen, Germany) and/or the EndoFree Plasmid Maxi Kit (Qiagen500-EF) according to manufacturer's instructions. The DNA concentration was determined by spectrophotometrical quantification at 260 nm by A260 * 50 = x µg/ml.

3.8 Isolation of recombinant fusion proteins

3.8.1 Induction of fusion protein synthesis (GST and MBP)

The LB culture medium containing 100 µg of ampicillin/ml was used for the induction. 100 ml of an overnight culture of *E. coli* (XL-1 Blue MRF') strain transformed with either empty pGEX or pMAL vector or with generated appropriate constructs was grown overnight at 37°C in bacterial shaker. On the next day, 1000 ml of LB culture media was inoculated with complete 100 ml of prepared overnight cultures and grown with shaking at 37°C until mid-log phase ($OD_{600nm} \approx 0.6$ - 0.7). The culture was induced with IPTG (isopropyl-f-D-l-thiogalactopyranoside) (final conc. 1 mM) for several hours. Then the bacteria were harvested by centrifugation at 6000 x g (Sorvall, rotor SLA 1500, Beckmann Instruments GmbH, Munich, Germany) for 5-10 minutes and fusion proteins were purified as described below.

3.8.2 Purification of fusion proteins

The bacterial pellet for each probe (from 1l LB medium culture) was resuspended in 35 ml TBS plus 1X CompleteTM protease inhibitor (Roche). Cells lysis was performed with a French Press (Spectronic Instruments Inc., Rochester, New York, USA). Then for GST-fusion proteins Triton X-100 was added to a final concentration of 1% and cell lysates were shaked gently for 1 hour at 4°C. The soluble fractions ware separated from the debris at 6000 x g for 30 minutes at 4°C (Sorvall, rotor SLA 1500, Beckmann Instruments GmbH, Munich, Germany). The cleared lysate was transferred to a clean 50 ml Falcon tube. In the meantime 1.7 ml Gluthation-Sepharose 4B Fast Flow (for GST-fusion proteins) or amylose beads (for MBP-fusion proteins) (GE Healthcare, England) was washed three times with ice cold TBS. The cleared lysates were added to the prewashed beads and shaken at 4°C to

allow binding of the fusion proteins to the resin. After overnight incubation, the beads were spun down at 500 x g for 10 minutes at 4°C and the unbound material was removed. The beads (matrix) were washed twice with cold TBS/1% Triton X-100 and kept at 4°C for further experiments.

3.9 Pull down assays

Pull down assays were done with different combinations of proteins in order to show direct interaction between them *in vitro*. The combinations of proteins were:

Pull down 1:

AKAP7-MBP (coupled to matrix) and PKAcsβ-GFP (expressed in COS-7 cells)

Pull down 2:

AKAP7-MBP (coupled to matrix) and PKARIIβ-c-myc (expressed in COS-7 cells)

Pull down 3:

AKAP7-GST (coupled to matrix) and caldendrin-no tag (expressed in COS-7 cells)

Pull down 4:

PKARIIβ-GST (coupled to matrix) and PKAcsβ-GFP (expressed in COS-7 cells)

Transfected COS-7 cells expressing one protein of interest tagged to GFP or c-myc tag were scraped in medium and transferred to 15 ml Falcon tube. Cell flask was washed with 2 ml of TBS and the solution was pulled with scraped cells. After centrifugation at 1000 x g for 5 min in cooled centrifuge (4°C), supernatant was discarded, the cells were resuspended in 1 ml of TBS and transferred to 1.5 ml Eppendorf tube. The cells were then centrifuged again at 1000 x g for 5 min at 4°C, supernatant was discarded and the pellet was frozen and thawed up 1-2 times using liquid nitrogen in order to disrupt cells. After careful resuspension in 200 µl of 1 x TBS/Triton X-100 and vortexing, lysat was mixed for 1h in cold room (4°C) at rotation wheel. Cleared lysat that was obtained after 20 min centrifugation on 14000 rpm at 4°C was diluted with TBS up to final concentration of 0.2% Triton X-100 and either used directly for pull down assay or stored at -20°C for further use.

Next, approx. 50 µl of prepared beads (matrix) coupled to other protein of interest with GST or MBP tag were washed 2x and equilibrated in 1 x TBS containing 0.1% Triton X-100. 200-300 µl of appropriate lysates from COS-7 cells were added and beads were gently shacked at rotation wheel overnight at 4°C. After 5 min centrifugation at 600 x g at 4°C, matrix was three times washed with 1 x TBS/0.2% Triton X-100 for 10 min on rotation wheel in order to remove unbound proteins. Bound proteins were eluted by 5 min boiling with 4 x SDS sample buffer and either loaded on SDS-PAGE gels directly or stored at -20°C for further use.

3.10 Sodium dodecyl sulphate polyacrylamide gel electrophoresis (SDS-PAGE)

In this work, proteins were separated using one-dimensional SDS-PAGE under fully denaturing and reducing conditions *(Laemmli, 1970)*. SDS-PAGE was performed in a 5 - 20% gradient gel. The samples were first incubated with SDS-sample buffer at 95°C for 5 minutes and then loaded onto the gel. Gels were allowed to run at a constant current strength of 12 mA in an electrophoresis chamber (Hoefer Mighty Small System SE 250 from Amersham Biosciences) filled with 1x electrophoresis buffer. Subsequently the gels were either stained with Coomassie blue or were used for immunoblotting.

3.10.1 Laemmli system

Buffer	**Composition**
4x SDS-sample buffer	250 mM Tris/HCl, pH 6.8, 1% (w/v) SDS, 40% (v/v), glycerol, 4% β-mercaptoethanol, 0.02% bromophenol blue
Electrophoresis buffer	192 mM glycine, 0.1% (w/v) SDS, 25 mM Tris-base, pH 8.3
4x separating buffer	0.4% (w/v) SDS, 1.5 M Tris/HCl, pH 6.8
Separation gel (20%)	8.25 ml separation buffer, 7.5 ml 87% Glycerol, 16.5 ml 40% Acrylamyde, 330 µl EDTA (0.2 M), 22 µl TEMED, 120 µl 0.5% Bromophenol blue and 75 µl 10% APS
Separation gel (5%)	8.25 ml separation buffer, 17.94 ml dH_2O, 1.89 ml 87% Glycerol, 4.12 ml 40% Acrylamide, 330 µl EDTA (0.2 M), 22 µl TEMED and 118 µl APS.
Stacking gel (5%)	6 ml stacking buffer, 7.95 ml dH_2O, 5.52 ml 87% Glycerol, 3.90 ml 30% Acrylamyde, 240 µl EDTA (0.2 M), 240 µl 10% SDS, 17.2 µl TEMED, 30 µl Phenol red and 137 µl 10% APS

3.10.2 Coomassie staining of SDS-polyacrylamide gels

Coomassie blue staining solution	1 mg/l Coomassie brilliant blue R-250, 60% (v/v) methanol, 10% (v/v) acetic acid
Distaining solution	7% (v/v) acetic acid, 5% (v/v) methanol
Drying solution	5% (v/v) glycerin, 50% (v/v) methanol

Polyacrylamide gels were stained with Coomassie solution for 10 minutes. Proteins were visualized by incubating the gel in distaining solution for 2 hours or overnight incubation by shaking. For preservation the distained gel was incubated for 15 minutes with drying solution and mounted between two cellophane membranes in a drying device.

3.11 Western blot analysis

Proteins were electrotransfered from polyacrylamide gels to nitro-cellulose membranes (Protran-BA nitrocellulose, 0,25 µm pore size, Schleicher & Schuell). The transfer was performed in blotting buffer at 4°C with 200 mA. Then, the membranes were stained for 5 minutes with Ponceau S solution to detect the molecular weight marker and the transferred proteins.

Buffer	**Composition**
Blotting buffer for Tris-acetate	25 mM Bicine, 25 mM BisTris, 1 mM EDTA, 5% methanol
Blotting buffer for TrisGlycin	192 mM Glycine, 0.2% (w/v) SDS, 18% (v/v) methanol, 25 mM Tris-Base, pH 8.3
Ponceau S solution	0.5% (w/v) Ponceau S, 3% Acetic Acid

3.12 Immunoblot detection

The immunodetection of Western blots started with a 5% Milk/TBST blockade of the membrane for one hour at room temperature. After this incubation, the membrane was washed with TBST for 5 minutes. Blots were incubated at 4°C overnight with the appropriate primary antibody diluted in TBST plus 0.02% sodium azide. After three washing steps with TBST for 10 minutes each time, the membrane was submerged into secondary antibody (anti-mouse, rabbit, or goat, depending on the nature of the primary antibody) for 90 minutes at room temperature in 5% Milk/TBST. After washing the blot as describe above, immunodetection was carried out using the ECL detection system (Pierce, IL 61105 USA) according to manufacturer's instructions. The blots were exposed for different times to ECL films (GE Healthcare, Amersham HyperfilmTM ECL), which were developed automatically using Agfa Curix 60 developing machine.

3.13 Immunoprecipitation

Immunoprecipitation is designed to detect protein-protein interactions. When a cell (for example, transfected COS-7) is lysed under nondenaturing conditions, many of the protein-protein associations that exist within the intact cell are preserved. First, antibody specific to the tag of one recombinant protein of interest (or antibody for one endogenous protein) is used to immunoprecipitate that protein. If there are any proteins that are stably associated with the protein of interest *in vivo*, they also may be co-precipitated. Identification of those proteins can be done by Western blot analysis.

AKAP5-GFP, co-expressed with PKARIIß-c-myc in COS-7 cells, was immunoprecipitated using µMACS™ Epitope Tag Protein Isolation Kit (Miltenyi Biotec, Germany) according to

manufacturer's instructions. Eluted probes were loaded on SDS-PAGE and presence of proteins interacting with AKAP5 was detected after Western blot analysis using PKARIIβ specific antibody (BD Bioscience, USA).

3.14 Mammalian cell cultures

All cells were cultivated at 37° C, with 5% CO_2 and 95% humidity.

3.14.1 COS-7 cell culture

3.14.1.1 Materials and culturing of COS-7 cells

Medium (DMEM+) and washing buffer were warmed in a water bath to 37°C and frozen 2 ml Trypsin dilution was thawed up at room temperature. One flask of COS-7 cells (grown to confluency) was taken out from the incubator and washed once with warm HBSS. After incubation for 5 minutes at room temperature with 2 ml Trypsin solution, the cells were collected with 10 ml cell culture medium and transferred into a 15 ml Falcon tube. Cell pellets obtained after centrifugation at 500 x g for 5 minutes at 4°C were resuspended in 10 ml of DMEM+ and diluted 1:10 into a new flask. Cells were split every 3 days.

3.14.1.2 COS-7 cells transfection

15 µg of DNA (for a double transfection 7.5 µg for each construct) was diluted in Optimem I up to final volume of 350 µl. 35 µl of Lipofectamine 2000 was mixed with 315 µl of Optimem I and left on room temperature for 5 minutes. DNA and Lipofectamine solutions were then combined and incubated at room temperature for 20 minutes. In the meantime, old cell culture medium from T75 flasks of COS-7 cells (one for each transfection) was changed with 10 ml of fresh, prewarmed DMEM. DNA-Lipofectamine complexes were added into the flask and cells were left in incubator for next two days. 24 hours after transfection sodium-butirate was added in order to enhance expression of transfected proteins. 48 hours after transfection, the cells were lysed and obtained lysates were either used immediately or stored at -20°C. For GFP constructs, transfection efficiency was analyzed under a fluorescence microscope (Zeiss axioplan microscope, Carl Zeiss, Jena, Germany).

3.14.2 Thalamic cultures

3.14.2.1 Preparation and culturing of dissociated cell cultures from the dorsal thalamus

Dorsal thalami were prepared from embryos (Long-Evans rats) at stage E19 and subsequently transferred into ice-cold HBSS without Ca/Mg. After triple washing with 5 ml HBSS each, 2.0 ml HBSS containing 0.5% trypsin was added to the tissue, followed by incubation at 37°C for 20 min. Tissue was washed again five times with 5 ml HBSS and finally transferred into tubes (2 ml) with HBSS containing 0.01% DNAseI. To dissociate thalamic tissue, it was pressed slowly three times through a 0.9 mm gauge needle followed by three passages through a 0.45 mm gauge needle. The remaining cell suspension was poured through a nylon tissue into a 50 ml tube and filled up with 18 ml Dulbecco's modified Eagle medium (DMEM; Gibco, Eggestain, Germany). After estimating cell quantity, the suspension was diluted with DMEM in order to achieve a cell density of 30,000 cells / ml. A 500 µl aliquot of this suspension was placed on each well of a 24-well plate, containing defatted, baked, and poly-D-lysine-coated coverslips. The cell cultures were incubated at 37°C and 5% CO_2 up to the appropriate time points. Between 3rd and 4th day of incubation AraC (final conc. 6 µM) which is known as mitotic inhibitor was added to 24-well plates with cell cultures to prevent further growth of glial cells.

3.14.3 Hippocampal cultures

Primary hippocampal cells were prepared as essentially described in section 3.14.2 and grown in culture until day 10. Some of the cover slips were taken out and immediately fixed with 4% paraformaldehyd acid (PFA). These cells were then stained with PKARIIβ antibody (1:500, BD Bioscience) and used as control cells (no treatment). Other cover slips were treated with β-AR agonist Isoproterenol hydrochloride (50 µM) for 5 minutes and then fixed. After washing, the cells were incubated with PKARIIβ antibody. All cells were then incubated with the appropriate secondary antibody, coversliped on microscope slides and analysed under the microscope. Finally, all results were quantified by measuring distances of PKA from the centre of the soma to dendrites in pixels using MetaMorph software (Visitron System).

3.15 Immunocytochemistry

After 10-14 days in vitro (DIV 10 - 14), PFA-fixed thalamic cells were washed two times with 25 mM glycine in PBS and one time with 10 mM PBS and subsequently preincubated at room

temperature in blocking solution (10 mM PBS, 10% horse normal serum, 2% bovine serum albumin, 5% sucrose, 0.3% Triton X-100). After 1h, primary antibodies were added to the blocking solution and incubated for 90 min at room temperature. The cultures were then washed with 10 mM PBS including 0.3% Triton X-100 and incubated with appropriate specific fluorescent secondary antibodies for 90 min, washed, and coverslipped with Mowiol. Omission of primary and secondary antibodies resulted in lack of fluorescent signals (controls).

3.16 Immunohistochemistry

Long–Evans rats P25–27 were deeply anesthetized using pentobarbital (50 mg/kg body weight) and transcardially perfused with PBS, followed by an icecold 4% PFA/PBS for 35–40 min. Brains were removed, postfixed for 4 h in 4% PFA/PBS, and cryoprotected with 30% sucrose. Coronal sections (20 μm) were cut at the level of the dLGN, mounted onto Polysine slide glass (Menzel, Germany), and air dried. For detection of $Ca_V1.2$, fresh-frozen sections were used. In this case, brains from isoflurane-anesthetized rats were removed and frozen in −50°C isopentane. Cryostat coronal sections of 20 μm thickness were cut at the level of the dLGN, thaw-mounted onto Polysine slide glass, air dried, and fixed in 4% PFA/PBS for 10 min. After permeabilization with 0.1% Triton X-100 in PBS for 10 min and several washings with PBS, sections were blocked with 10% normal horse serum (NHS), 2% BSA in PBS for 3 h to minimize nonspecific binding before incubation of slices with primary antibodies: rabbit anti - $Ca_V1.2$ (1:200, Alomone Labs, Israel), mouse anti-PKARIIβ (1:500, BD Bioscience, USA) in 2% NHS, 2% BSA in PBS at 4°C for 16–18 h. After washing (3±10 min with PBS), sections were exposed to Cy3-conjugated donkey anti rabbit IgG (1:400 in 2% NHS, 2% BSA in PBS, Dianova, Germany) or Alexa488 goat anti-mouse IgG (1:750 in 2% NHS, 2% BSA in PBS, Molecular probes, Invitrogen, Germany) for 1.5 h, washed again, and coverslipped with Immumount. For the negative controls, omission of the primary antibodies from the staining procedure was routinely performed with no positive immunological signal detected.

3.17 Microscopy

Immunofluorescence analysis was done using a laser scanning microscope (Leica, Leica Bensheim, Germany). Images were recorded digitally and processed using MetaMorph (Visitron System), ImageJ (NIH) and Adobe Photoshop CS (version 9.0 CS2).

3.18 Data analysis

Statistic analysis of the data was done by Student's t test or one way ANOVA as indicated using GraphPad, Prism 5 and Microcal, Origin 6.

4. Results

4.1 PCR expression patterns of the main components of the β-AR signalling cascade

4.1.1 $Ca_V1.2$ expression in whole brain and dLGN

In a first set of experiments, we analyzed the proposed modulation of CDI by β-AR signalling. To investigate expression patterns of the main components of the β-AR signalling in dLGN TC neurons, we performed RT-PCR analyses on tissue and single cell level.

By this approach, we have probed for expression of three types of β-ARs, different types of adenylate cyclases, G proteins coupled to the adrenergic receptors and different types of Ca^{2+} channels. As Fig. 6 shows, we could confirm the expression of all main components of the β-AR signalling cascade supposed to be involved in CDI modulation in TC neurons.

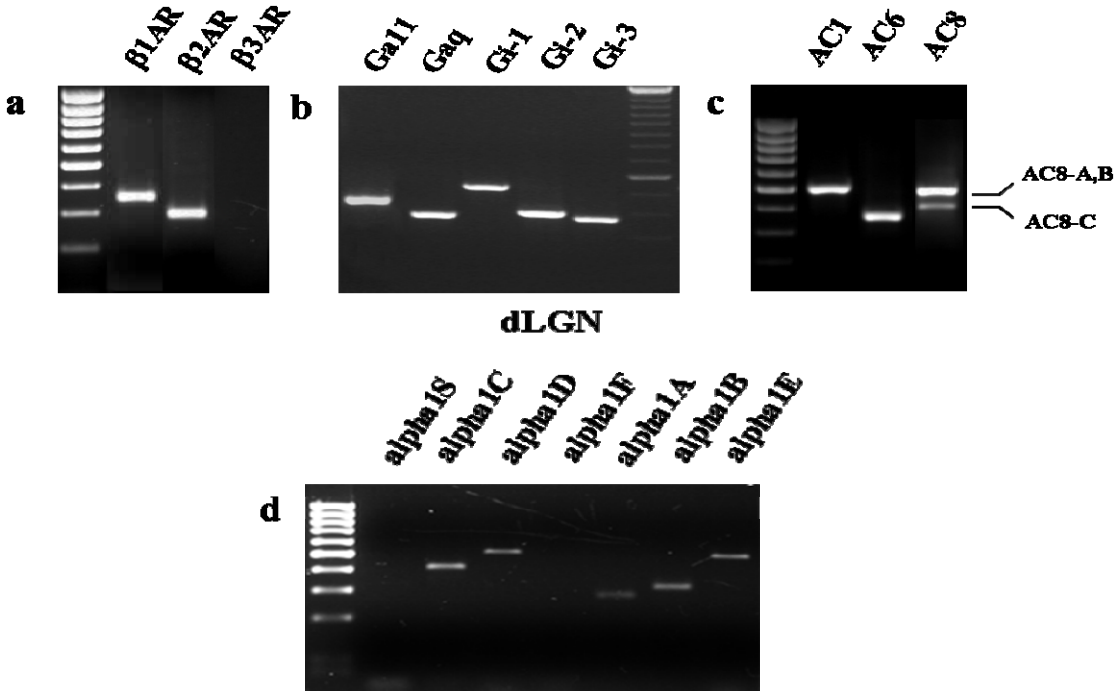

Figure 6. Expression patterns of mRNAs of main components of β-AR signalling cascade in the dLGN of Long Evans rats. (**a**) Using specific primers for all three types of β-AR, we have shown specific expression of only β_1 and β_2-AR. β_3-AR receptor was completely not expressed in thalamus. (**b**) Following the same procedure, we have shown the expression of some of the G proteins coupled with metabotropic receptors (Gα and Gi) in dLGN. In all experiments specific markers for size were used. (**c**) Expression of three different adenylate cyclases, namely type 1, 6 and 8 with two isoforms A/B and C in dLGN. (**d**) RT-PCRs from mRNAs of dLGN showed that L-type (α1C) Ca^{2+} channels are one of the dominant types of Ca^{2+} channels in dLGN.

For comparison, we have analyzed the expression of different types of Ca^{2+} channels in the ventrobasal thalamic complex (VB) as well as in whole brain extracts. This clearly indicates that L-type of Ca^{2+} channels are indeed one of the dominant forms in the brain including the thalamus (Fig. 7).

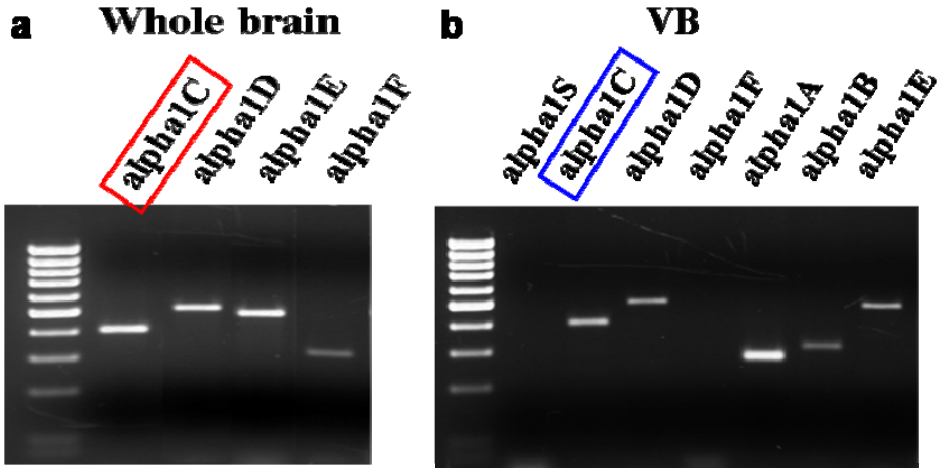

Figure 7. Expression pattern of HVA Ca^{2+} channels in extracts from whole brain and the VB region of thalamus of LE rats. RT-PCRs of mRNA from whole brain extracts (**a**) and VB (**b**) show that the α1C subunit (colored squares) as well as other Ca^{2+} channels forms are widely expressed. The skeletal muscle form α1S was not found in both regions (as well as in dLGN, see Fig. 6d). In all experiments, appropriate markers for size were used in order to assure detection of specific forms of Ca^{2+} channels.

4.1.2 Other components supposed to be involved in CDI modulation are also expressed in TC neurons

In order to achieve cell type-specific results, we next used single cells obtained from dLGN tissue. Acutely dissociated cells were observed under an inverted microscope and small bipolar interneurons and larger multipolar TC neurons were visually identified by using established criteria *(Pape et al., 1994; Broicher et al., 2007)*. While the former cells appear positive in immunostaining for glutamic acid decarboxylase 67 (GAD67), the latter cells were immunonegative (Fig. 8a-b). Single cells were collected by means of a suction pipette and used in standard RT-PCR or quantitative Real-Time PCR (qRT-PCR). Because of very low amounts of the mRNA species targeted here, in some sets of experiments it was necessary to pull cells together (up to 10 cells). As Fig. 8c shows, the Gs subunit (Gnas) was expressed in both types of neurons, AKAP5 was only expressed in TC neurons, and AKAP7 was not detected.

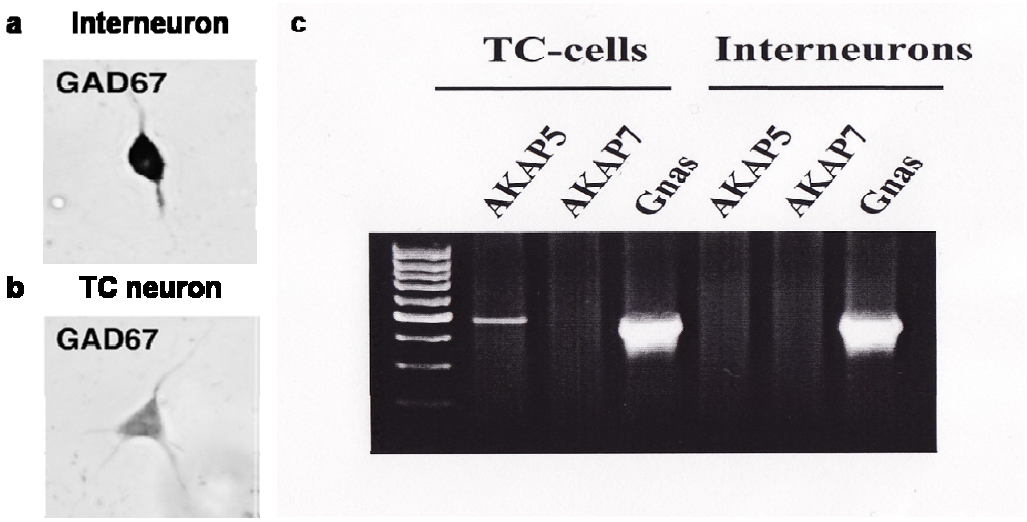

Figure 8. Single cell expression profiles of AKAP5, AKAP7 and the Gs subunit of G proteins (Gnas). Two different cell types are expressed in LGN, interneurons that are GAD67 positive (**a**) and TC neurons that are GAD67 negative (**b**) (taken from *Broicher et al., 2007*). These types of cells were collected under visual control and classified based on their morphological differences and mRNA was extracted. (**c**) Representative PCR gel with bands specific for AKAP5, AKAP7, and the Gs subunit of G proteins. Note that AKAP5 is only expressed in TC neurons while AKAP7 was not detectable.

To increase specificity, we also performed qRT-PCR with samples from different brain regions including the somato-sensory part of the cortex (SSC), visual cortex, VB, dLGN, NRT and hippocampus. Using specific primers for each gene (AKAP5 and AKAP7), we were now able to obtain expression profiles for these two proteins from all brain regions investigated, as shown in Fig. 9. Note that while AKAP7 is nearly equally expressed in the brain, AKAP5 has slightly higher expression in the SSC and hippocampus. Expression of both genes in thalamic regions was almost identical.

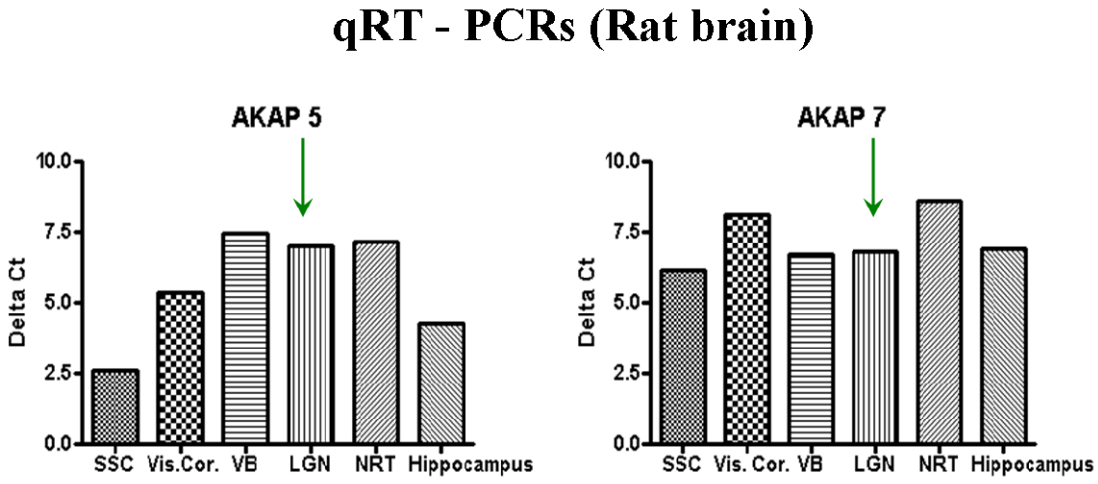

Figure 9. Expression profiles of AKAP5 and AKAP7 obtained by qRT-PCR from LE rat brain tissue. Messenger RNAs were isolated from the indicated brain tissues. qRT-PCRs analysis showed expression of both AKAP5 and AKAP7 genes in the brain with slightly higher expression of AKAP5 in SSC and hippocampus. In comparison to cortical and hippocampal areas, expression levels in thalamic regions were generally lower.

4.2 CDI is active in TC neurons in brain slices

Next, we demonstrated the occurrence of CDI in TC neurons in brain slices. Total HVA Ca^{2+} current, which is composed of about 50% current through L-type channels, was measured in the presence of TTX *(Budde et al., 1998)*. Blocking of L-type calcium channels using nifedipine significantly reduced CDI (data not shown). To confirm the presence of CDI in dLGN TC neurons in thalamic slices, HVA Ca^{2+} currents were recorded in a total of more than 150 cells and a double pulse voltage protocol (Fig. 10a; see "Methods") was used that effectively discloses VDI *(Budde et al., 2002)*. If CDI is operative, the current evoked by the test pulse should exhibit a U-shaped dependence on the conditioning pulse potential, with maximal inactivation occurring at the peak of the conditioning pulse current-voltage (*I-V*) relationship. In the present study, the results are presented as inverted U-shape curves due to normalization. Under standard conditions the *I-V* relationship of the conditioning pulse demonstrated HVA Ca^{2+} currents with an activation threshold of –40 mV, maximal inward current at around +10 mV, and an apparent reversal potential at around +60 mV (Fig. 10b). The test pulse *I-V* (peak amplitude of the test pulse current plotted vs. conditioning pulse voltage) was inverted U-shaped with minimal current occurring at +10 mV (Fig. 10c) as expected for a CDI mechanism. With respect to the amplitude of the test pulse current elicited from the holding potential of –40 mV, the degree of inactivation (D_{inact}) was 39.5 ± 0.5% (n = 100; Fig. 10c). By default, the test pulse *I-V* was obtained with the conditioning pulses altered in 10 mV increments from -40 mV (Fig. 10a). As is obvious from the presented data, there is no full recovery of the test pulse current amplitude to baseline levels at the most depolarized potentials. The hysteresis found in these type of experiments most probably resulted from the incapability of the cells to fully recover the intracellular Ca^{2+} concentration between stimulations to baseline levels *(Meuth et al., 2002)*. For reasons of recording stability it was not possible to use time periods >10 s between stimulations.

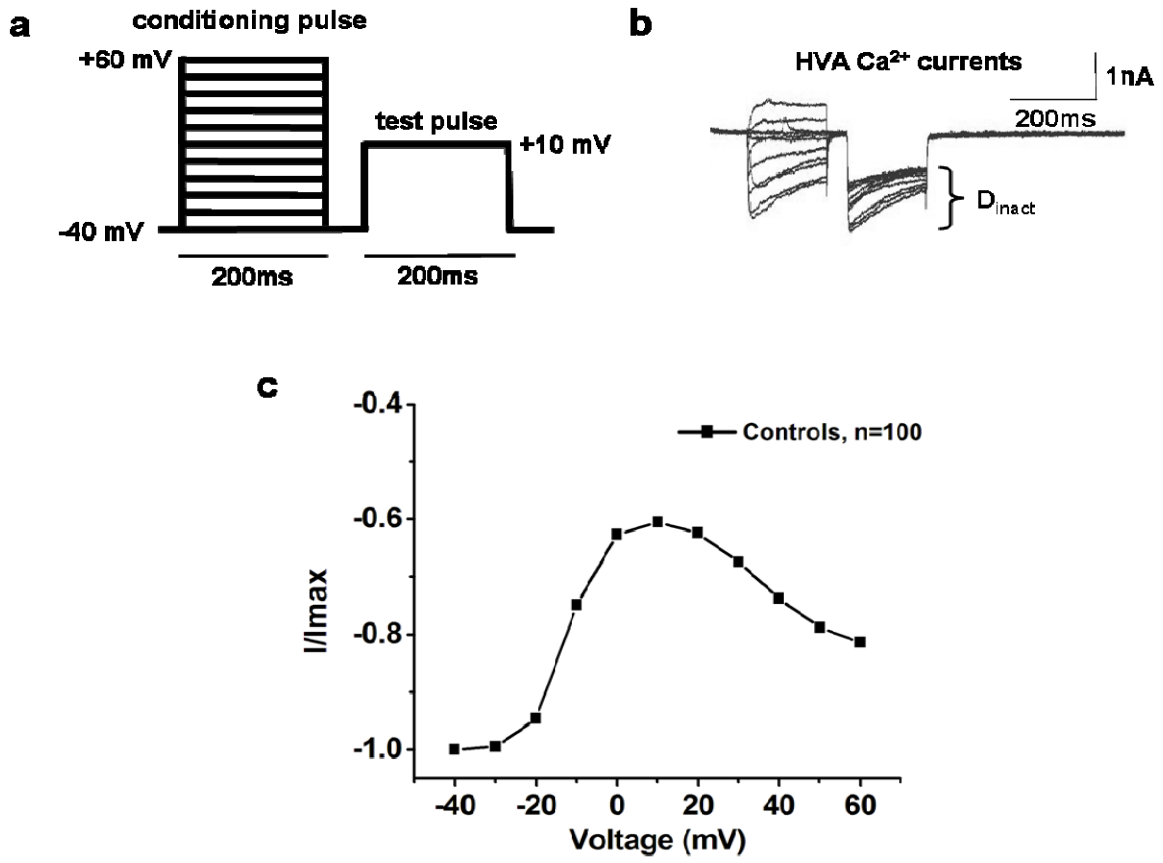

Figure 10. Identification of CDI in TC neurons in the slice preparation. (**a**) Scheme of the double pulse protocol used to elicit HVA Ca^{2+} currents. TC neurons were held at -40 mV and conditioning pulses to varying potentials (-40 to +60 mV, 200 ms duration) were followed by a brief gap (-40 mV, 50 ms) and a subsequent analyzing test pulse to a fixed potential of +10 mV (200 ms). (**b**) Family of representative current traces elicited by the pulse protocol shown in (**a**). (**c**) Mean *I-V* relationship of currents evoked by the pulse protocol shown in (**a**). Normalized test pulse amplitudes are plotted vs. the conditioning pulse potential (filled squares).

As has been noted before *(Budde et al., 1998)*, HVA Ca^{2+} currents showed a 7 ± 1% (n = 10) rundown over the course (~20 min) of a typical experiment (data not shown). To exclude that rundown has influenced the degree of CDI, the extracellular Ca^{2+} concentration was reduced from 2 to 1 and 3 to 1.5 mM, resulting in a 40.2 ± 1.8% (n = 6) and 39.4 ± 0.1% (n = 7) reduction in peak current amplitude, respectively (data not shown). Despite significantly smaller ($p < 0.01$) overall current amplitudes, the degree of inactivation was not significantly reduced when the driving force decreased (3 mM: 38.9 ± 3.1%; 2 mM: 42.2 ± 2.2%; 1.5 mM: 37.2 ± 2.0%; 1 mM: 40.2 ± 1.8%). Taken together, these findings demonstrate a CDI mechanism in TC neurons in the slice preparation that is very similar to the cells after acute isolation *(Meuth et al., 2002)*.

4.2.1 The role of β-ARs in CDI modulation of L-type Ca^{2+} channels

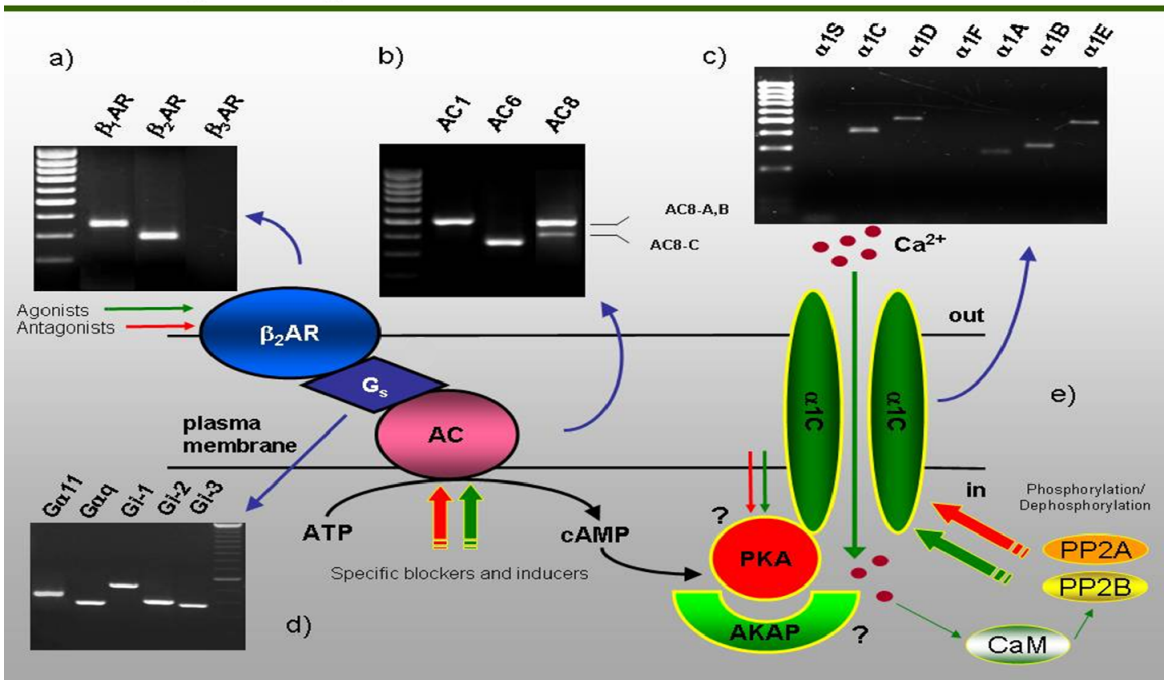

Figure 11. From receptors to CDI modulation of calcium channels $Ca_V1.2$. Hypothetical β-AR signalling cascade supposed to be involved in CDI modulation of Ca^{2+} channels (**e**) with indicated main components presented earlier (**a, b, c, d**). Scheme is also showing possible sites for modulation of the cascade with specific proteins and/or agonists or antagonists.

As outlined in the introduction, activation of β-ARs might modulate CDI of L-type calcium channels in the dLGN. β-ARs consist of three different but very similar receptor types (β_1, β_2, β_3). Using commercially available pharmacological substances, we were able to stimulate or block certain types of receptors and therefore look for the possible relevance in terms of CDI modulation of Ca^{2+} channels (see Fig. 11 above with indicated possible sites for modulation). First, we used general agonists and antagonists for β-ARs, namely Isoproterenol hydrochloride and Propranolol hydrochloride, respectively (Fig. 12). One mM ascorbic acid was added to the extracellular bath solution in order to prevent oxidation of the drugs. Experiments testing β-AR activation alone using 10 µM Isoproterenol (Fig. 12a) revealed a negative influence of β-AR stimulation on CDI. Maximal inactivation was decreased, D_{inact} to 35.7 ± 2% (n = 4, p > 0.05) as compared to control. The effect of Isoproterenol on CDI was reversed by co-application of the β-AR antagonist Propranolol (100 µM, D_{inact} = 43.68 ± 5.6, n=5; p > 0.05; Fig. 12b). These experiments generally demonstrate a role of β-AR in modulation of CDI in TC neurons. Note that the inactivation after β-AR stimulation most probably would be higher, but due to the fact that dephosphorylation processes occur at the same time these

effects may be lower than excepted. The possible role of dephosphorylation processes was tested later in this study (see Chapter *4.5*).

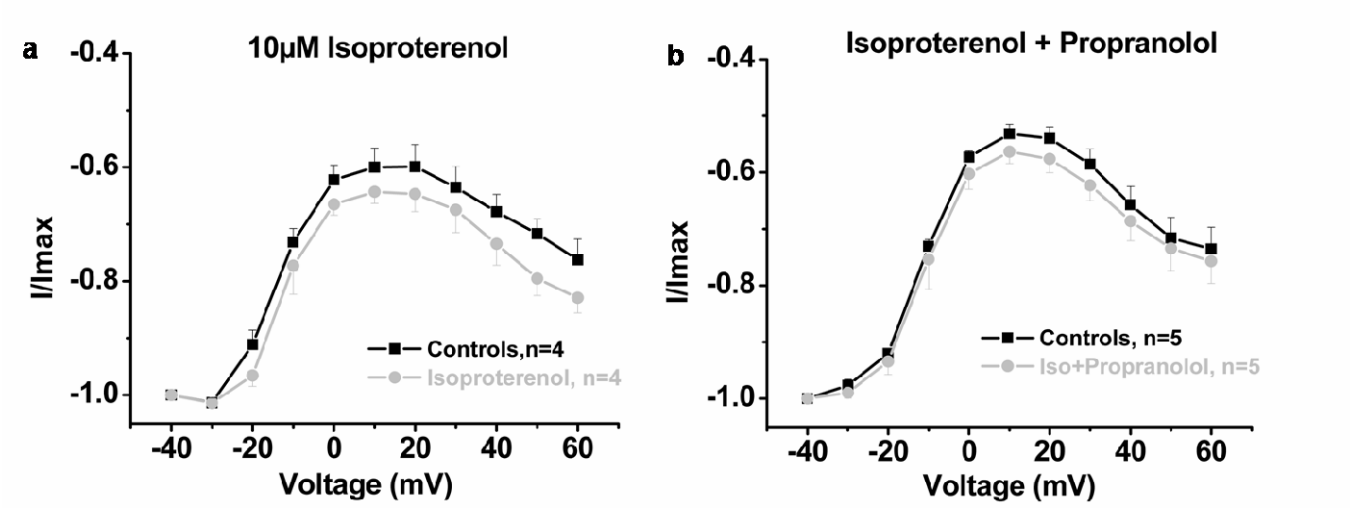

Figure 12. Modulation of β-AR influences properties of CDI inactivation in TC neurons. (**a**) Mean *I-V* relationship of normalized currents evoked by the test pulse under control conditions (filled squares) and in the presence of 10 µM Isoproterenol hydrochloride (filled circles). (**b**) Mean *I-V* relationship of normalized currents evoked by the test pulse under control conditions (filled squares) and in the presence of 10 µM Isoproterenol hydrochloride in combination with 100 µM Propranolol hydrochloride (filled circles). Data are presented as means ± SEM of several independent experiments.

4.2.2 β_2-ARs of dLGN are adrenergic receptors that mostly contribute to CDI modulation

Next, we tested agonists which bind preferentially to one of the β-AR subtypes (β_1, β_2 or β_3,). Therefore Xamoterol hemifumarate (β_1-AR agonist), Salmeterol (β_2-AR agonist), and BRL 37344, sodium salt (β_3-AR agonist) were tested. As shown in Fig. 13a & d, challenging of TC neurons with extracellular Xamoterol hemifumarate (10 µM), reduced the degree of inactivation from 43.8 ± 2.3% to 37.4.5 ± 1.8% (n = 4, $p < 0.05$). This decrease was similar in the case of extracellular Salmeterol application (reduction of D_{inact} from 39 ± 2.2% to 34.5± 0.3%, n = 4; $p < 0.05$; Fig. 13b, e) and BRL 37344, sodium salt (reduction of D_{inact} from 43.75 ± 0.6% to 38.3± 0.8%, n = 4; $p < 0.05$; Fig. 13c, f). These results raise some doubts on the selectivity of these pharmacological tools, which are due to the very similar chemical structure of all three types of receptors agonists which may therefore act on other receptor subtypes as well.

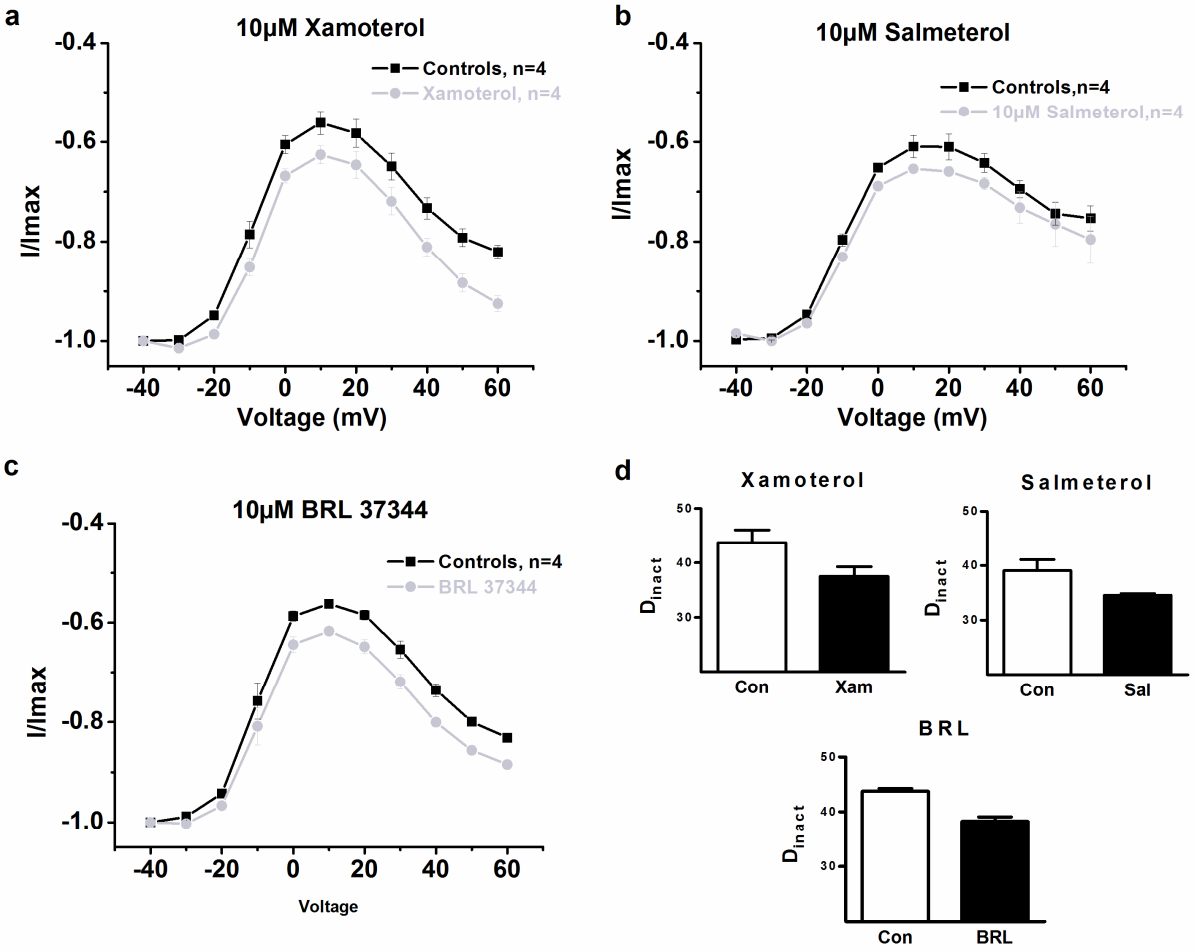

Figure 13. Type specific activation of β-ARs and effects on CDI modulation in TC neurons. (**a**) Mean *I-V* relationship of normalized currents evoked by the test pulse under control conditions (filled squares) and in the presence of specific β_1-AR agonist Xamoterol hemifumarate (filled circles). (**b**) Mean *I-V* relationship of normalized currents evoked by the test pulse under control conditions (filled squares) and in the presence of specific β_2-AR agonist, Salmeterol (filled circles). (**c**) Mean *I-V* relationship of normalized currents evoked by the test pulse under control conditions (filled squares) and in the presence of specific β_3-AR agonist BRL 37344, sodium salt (filled circles). (**d**) The degrees of inactivation are given by the normalized current value of the mean postpulse I/V at +10 mV. Data are presented as means ± SEM of several independent experiments.

To further enhance the specificity of our pharmacological approach we used the agonist that is specific for one type of receptor (in 10 µM concentration) in combination with antagonists for the other two receptor types (in 100 µM concentration), thereby allowing to investigate the role of each type of receptor in CDI modulation separately. The following antagonists were used: CGP 20712 dihydrochloride (β_1 antagonist), ICI 118,551 hydrochloride (β_2 antagonist), and SR 59230A hydrochloride (β_3 antagonist). Using this approach, effects on CDI were detected only when the β_2 agonist Salmeterol was used in combination with antagonists for the other two types of receptors (Fig. 14a, b). For the other two isoforms of β-ARs, no significant modulation of CDI effects was obtained

in this set of experiments (data not shown). These results clearly demonstrate that β_2-ARs of dLGN specifically contribute to CDI modulation in dLGN TC neurons.

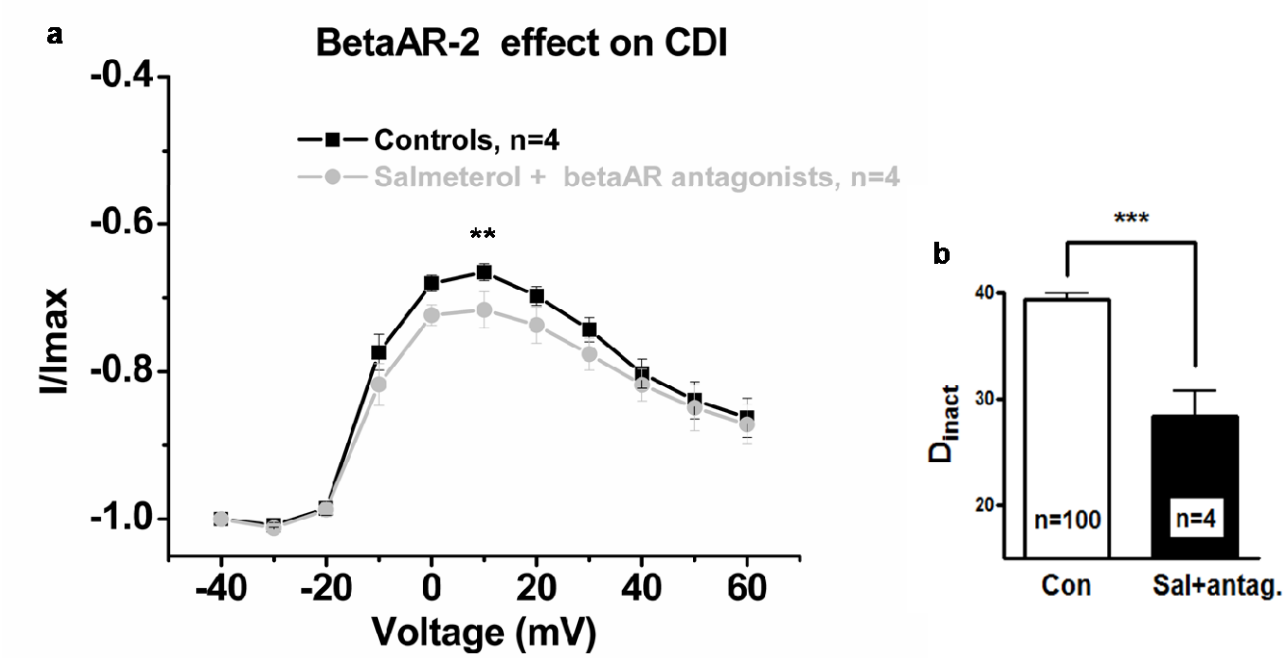

Figure 14. β_2-AR specifically modulates CDI in TC neurons of dLGN. (**a**) Mean *I-V* relationship of normalized currents evoked by the test pulse under control conditions (filled squares) and in the presence of specific β_2-AR agonist Salmeterol plus antagonists for other two types of receptor (CGP 20712 dihydrochloride-β_1 antagonist and SR 59230A hydrochloride-β_3-antagonist), (filled circles). ** = $p<0.01$ Salmeterol plus antagonists (10 mV) versus control was calculated by Student's t test. (**b**) Bar graph representation of normalized amplitudes of the test pulse current conditioned with a pulse to +10 mV under different recording conditions. The mean value of 100 cells recorded under control conditions was taken for comparison with four cells recorded under 10 µM Salmeterol plus 100 µM β_1+β_3 antagonists. Data are presented as means ± SEM of several independent experiments. . *** = $p<0.001$. Significance of Salmeterol plus antagonists versus control (n=100) was calculated by Student's t test. The degree of inactivation is given by the normalized current amplitude of the mean postpulse I/V at +10 mV.

4.2.3 Localization of β_2-ARs in cultured TC neurons

Next we analyzed the specific expression and localization of β_2-AR in 10 days old cultured thalamic neurons. We performed double immunostaining of cultured thalamic neurons using an antibody against β_2-AR (1:400, Santa Cruz) (Fig. 15b) in combination with an antibody against the neuronal marker protein microtubule associated protein 2b (MAP2b; 1:1000, BD Bioscience) which is also one of the members of AKAP family (Fig. 15a). The expression of both proteins was detected with β_2-AR mainly localized in somatic and proximal dendrites regions of TC neurons (Fig. 15b, c).

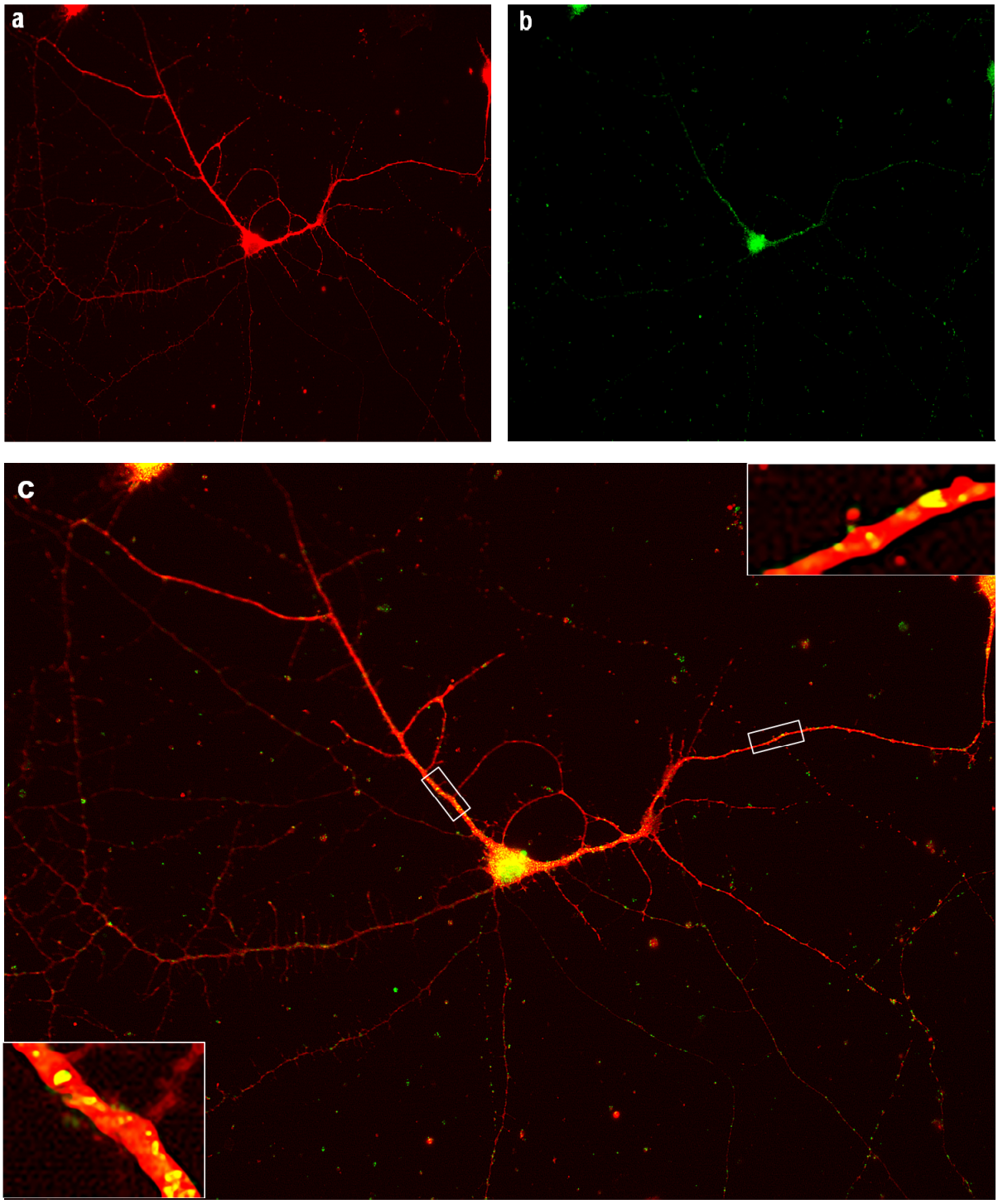

Figure 15. Localization of β_2-AR in cultured TC neurons. (**a,b,c**) Immunocytochemical analysis of primary cultures of the dorsal thalamus using (**a**) MAP2b specific antibody (red) and (**b**) β_2-AR specific antibody (green). (**c**) The merged picture revealed the co-expression of these two proteins in somatic regions and proximal dendrites. Enlarged inlay represents magnification of the area indicated by the rectangle. Yellow dots represent places were these two proteins are in close proximity.

Summarizing, these results demonstrate for the first time that β_2-ARs are involved in modulation of CDI in TC neurons. The main findings can be summarized as follows: (i) Classical double pulse protocols reveal the occurrence of CDI in TC neurons in the slice preparation. (ii) Specific activation of β_2-ARs leads to a reduction of CDI in TC neurons. (iv) β_2-ARs are localized primarily in somatic regions and proximal dendrites of TC relay neurons.

4.3 Modulators of RyR alter CDI in TC neurons

CICR is a prominent feature of TC neurons *(Budde et al., 2000)* that is based on close spatial interaction between L-type Ca^{2+} channels and RyR *(Chavis et al., 1996)*. Therefore, we probed the possibility of a negative feedback between intracellular Ca^{2+} release and HVA Ca^{2+} current amplitude by stimulating CICR with Caffeine (a commonly used drug to mobilize Ca^{2+} from intracellular stores). Extracellular application of Caffeine induced a significant ($p < 0.001$) and concentration-dependent (5 mM: 46.7 ± 2%; n = 5; 10 mM: 52.6 ± 0.2%; n = 6; 20 mM: 55.6 ± 0.9%; n = 5) increase in the degree of inactivation (Fig. 16c). These data suggest that intracellular Ca^{2+} stores might have a significant influence on CDI in TC neurons.

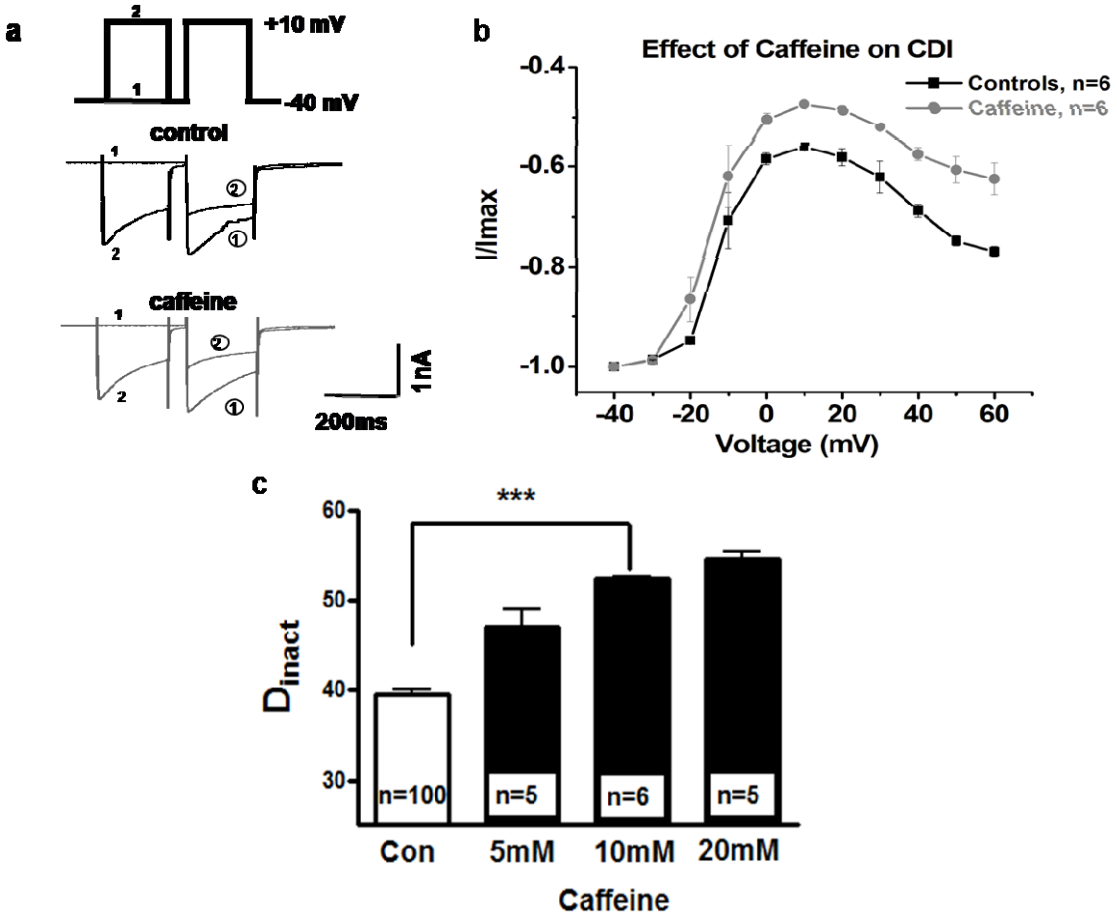

Figure 16. **Effect of Caffeine on CDI.** (**a**) Representative current traces recorded under control conditions (middle panel) and during extracellular application of Caffeine (10 mM) with no conditioning pulse (1) and a conditioning pulse to +10 mV (2) are shown (see upper panel for pulse protocol; traces were taken from the same cell). (**b**) Mean *I-V* relationship of normalized currents evoked by the test pulse under control conditions (filled squares) and in the presence of 10 mM Caffeine (filled circles). (**c**) Concentration-dependent effect of Caffeine on CDI. Normalized amplitudes of the test pulse current conditioned with a pulse to +10 mV are shown. Data are presented as means ± SEM of several independent experiments. *** = $p<0.001$. Significance of Caffeine versus control was calculated by Student's t test. The degree of inactivation is given by the normalized current amplitude of the mean postpulse I/V at +10 mV.

To further investigate which type of intracellular Ca^{2+} channels are involved in CDI modulation in TC neurons, we first applied ryanodine (10 µM) which is a specific ryanodine receptor blocker and found a significant ($p < 0.001$) reduction in D_{inact} to 30.5 ± 1.3% (n = 6; Fig. 17a, d). On the other hand, intracellular application of two inhibitors of inositol 1,4,5-tris-phosphate (IP_3)-induced Ca^{2+} release, namely 2-aminoethoxydiphenyl borate (2APB) (100 µM; 40.75 ± 2.1%; n = 6; Fig. 17b, d) and heparin (2 mg/ml; 42.05 ± 1.5%; n = 4; Fig. 17c, d) had no effect on the degree of inactivation. This suggests that RyR are critically involved in CDI modulation in TC neurons.

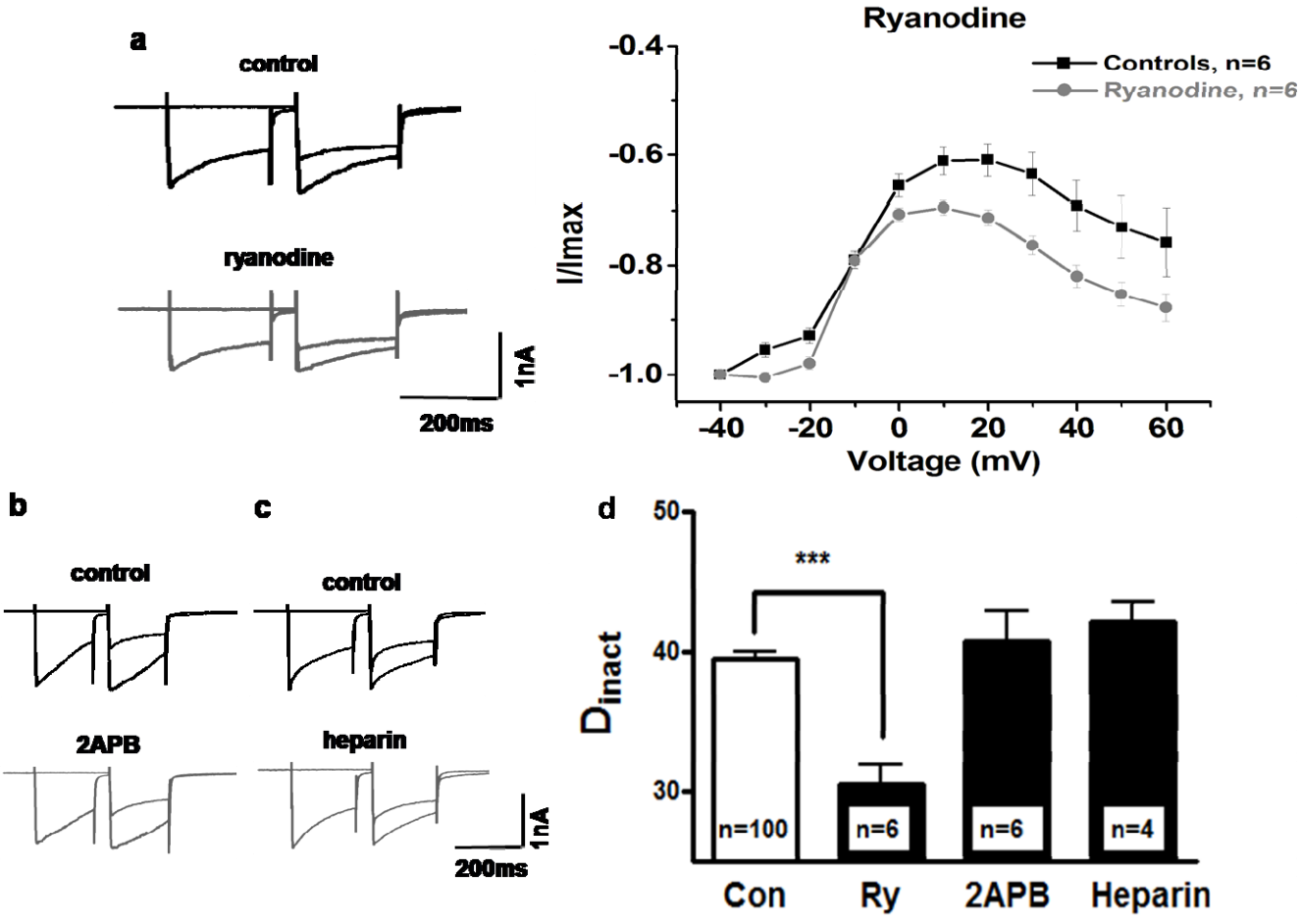

Figure 17. **Influence of different types of intracellular Ca^{2+} release channels on CDI.** (**a**) Representative current traces recorded under control conditions (upper left panel) and during application of ryanodine (10 µM, extracellular application; lower left panel; conditioning pulses as in Fig. 11a; traces were taken from the same cell). Mean *I-V* relationship of normalized currents (right panel) evoked by the test pulse under control conditions (filled squares) and in the presence of 10 µM ryanodine (filled circles). (**b, c**) Current traces recorded under control conditions (upper panel) and during application of 2APB (100 µM, intracellular application; traces in the lower panel were taken from different cells) and heparin (2 mg/ml; lower panel; intracellular application; traces were taken from different cells) are shown in **b** and **c**, respectively. (**d**) Bar graph representation of normalized amplitudes of the test pulse current conditioned with a pulse to +10 mV under different recording conditions. Since no paired statistical tests were possible for experiments with intracellular substance application, the mean value of 100 cells recorded under control conditions was taken for comparison. Data are presented as means ± SEM of several independent experiments. *** = $p<0.001$. Significance of ryanodine versus control was calculated by Student's t test. The degree of inactivation is given by the normalized current amplitude of the mean postpulse I/V at +10 mV.

The possible contribution of store-operated calcium entry was probed by extracellular application of 2APB which is also a blocker of multiple types of transient receptor potential (TRP) channels *(Iwasaki et al., 2001)*. As shown in Fig. 18, the degree of inactivation was significantly reduced to 26.5 ± 1.8% (n = 6; Fig. 18a, b) when TC neurons were challenged with extracellular 2APB (100 µM). Taken together, these findings indicate a contribution of CICR which depends on store replenishment by extracellular Ca^{2+} to the degree CDI.

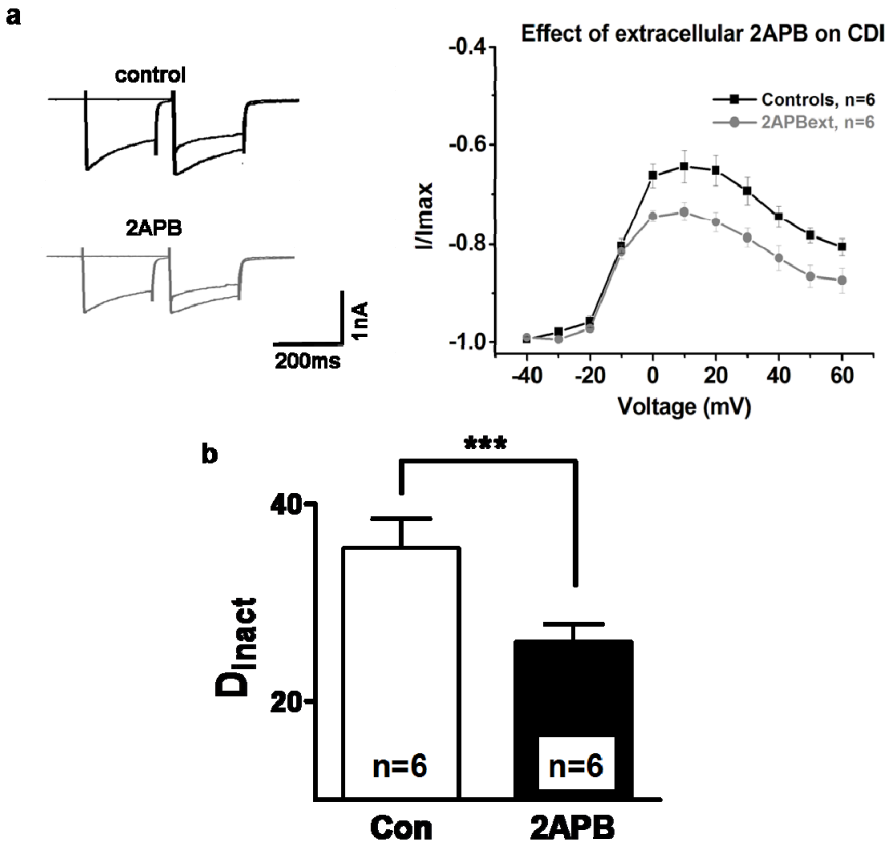

Figure 18. **Influence of store-operated Ca^{2+} influx on CDI.** (**a**) Representative current traces recorded under control conditions (upper left panel) and during extracellular application of 2APB (100 µM; lower panel; pulse protocol as in Fig. 10a; traces were taken from the same cell). Mean *I-V* relationship of normalized currents (right panel) evoked by the test pulse under control conditions (filled squares) and in the presence of 2APB (filled circles). (**b**) Bar graph representation of normalized amplitudes of the test pulse current conditioned with a pulse to +10 mV under different recording conditions. Data are presented as means ± SEM of several independent experiments. *** = $p<0.001$. Significance of 2APB versus control was calculated by Student's t test. The degree of inactivation is given by the normalized current amplitude of the mean postpulse I/V at +10 mV.

4.3.1 Control of HVA Ca^{2+} current amplitude by CICR during trains of mock action potentials

In order to test the functional aspects of the influence of CIRC on CDI, trains (200 pulses) of action potential-like pulses (-50 – -45 mV, 1 ms; -45 – +50 mV, 3 ms; +50 mV, 1 ms; +50 – -50 mV, 3 ms) were applied at 30 Hz, a typical frequency of tonic firing during slice recordings, from a holding potential of -50 mV. Control and test pulses (200 ms, from -40 to 0 mV) were applied 60 s before and immediately after the train, respectively (Fig. 19a). To assure minimal interference with exogenous Ca^{2+} buffering, recordings were performed in the absence of the low affinity Ca^{2+} buffer citrate. Under these conditions the inward current amplitude during train stimulation gradually declined and the peak current amplitude of the test pulse with respect to the control pulse was decreased by 36.3 ± 0.1% (n = 5; Fig. 19b, e). When thapsigargin (blocks the SERCA-pump and consequently, intracellular stores are drained) (10 µM) was present in the intracellular solution, the effect of train stimulation was significantly ($p < 0.01$) reduced with the decrease in test pulse amplitude averaging 21.9 ± 0.1% (n = 8; Fig. 19c, e). To further assess the relative contribution of CDI vs. voltage-dependent inactivation (VDI), Ba^{2+} (3 mM) was used as charge carrier while 11 mM BAPTA was included to the intracellular solution. Under these conditions the degree of current amplitude reduction was 12.5 ± 0.1% (n = 6; Fig. 19d, e). Taken together these findings indicate that CICR triggered by trains of mock action potentials is contributing to CDI in TC neurons.

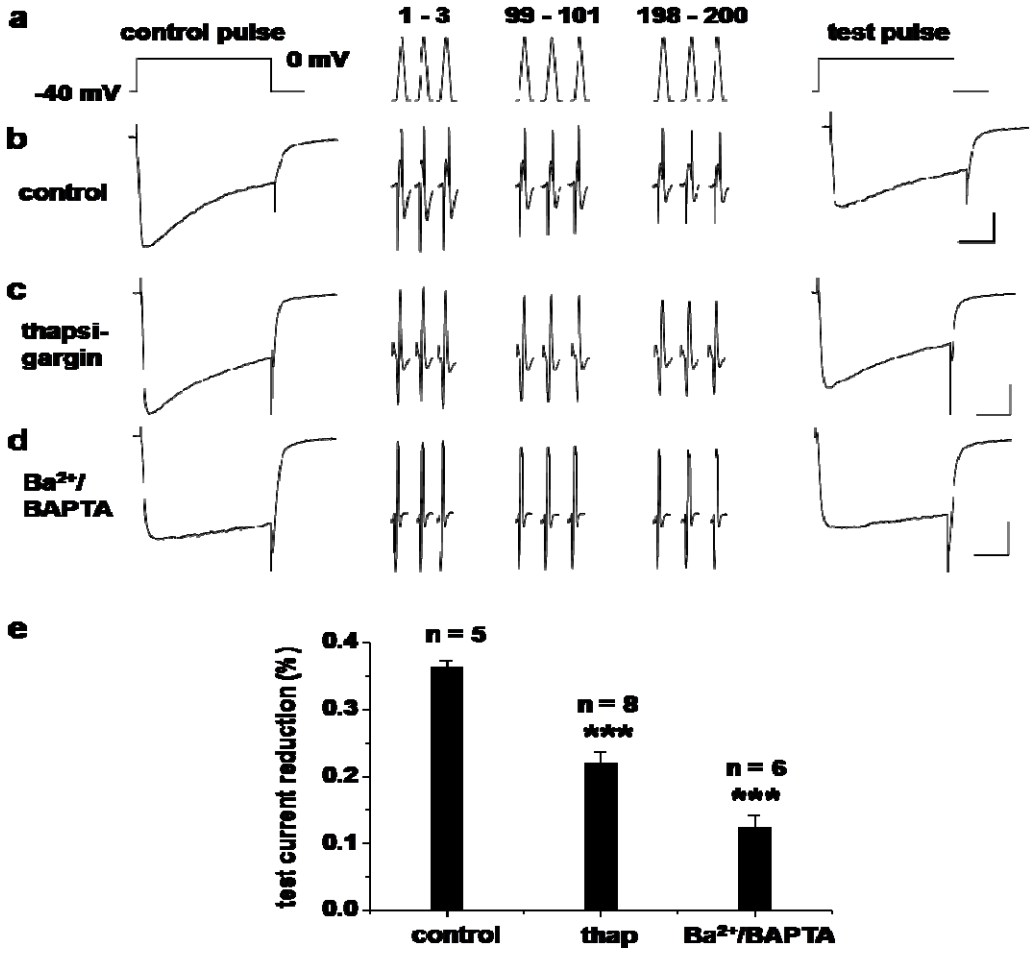

Figure 19. **Interaction between CDI and intracellular Ca^{2+} stores during trains of action potential-like stimuli.** (**a**) Scheme of the stimulation protocol. A voltage step (200 ms, from -40 to 0 mV) was applied 1 min before (control pulse) and immediately after (test pulse) a train (200 pulses @ 30 Hz) of short depolarizations (-50 – -45 mV, 1 ms; -45 – +50 mV, 3ms; +50 mV, 1 ms; +50 – -50 mV, 3 ms). (**b-d**) Current traces evoked by pulses before (left column), during (three middle columns; responses to the 1st, 2nd, 3rd, 99th, 100th, 101st, 198th, 199th, and 200th pulse in a train are shown), and following (right column) train stimulation under control conditions (**b**), during intracellular application of thapsigargin (10 µM, **c**), and using Ba^{2+} (3 mM, as charge carrier) / BAPTA (11 mM, as Ca^{2+} chelator, **d**). (**e**) Mean bar graph representation of the reduction of the test current peak amplitude in relation to the control current. Data are presented as means ± SEM of several independent experiments. *** = $p<0.001$. Significance of thapsigargin and Ba^{2+}/BAPTA versus control was calculated by Student's t test.

4.3.2 Control of basal level of Ca^{2+} in TC neurons

To further establish a specific contribution of CICR to CDI, we combined whole cell patch clamp and Ca^{2+} imaging techniques. TC neurons were loaded with the Ca^{2+} indicator dye bis-fura-2

(100 µM) via the recording pipette. Calcium currents were evoked by using double-pulses with conditioning voltage steps to -40, +10, and +60 mV (see pulse protocol in Fig. 20c). Under control conditions the fluorescence ratio averaged 0.50 ± 0.015 (n = 3). When double pulses were applied, amplitudes of the Ca^{2+} transients under control conditions with respect to the basal Ca^{2+} level were 0.077 ± 0.015 (1^{st} double pulse), 0.14 ± 0.018 (2^{nd} double pulse), and 0.142 ± 0.025 (3^{rd} double pulse) (Fig. 20d). To achieve a rough estimation of the duration of each transient, we determined the fluorescence ratios reached at the end of each double pulse sweep (i.e, 10, 20, and 30 seconds after starting the electrophysiological stimulation) and calculated the degree of recovery with respect to the maximal amplitude of each transient. Under control conditions Ca^{2+} transients recovered by 85.8 ± 2.15% (1^{st} double pulse), 66.9 ± 2.34% (2^{nd} double pulse), and 52.14 ± 5.7% (3^{rd} double pulse) (Fig. 20e). After application of 10 mM Caffeine, basal Ca^{2+} levels increased to ratio values of 0.552 ± 0.012% (Fig. 20c, < 10%). Under these conditions amplitudes of the Ca^{2+} transients with respect to the basal Ca^{2+} level were 0.095 ± 0.024% (1^{st} double pulse), 0.158 ± 0.032% (2^{nd} double pulse), and 0.143 ± 0.034% (3^{rd} double pulse) (Fig 20d) and recovered by 58.7 ± 2% (1^{st} double pulse), 37.1 ± 5.9% (2^{nd} double pulse), and 26.9 ± 6.1% (3^{rd} double pulse) (Fig. 20e). These findings indicate that Caffeine had only little influence on the amplitudes of Ca^{2+} transients but significantly increased their duration (see Fig. legend of 20d & e for significance values).

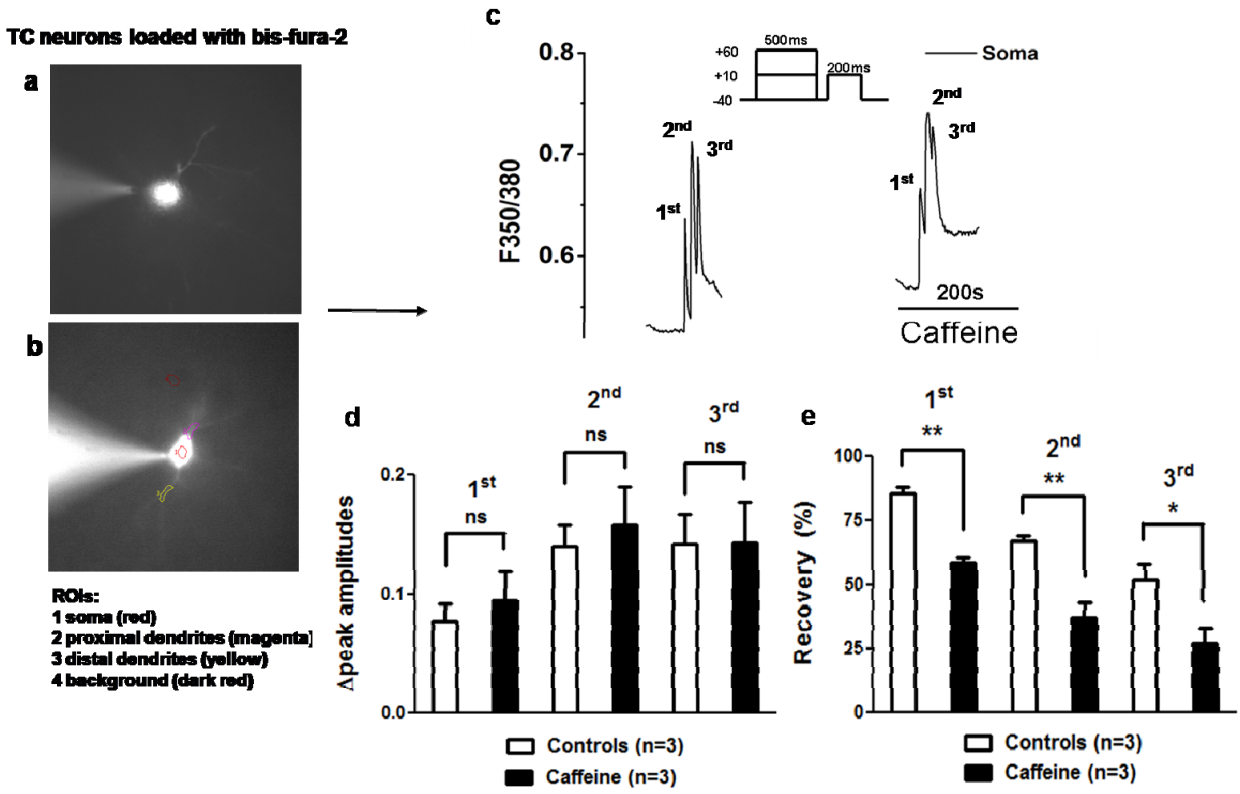

Figure 20. **Calcium imaging of TC neurons after Caffeine stimulation.** (**a, b**) TC neurons loaded with 100 µM bis-fura-2. Regions of interest (ROIs) in different cellular compartments are indicated. (**c**) Recording of somatic fluorescence ratio changes in TC neurons under control conditions and during application of 10 mM Caffeine with indicated measured peaks (1st, 2nd and 3rd). In this set of experiments double pulse protocol was used consisting of conditioning pulse (-40, +10, and +60 mV, 500 ms), pause of 50 ms and test pulse fixed to +10 mV (200 ms) to evoke calcium currents. (**d, e**) Bars represent quantified data after Student's t test (n=3). (**d**) Here differences in Δpeaks amplitudes in control condition in comparison to Δpeaks in presence of Caffeine were measured. P values of Δpeak amplitudes were after 1st peak, p = 0.75, 2nd peak, p = 0.39, and after 3rd peak, p = 0.42. (**e**) Recovery rates of the transients were calculated in control conditions and after application of Caffeine. Significance of recovery were after 1st peak ** = p = 0.0013, 2nd peak ** = p = 0.0093, and after 3rd peak * = p = 0.014.

4.3.3 Localization of CDI and CICR relevant channels

Next, we investigated the localisation of RyR2 and $Ca_V1.2$ channels in TC neurons by co-immunostaining with specific antibodies (RyR2, 1:200; Fig. 21a) and $Ca_V1.2$ (1:200, L-type Ca^{2+} channel of the α1C subtype; Fig. 21b) in thalamic primary cell cultures. Both Ca^{2+} channels were detected in TC neurons. To verify the expression of $Ca_V1.2$ in different brain regions, a Western blot analysis of the membrane fraction of rat hippocampus, thalamus, and liver (as negative control) was performed. In hippocampus and thalamus, a band of the predicted size was detected, while no band was found in liver samples, as expected (Fig. 21c).

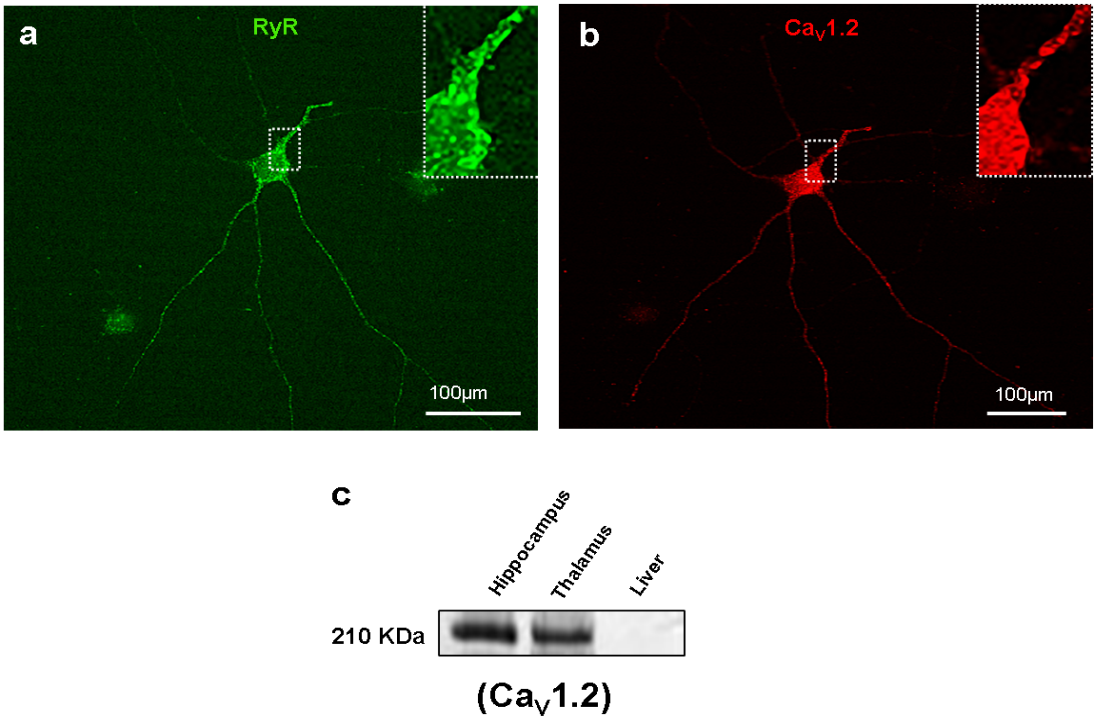

Figure 21. **Localization of RyR2 and $Ca_V1.2$ in cultured TC neurons.** (**a, b**) Immunocytochemical analysis of primary cultures of the dorsal thalamus using RyR2- (**a**) and $Ca_V1.2$- (**b**) specific antibodies. Enlarged inlay represents magnification of the area indicated by the dotted rectangle. (**c**) Western blot analysis of the membrane fraction of hippocampal, thalamic and liver tissues was performed to test the $Ca_V1.2$ antibody specificity and also to look for expression of channels in different brain compartments as well as in liver (negative control). Bands of the expected size (~210 kDa) were present in membrane fractions of hippocampal and thalamic origin, but were absent in membrane fractions of the liver.

Altogether, our results in this section demonstrate the negative feedback of intracellular Ca^{2+} release on CDI of HVA Ca^{2+} channels in central neurons and can be summarized as follows: (i) Classical double pulse protocols reveal the occurrence of CDI in TC neurons in the slice preparation. (ii) Activators and inhibitors of CICR increase and decrease the degree of CDI, respectively. (iii) Inhibition of store-operated Ca^{2+} influx reduces the degree of CDI. (iv) Trains of action potential-like stimuli induce an ER-dependent reduction in HVA Ca^{2+} current amplitude. (v) $Ca_V1.2$ and RyR2 channels are localized near the plasma membrane of identified TC neurons.

4.4 Downstream β-AR signalling molecules supposed to be involved in CDI modulation of TC neurons

4.4.1 Blocking of PKA completely suppresses the modulation of CDI in TC neurons

Next, we probed the possible contribution of PKA in CDI modulation of TC neurons in whole cell patch clamp studies. The possible contribution of PKA was probed using intracellular application of PKA inhibitor myristoylated PKI 14-22 amide (10 μM, Tocris). As is shown in Fig. 22, the degree of inactivation was significantly reduced from of 44.6 ± 2.3% (n=5) under control conditions to 34.5 ± 0.3% (n = 4; $p < 0.001$; Fig. 22a, 22b) when TC neurons were challenged with extracellular Salmeterol (10 μM; filled squares), while in combination with PKI the inhibitory effect of β-AR stimulation was suppressed (D_{inact} = 43.2 ± 1%; n=5). These findings indicate a contribution of PKA to the degree of CDI that depends on phosphorylation by PKA.

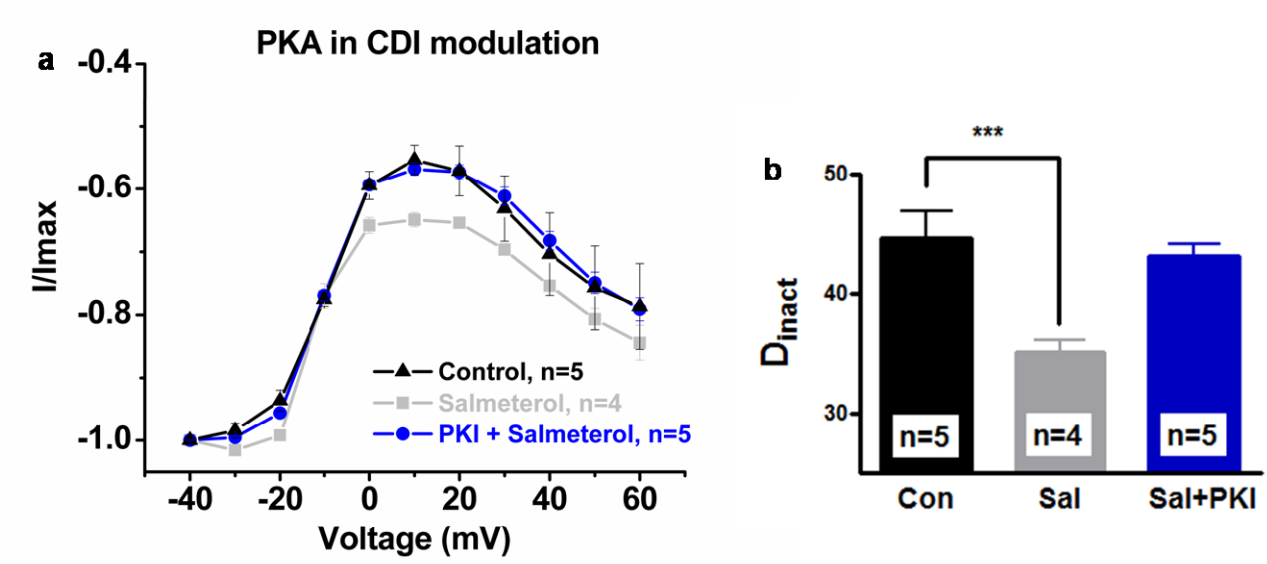

Figure 22. Inhibition of PKA completely suppresses the effect of β-AR stimulation on CDI in TC neurons. (**a**) Mean *I-V* relationship of normalized currents evoked by the test pulse under control conditions (filled triangles) in the presence of the specific β_2-AR agonist Salmeterol alone (filled squares) or in combination with PKI 14-22 amide (filled circles, blue line). (**b**) The bar graph represents test current peak amplitudes in relation to the control current (black bar are controls, grey are Salmeterol and blue Salmeterol plus PKI). Data are presented as means ± SEM of several independent experiments. *** = $p<0.001$. Significance of Salmeterol (10mV) versus control was calculated by Student's t test.

4.4.2 AKAPs play a crucial role in the modulation of CDI in TC neurons

Next, we investigated contribution of AKAPs in CDI modulation of Ca^{2+} channels in TC neurons. AKAPs are assumed to simultaneously bind to PKA, Ca^{2+} channel and protein phosphatase (like Calcineurin, for example). Therefore we tested our hypothesis that AKAPs might play an important role in PKA phosphorylation of Ca^{2+} channels by combining patch clamp experiments and immunocytochemistry. The selective AKAP inhibitor InCELLect™ AKAP St-Ht31 and the corresponding control peptide (Promega, Germany) were used to specifically manipulate binding of AKAP to PKA. Inhibitory peptide specifically binds to PKA binding sites of AKAPs thereby blocking the binding of intracellular PKA. In the case of control peptide, PKA binds normally. When Salmeterol (10 µM in bath solution) was applied in the presence of InCELLect™ AKAP St-Ht31 inhibitory peptide (10 µM in pipette solution) the degree of inactivation (37.6 ± 1.5%, n = 9; Fig. 23b) was comparable to control conditions but different in comparison to application of Salmeterol alone (34.5 ± 0.3%, n = 4; Fig. 23b). Using the same experimental protocol co-application of Salmeterol and control peptide did not change the reduction in CDI (data not shown). Therefore, these experiments point to a role of AKAPs in modulation of CDI of Ca^{2+} channels.

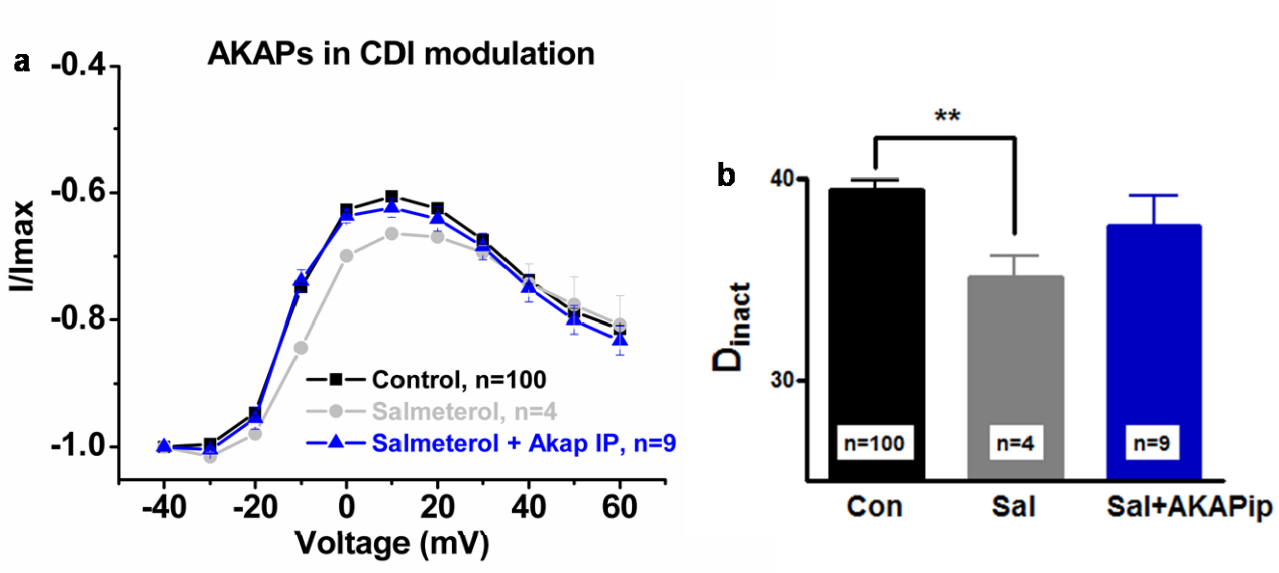

Figure 23. Inhibition of PKA binding to AKAPs suppresses the effect of β-AR stimulation in TC neurons. (**a**) Mean *I-V* relationship of normalized currents evoked by the test pulse under control conditions (filled squares) in the presence of the specific β_2-AR agonist Salmeterol alone (filled circles), or in combination with InCELLect™ AKAP St-Ht31 inhibitory peptide (filled triangles, blue line). (**b**) Bar graphs represent test current peak amplitudes in relation to the control current (black bar are controls, grey are Salmeterol and blue Salmeterol plus AKAP St-Ht31 inhibitory peptide). Since no paired statistical tests were possible for experiments with intracellular substance application, the mean value of 100 cells recorded under control conditions was taken for comparison. Data are presented as means ± SEM of several independent experiments. ** = $p<0.01$. Significance of Salmeterol (10 mV) versus control was calculated by Student's t test.

4.4.3 AKAPs assist in PKA translocation from somatic regions to the plasma membrane

In order to demonstrate that PKA translocates close to the Ca^{2+} channels to phosphorylate them after β-AR stimulation and to further confirm the role of AKAPs, we performed the following set of experiments. First, we looked for localization and possible translocation of PKA after stimulation of the β-AR cascade. Since cultured hippocampal neurons represent a robust and widely used model system to investigate neuronal processes, in the following experiment 10 days old hippocampal neurons were used. Moreover, both hippocampal as well as thalamic cells express $Ca_V1.2$ and PKA (data not shown). During this study, we focused on the regulatory subunit IIβ of PKA which is the dominant neuronal form of this enzyme and therefore a candidate involved in phosphorylation of $Ca_V1.2$. Thus, it was reasonable to investigate this isoform in regulation of CDI in TC neurons.

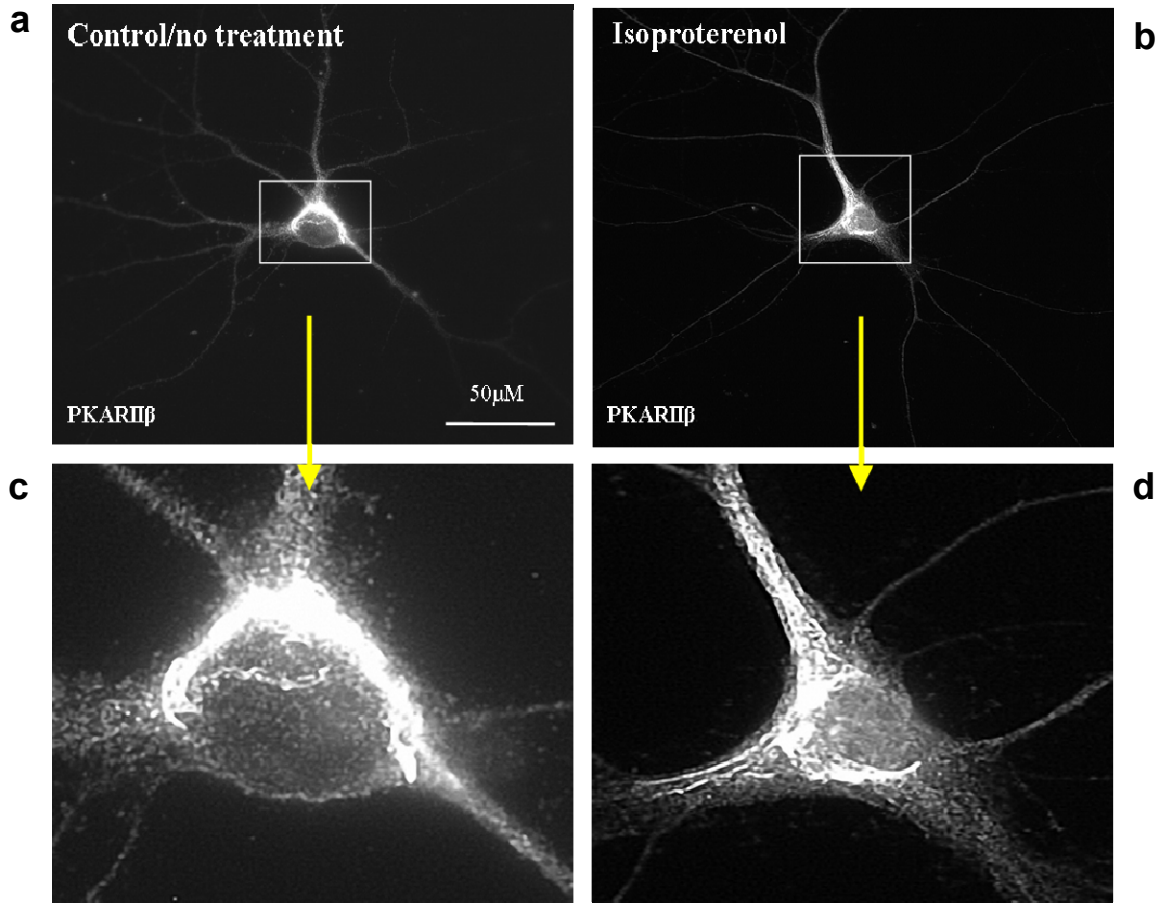

Figure 24. Translocation of PKA after β-AR stimulation in 10 days old cultured hippocampal neurons. (**a, b**) Cultured hippocampal cells were treated or kept under control conditions (control/no treatment) with 50 μM Isoproterenol, fixed and immunostained with PKARIIβ antibody. Enlarged inlays (**c, d**) represent magnification of the area indicated by the rectangle. Note translocation of PKA from somatic perinuclear region in control cells to more distal regions close to the plasma membrane and probably Ca^{2+} channels in cells treated with Isoproterenol.

Figure 24 shows a PKARIIβ immunostaining of control (no treatment) cells and cells treated with Isoproterenol for 5 minutes. It is evident that in untreated cells PKARIIβ was mostly localised in somatic perinuclear regions (24a, c), whereas after Isoproterenol treatment PKA translocates from this regions to more distal sites and most probably close to the membrane and Ca^{2+} channels (Fig. 24b, d). Note that translocated PKA shows a specific staining pattern in dendrites (looking like straight lines) giving us a reason to believe that this movement is supported by scaffolding proteins, namely the cytoskeleton (microtubule) and probably proteins from the AKAP family.

Therefore, it was reasonable to test a possible role of AKAPs in PKA translocation after β-AR stimulation. To do this, we again used an inhibitory peptide AKAP St-Ht31 which specifically blocks binding between PKA and AKAPs. According to our hypothesis, when the binding of intracellular PKA to AKAPs is blocked, PKA cannot be translocated to Ca^{2+} channels. Data obtained in this set of experiments are shown in Fig. 25. As expected, application of AKAP inhibitory peptide AKAP St-

Ht31 strongly decreased PKA translocation induced by 5 minutes of treatment with Isoproterenol (50 µM) (Fig. 25b), whilst the control peptide had no significant effect (Fig. 25a). Using Anisomycine (7.5 µM) to block *de novo* synthesis of proteins, we showed that PKA translocation is due to the stimulation of adrenergic receptors and not a consequence of new synthesis of the enzyme (Fig. 25c). Significant differences were found between the group of cells treated only with Isoproterenol and the group treated with Isoproterenol together with the inhibitory peptide AKAP St-Ht31. Control peptide showed no significant effects on translocation of PKA after Isoproterenol treatment.

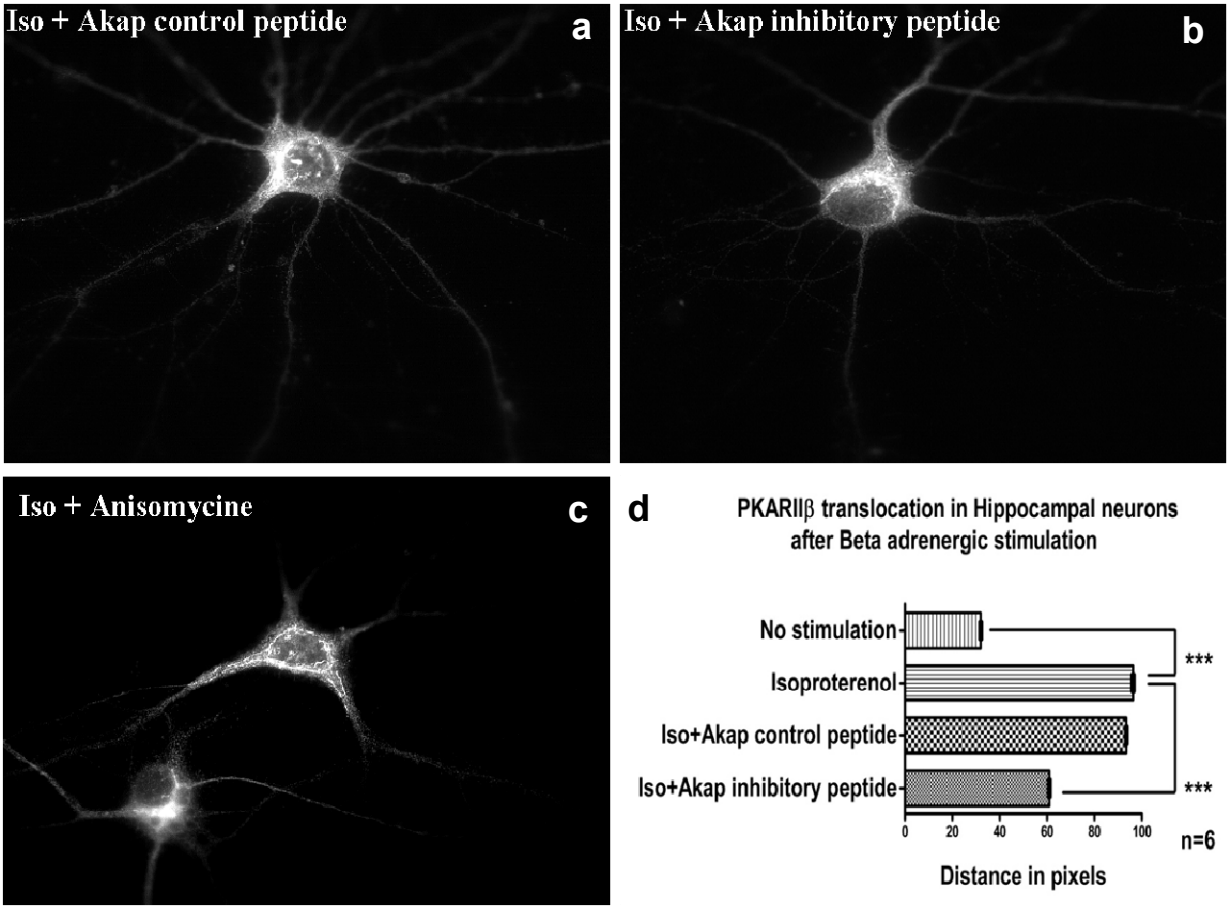

Figure 25. PKA translocation after β-AR stimulation is dependent on AKAPs in hippocampal neurons. Ten days old hippocampal cultures were treated for 5 minutes with **(a)** 50 µM Isoproterenol in combination with 50 µM control peptide AKAP St-Ht31**, (b)** 50 µM Isoproterenol in combination with 50 µM AKAP St-Ht31 inhibitory peptide and **(c)** 50 µM Isoproterenol in combination with 7.5 µM Anisomycine. The cells were then fixed and immunostained with PKARIIβ antibody. Note that PKA is still translocated to proximal dendrites **(a)**, after blocking the association of PKA with AKAPs, translocation is almost completely inhibited **(b)** and anisomycine treatment did not block PKA translocation **(c)**. **(d)** Quantification of translocation experiments using MetaMorph was done by measurement of PKA distance from centre of the soma to dendrites in pixels after different treatments. Data are presented as means ± SEM of several independent experiments. *** = $p<0.0001$, Anova test.

4.4.4 Ternary complex formation by the main components of the β-AR signalling cascade in TC neurons

After stimulation of the β-AR signalling cascade it is assumed that a ternary complex is formed between PKA, AKAP, and $Ca_V1.2$, the formation of which is important for CDI modulation in TC neurons. In order to prove this assumption, we next performed immunocytochemical staining.

Using antibodies specific for rabbit α $Ca_V1.2$ (1:200, Alomone Labs) (Fig. 26a), goat α AKAP 150, (1:200, Santa Cruz) (Fig. 26b) and mouse α PKARIIβ (1:500, BD Bioscience) (Fig. 26c), we labelled the respective proteins in 10 days old cultured thalamic neurons. Fluorescence imaging revealed that all three proteins are densely expressed in somatic regions and proximal dendrites of TC neurons. Merged images pointed to rather close spatial association of the three proteins (Fig 26d, merge and enlarged pictures).

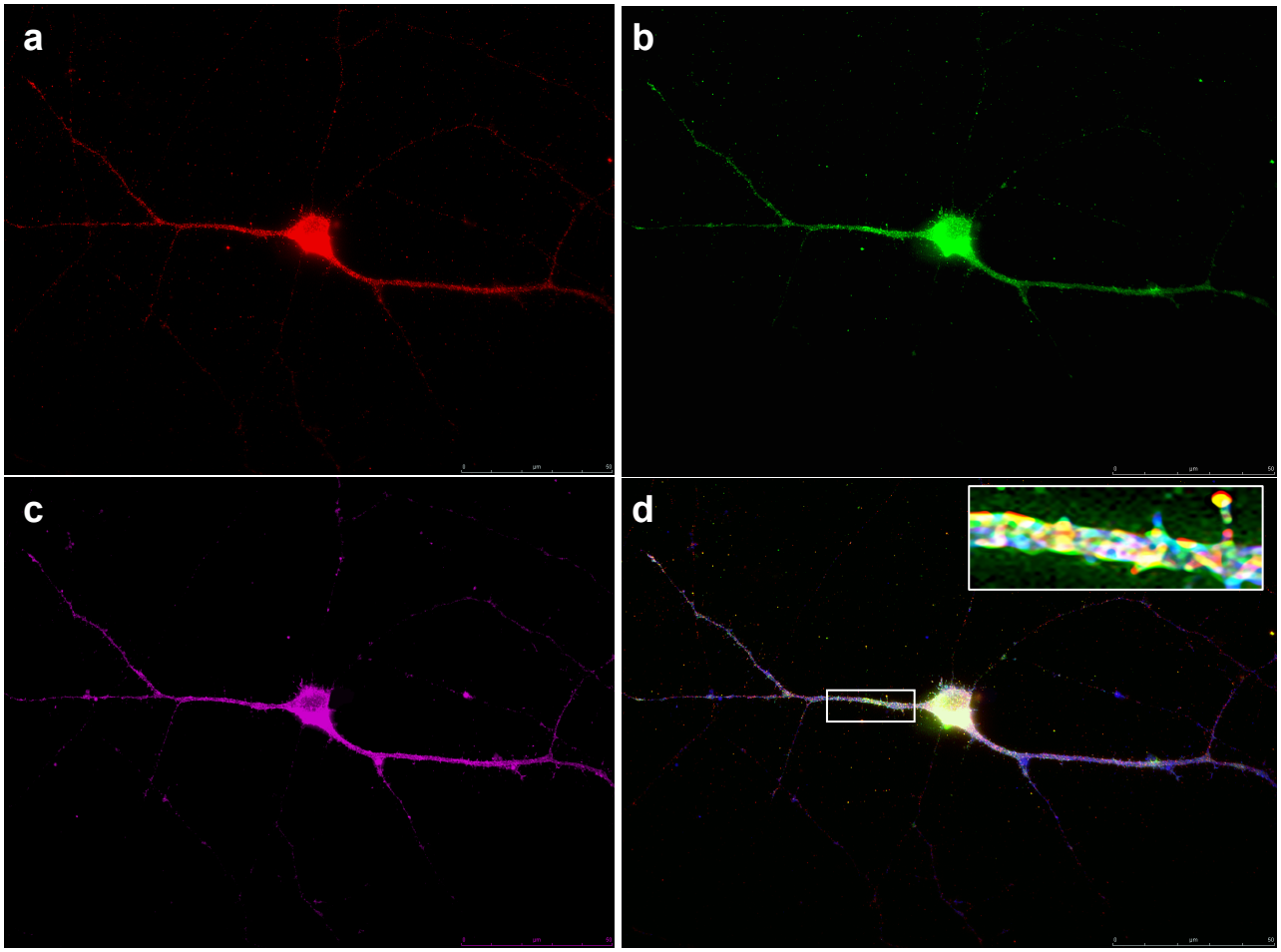

Figure 26. **Localization of $Ca_V1.2$, AKAP 150 and PKARIIβ in cultured TC neurons.** (**a, b, c**) Immunocytochemical analysis of primary cultures of the dorsal thalamus using $Ca_V1.2$- (**a**) AKAP150- (**b**) and PKARIIβ- specific antibodies (**c**). (**d**) Merged picture shows the close connection of the components of the proposed ternary complex, especially in somatic regions and proximal

dendrites. Enlarged inlay represents a magnification of the area indicated by the rectangle. Data shown are representative pictures from several independent immunostainings and preparations of neurons. In all cases, omission of primary antibodies resulted without signal (negative control).

To analyze the possible association between PKARIIβ and $Ca_V1.2$, additional immunostaining was performed. The use of appropriate antibodies demonstrated a close spatial proximity of the two proteins in dLGN as well as hippocampal slices (Fig. 27). As judged from the merged pictures, the interaction was more intensive in thalamic regions in comparison to the hippocampus.

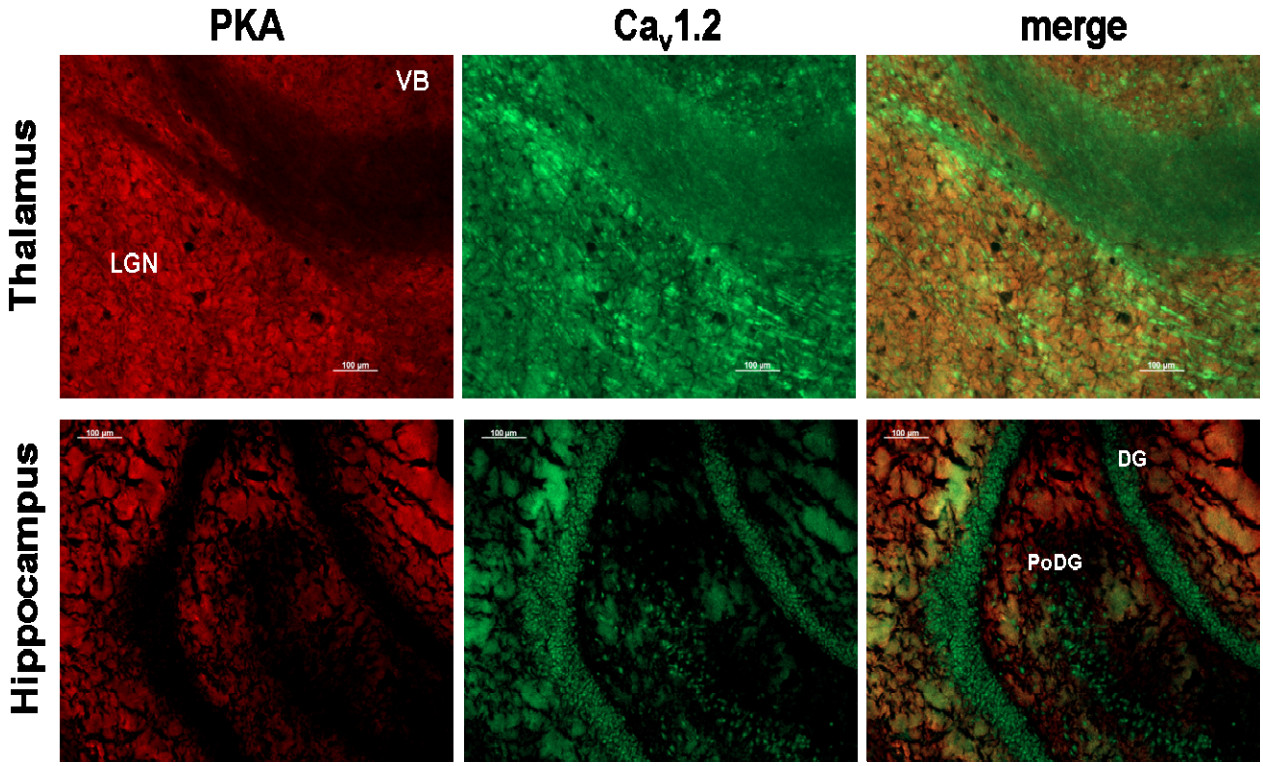

Figure 27. **Localization of $Ca_V1.2$ and PKARIIβ in brain tissues.** Indicated brain regions were immunostained with antibodies specific for PKARIIβ and $Ca_V1.2$. Thalamic regions LGN and VB (ventrobasal thalamic complex) revealed very strong interaction patterns in merged pictures. Association of these proteins is still present in hippocampus but on lower level. DG (dentate gyrus), PoDG (polymorph layer of the dentate gyrus).

As a control, the localization of two other types of calcium channels, namely $Ca_V3.3$ (α1I) and $Ca_V2.1$ (α1A) was investigated in dLGN. All experiments were done in 10 days old thalamic neurons. In the case of $Ca_V3.3$, antibodies against GABA (tissue level) and GAD65 (culture level) were used in order to estimate a cell type-specific expression in interneurons. In the case of $Ca_V2.1$ the neuronal marker MAP2b was used for double staining. It can be seen that $Ca_V3.3$ is predominantly expressed in thalamic interneurons (Fig. 28a-f) as previously described *(Broicher at al., 2007)*. On the

other hand, $Ca_V2.1$ (Fig. 28g-i) is expressed in TC neurons similarly like $Ca_V1.2$ (see Fig. 26a for comparison) but with different pattern. Namely, $Ca_V2.1$ can be found in dendrites that are more distal, beside somatic and proximal dendrites. Moreover, double staining with synaptophysin-specific antibodies revealed $Ca_V2.1$ expression in synaptic regions (data not shown).

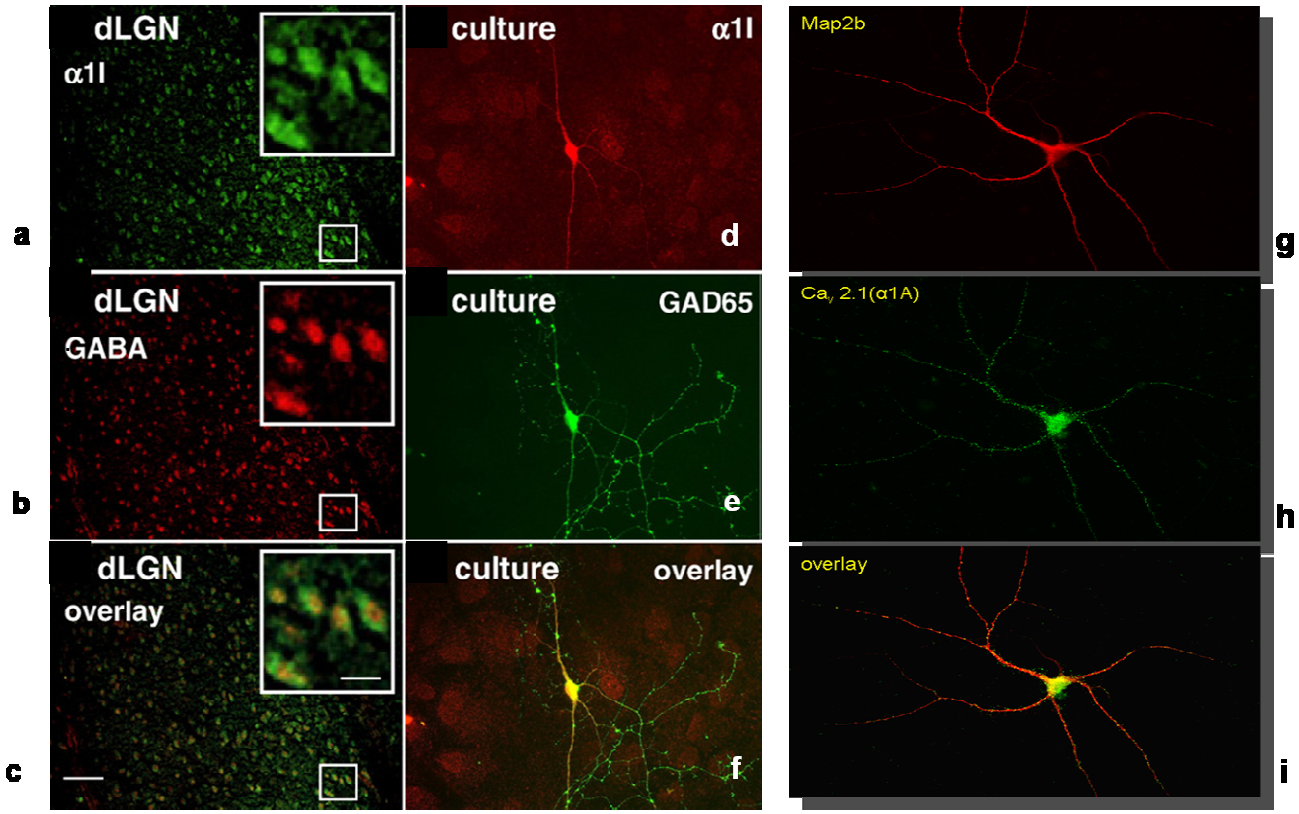

Figure 28. **Expression of $Ca_V3.3$ and $Ca_V2.1$ in thalamus.** Immunocytochemical analysis of thalamic tissue and primary cultures of the dorsal thalamus using $Ca_V3.3$- (**a, d**), GABA- (**b**) or GAD65-specific (**e**) antibodies. Merge pictures (**c, f**) indicated co-expression of calcium channels and markers for interneurons, namely GABA or GAD65. Enlarged inlay represents magnification of the area indicated by the rectangle. (**g, h**) Immunocytochemical analysis of primary cultures of the dorsal thalamus using $Ca_V2.1$- **(g)** and MAP2b-specific (neuronal marker) **(h)** antibodies. Merge picture (**i**) showed expression of these two proteins in somatic, proximal and in distal regions of TC neurons. Data shown are representative pictures from several independent experiments. In all cases, omission of primary antibodies resulted in staining without signal (negative control).

4.4.5 Protein-protein interactions between components of the ternary inactivation complex

After gaining evidence for a possible inactivation complex for CDI in TC neurons by means of immunocytochemical staining and probing its functionality by means of whole cell patch clamp experiments, we next tested the possibility of direct interactions between components of the proposed complex. Standard pull down assays showed interaction between two important molecules for

modulation of CDI in TC neurons, namely PKARIIβ and AKAPs. As shown in Fig. 29, Western blot analysis after pull down assays revealed the existence of direct interactions between the catalytic subunit β of PKA (PKAcsβ) and AKAP7 (Fig. 29a), regulatory subunit β (PKARIIβ) and AKAP7 (Fig. 29b) as well as an interaction of PKARIIβ and PKAcsβ (Fig. 29c). Control incubations of samples of interest with the appropriate fusion-protein partner (empty vector) showed no signal in Western blots. These results provided further evidence for a close coupling between PKA and AKAPs in the thalamus. Moreover, indications for an interaction of PKARIIβ and another member of the AKAP family, namely AKAP5, were obtained by immunoprecipitation experiments (IP). For these experiments, magnetic beads coupled to GFP antibody (μMACS™ Epitope Tag) were used to immunoprecipitate GFP-tagged AKAP5 and PKARIIβ. Western blotting using PKARIIβ-specific antibody (1:500, BD Bioscience) was used to identify a potential interacting partner (Fig. 29d). Control incubations of samples of interest (c-myc PKARIIß) with the appropriate fusion-protein partner (empty GFP vector) showed no signal in Western blots (data not shown).

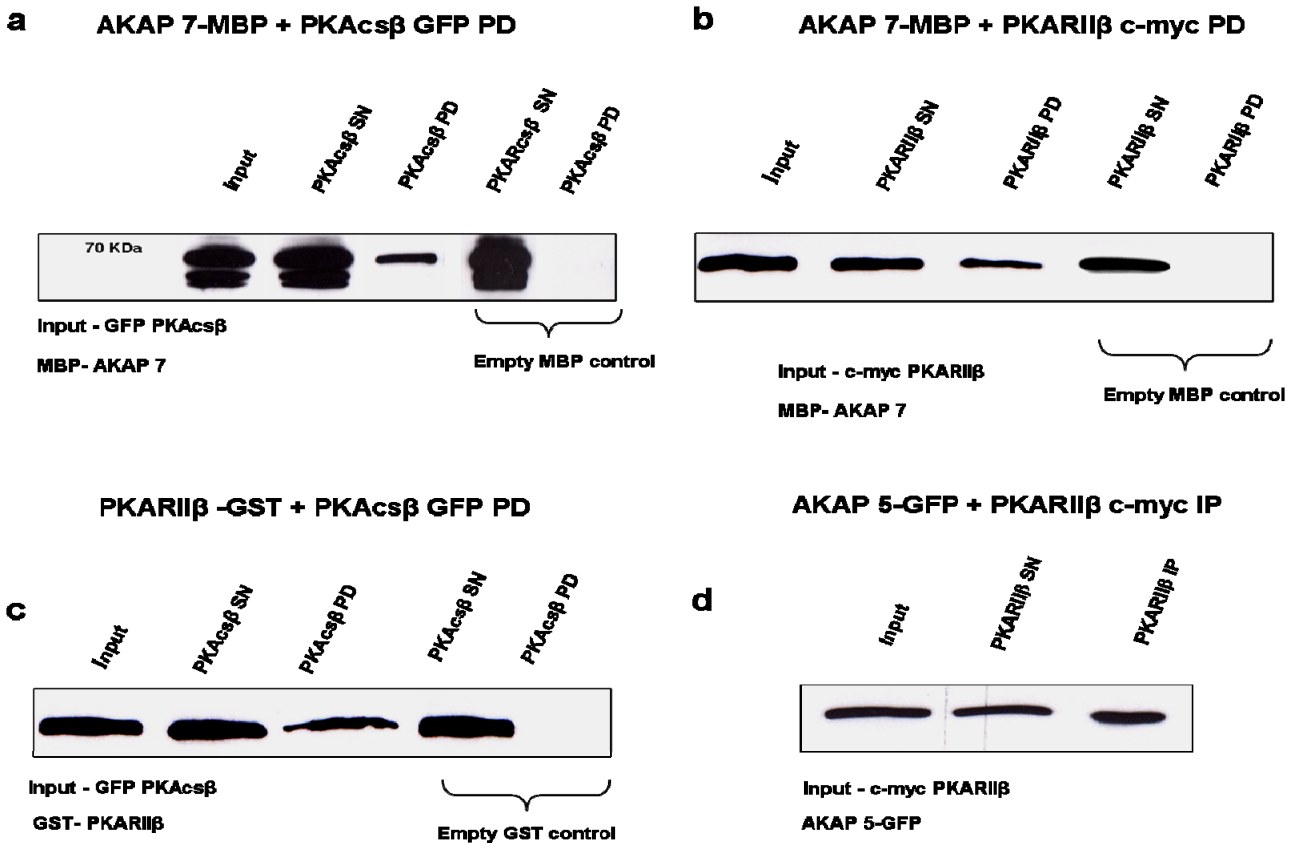

Figure 29. **Interaction partners important for CDI modulation in TC neurons.** Western blot analysis and pull down assays were done as described in "Methods". (**a**) Interaction of AKAP7-MBP and PKAcsβ-GFP was detected using antibodies against GFP protein. (**b**) Interaction of PKARIIβ-c-myc and AKAP7-MBP after detection with antibodies against c-myc. (**c**) Existence of PKA holoenzyme consisting of PKARIIβ-GST and PKAcsβ-GFP was detected with antibodies against

GFP protein. (**d**) IP of PKARIIβ-c-myc and AKAP5-GFP detected after incubation with GFP-coupled magnetic beads using antibodies derived against PKARIIβ.

4.5 Phosphorylation and dephosphorylation processes in modulation of CDI

It has been suggested previously that phosphorylation and dephosphorylation processes might have important roles in the regulation of calcium channels physiology *(Budde at al., 2002)*. In the present study, we focused on the role of these processes in the modulation of CDI in TC neurons after β-AR stimulation. As shown above, PKA is one of the main molecules which phosphorylates $Ca_V1.2$ channels, thereby keeping them in open state (increasing their open probability) and restraining the effects of CDI. Besides this phosphorylation processes that occur after β-AR stimulation, there might be constant dephosphorylation driven by protein phosphatases 1 and 2 (PP1 and PP2). To investigate their role in CDI modulation after β-AR stimulation, additional series of patch clamp experiments were performed on thalamic slices. The β-AR signalling cascade was stimulated while using Okadaic Acid (OA; a well known general inhibitor of protein phosphatases; 10µM, Tocris) alone (Fig. 30a, b), or in combination with Isoproterenol (10 µM; Fig. 30c, d). Figure 30 shows that after blocking dephosphorylation processes, degree of inactivation is even more decreased to 29.3 ± 1.2% (n = 5) in comparison to β-AR stimulation alone (35.7 ± 2%, n = 5). Control cells showed D_{inact} of 40 ± 3.3% in these experiments.

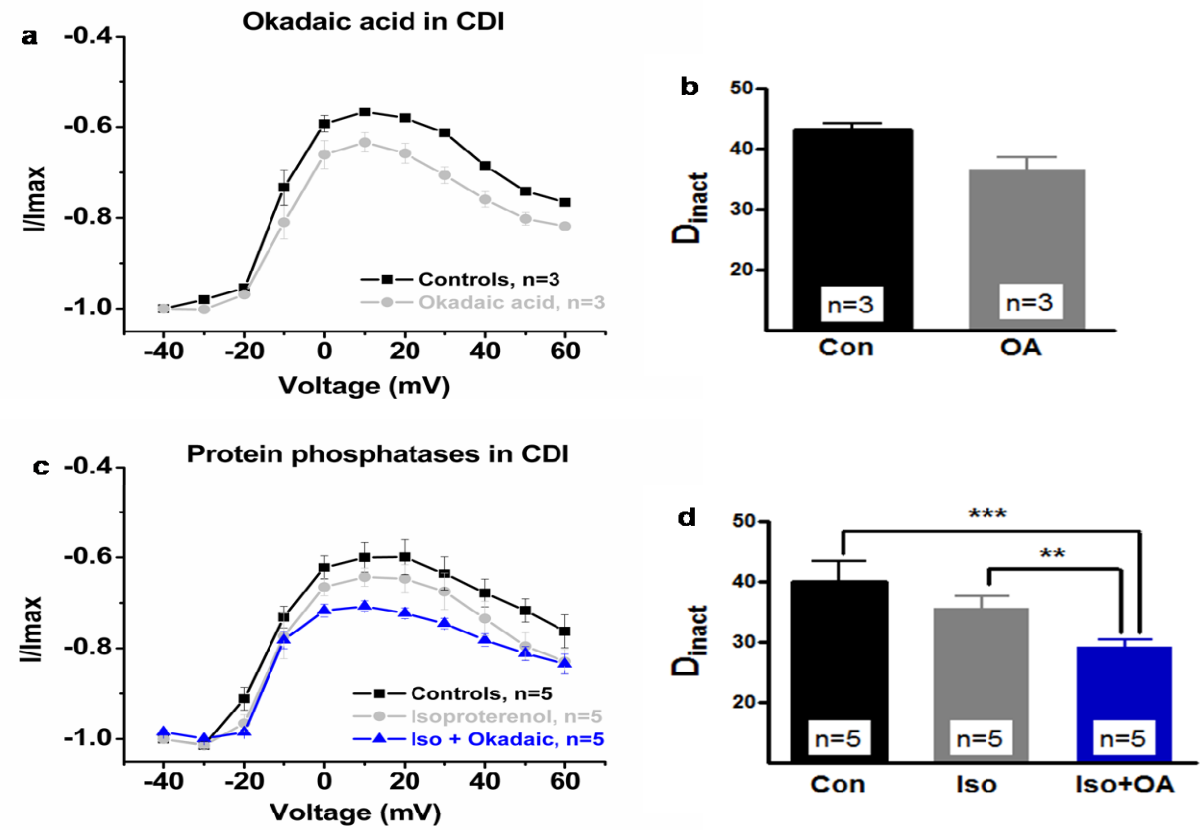

Figure 30. **The role of dephosphorylation processes in CDI modulation of TC neurons.** (**a**) Mean *I-V* relationship of normalized currents evoked by the test pulse under control conditions (filled squares) and in the presence of OA alone (filled circles). **(b)** Bar graphs represent test current peak amplitudes in relation to the control current (black bar are controls, grey are Isoproterenol). (**c**) Mean *I-V* relationship of normalized currents evoked by the test pulse under control conditions (filled squares) in the presence of Isoproterenol alone (filled circles, gray line) or in combination with OA (filled triangles, blue line). **(d)** Bar graphs represent test current peak amplitudes in relation to the control current (black bar are controls, grey are Isoproterenol and blue Isoproterenol plus OA). Data are presented as means ± SEM of several independent experiments. ** = $p<0.01$; *** = $p<0.001$. Significance of Isoproterenol versus Isoproterenol plus OA and Isoproterenol plus OA versus control was calculated by Student's t test.

Next, the specific expression and localization of PP2A enzyme in 10 days old cultured thalamic neurons was investigated by means of double immunostaining. Using an antibody for PP2A (1:500, Acris) (Fig. 31b) in combination with $Ca_V1.2$ (1:200, Alomone Labs) (Fig. 31a), the expression of both proteins was detected. PP2A as well as $Ca_V1.2$ were mainly localized in somatic region and proximal dendrites of TC neurons (Fig. 31c). Merged pictures pointed to a rather close spatial arrangement.

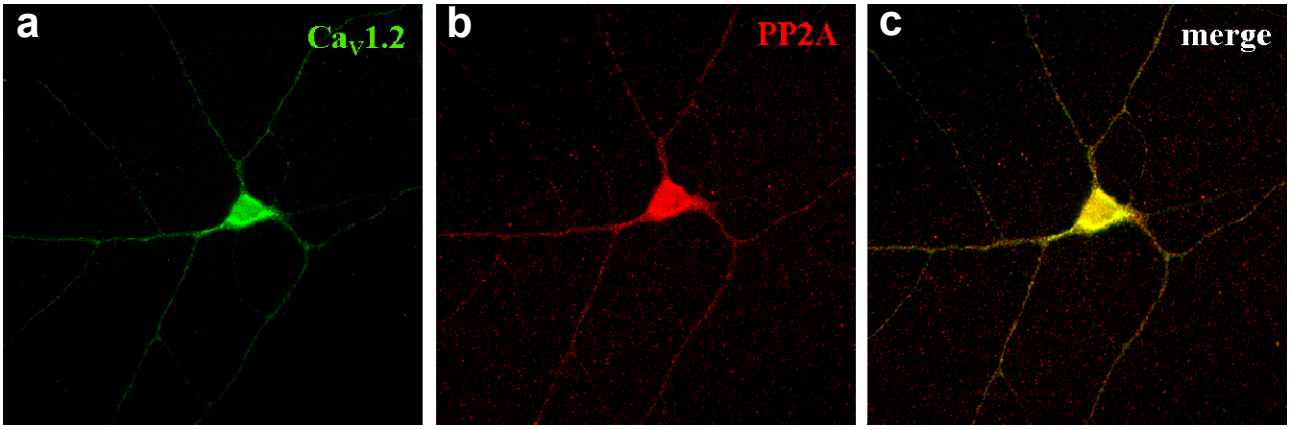

Figure 31. **Localization of $Ca_V1.2$ and PP2A in cultured TC neurons.** (**a, b, c**) Immunocytochemical analysis of primary cultures of the dorsal thalamus using $Ca_V1.2$- (**a**) and PP2A-specific antibodies (**b**). (**c**) Merge picture showed close association of the two proteins, especially in somatic regions and proximal dendrites. Data shown are representative pictures from several independent immunostainings and thalamic neurons preparations. In all cases, omission of primary antibodies resulted in staining without signal (negative control).

4.6 Role of the cytoskeleton in modulation of CDI in TC neurons

Scaffold molecules, such as the AKAPs, have been shown to orchestrate the binding of GPCRs to protein kinases, protein phosphatases and cytoskeletal elements. To test the role of the cytoskeleton in CDI, agents that act on microfilaments (cytochalasin D, Tocris) and microtubules (taxol and colchicine, Tocris) were applied. When the cytoskeletal stabilizer taxol (5 µM) and the β_2-AR agonist Salmeterol (10 µM) were applied together, the decrease of inactivation (40.7 ± 0.5%, n =

3) was comparable to control conditions (43.7 ± 1%, n = 4). Salmeterol alone reduced D_{inact} to 34.5 ± 0.3% (n=4; Fig. 32a, c). Colchicine (100 µM) had a similar effect on D_{inact} (data not shown). The actin microfilament disrupter cytochalasin D (50 µM) also significantly influenced D_{inact} after stimulation of β-ARs by Salmeterol. Similarly to microtubules, data showed that microfilaments were also important in modulation of CDI of TC neurons since D_{inact} was decreased to 39 ± 2.1% (n = 4; Fig. 32b, c). Together, these data indicated that agents interfering with the normal ability of the cytoskeleton for self-sustained reconstruction are one important element for CDI modulation after β-AR stimulation in TC neurons.

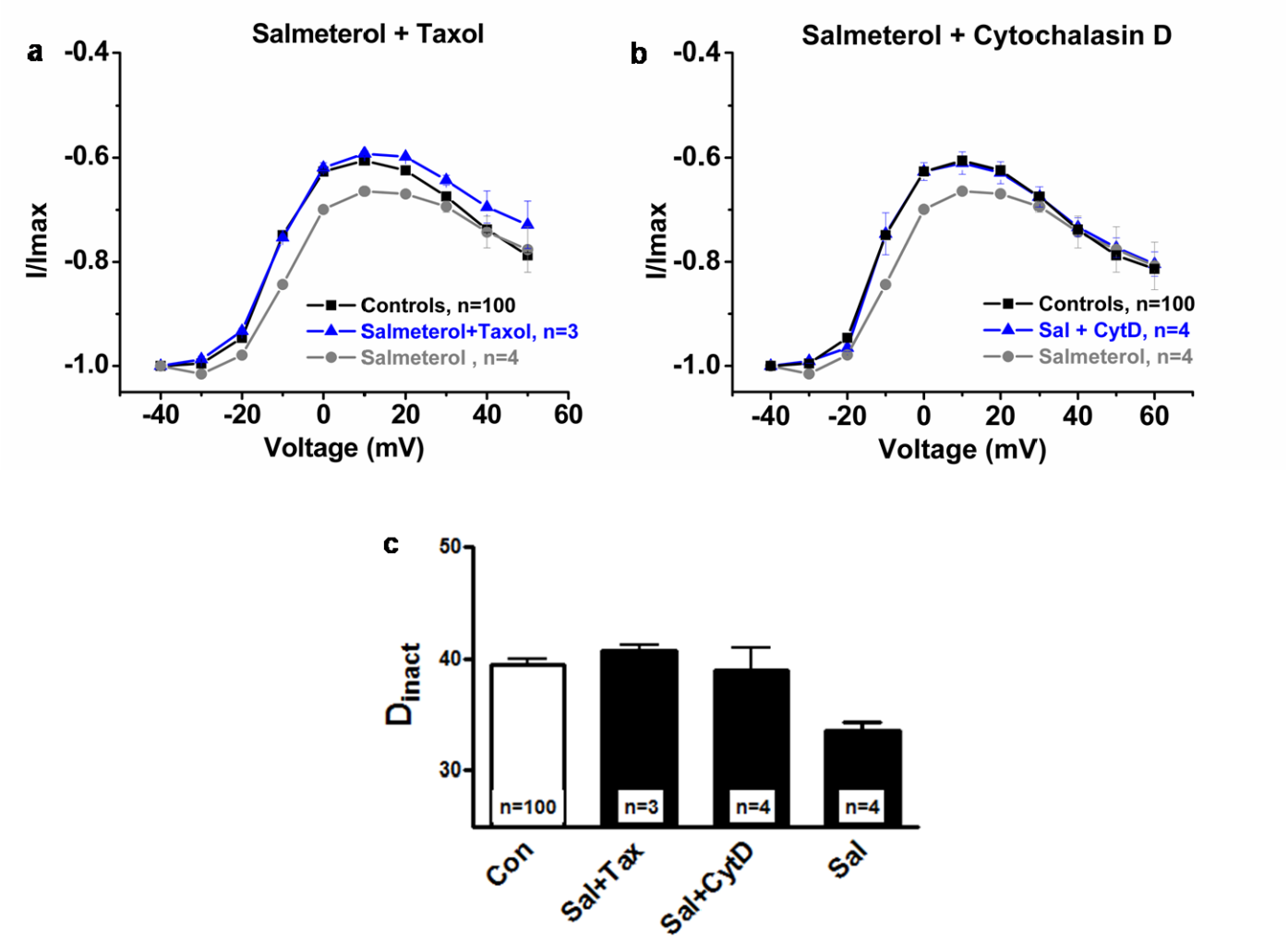

Figure 32. **Involvement of the cytoskeleton in CDI of TC neurons.** (**a**) Mean *I-V* relationship of normalized currents evoked by the test pulse under control conditions (filled squares), in the presence of specific β_2-AR agonist Salmeterol alone (filled circles) or in combination with Taxol (filled triangles, blue line). (**b**) Mean *I-V* relationship of normalized currents evoked by the test pulse under control conditions (filled squares), in the presence of specific β_2-AR agonist Salmeterol alone (filled circles) or in combination with Cytochalasin D (filled triangles, blue line). **(d)** Bar graphs represent test current peak amplitudes in relation to the control current. Data are presented as means ± SEM of several independent experiments. Since no paired statistical tests were possible for experiments with

intracellular substance application, the mean value of 100 cells recorded under control conditions was taken for comparison.

4.7 Role of calcium binding proteins in CDI

Recently important roles of the calcium binding proteins calmodulin, calbindin, calretinin, and parvalbumin in CDI have been shown *(Meuth et al., 2005)*. Therefore, we here addressed the calcium binding protein caldendrin (CDD) *(Seidenbecher et al., 1998)* as a possible molecule involved in modulation of CDI in TC neurons after β-AR stimulation. We looked for localisation of CDD (Fig. 33b) in cultured TC neurons with respect to $Ca_V1.2$ (Fig. 33a). The use of specific antibodies for CDD (1:200) and $Ca_V1.2$ revealed co-expression of the two proteins in somatic and proximal dendrites regions of TC neurons (Fig. 33c).

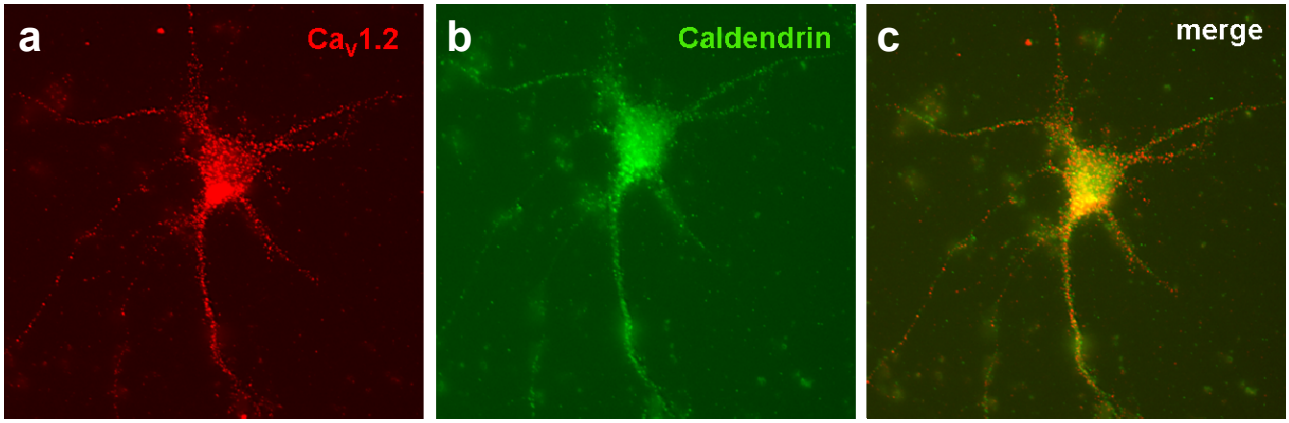

Figure 33. **Localization of $Ca_V1.2$ and caldendrin in cultured TC neurons.** (**a, b, c**) Immunocytochemical analysis of primary cultures of the dorsal thalamus using $Ca_V1.2$- (**a**) and CDD-specific antibodies (**b**). (**c**) Merge picture showed close association of the two proteins especially in somatic regions and proximal dendrites. Data shown are representative pictures from several independent immunostainings and thalamic neurons preparations. In all cases, omission of primary antibodies resulted in staining without signal (negative control).

Finally, we looked for the possible interaction of caldendrin with AKAPs as one of the major molecules that provide translocation of PKA to sites close to $Ca_V1.2$. After performing pull down assay with CDD without tag and AKAP 7-GST as one of the members of the AKAP family of proteins, we detected for the first time a clear interaction between these two proteins using a caldendrin antibody (Fig. 34). Interaction of CDD with an empty GST vector (negative control) resulted in no Western blot signal. Taken together, these data suggested that the Ca^{2+} binding protein CDD might play a role as a linker protein between AKAPs and $Ca_V1.2$ in CDI modulation. However, more experiments have to be performed to directly look for possible role of CDD in CDI modulation of L-type of Ca^{2+} channels.

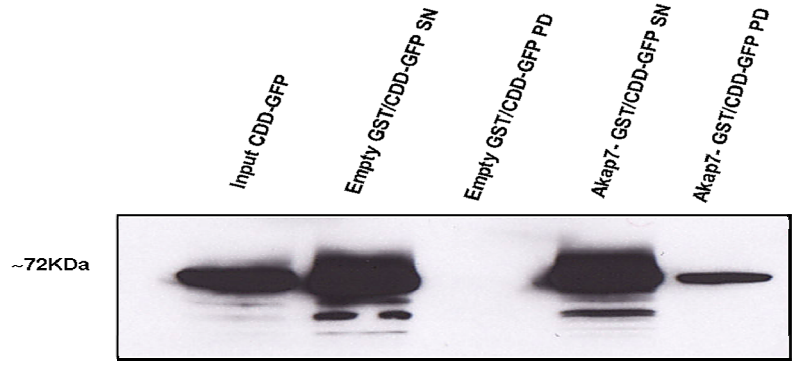

Figure 34. **Interaction between AKAPs and CDD.** Western blot analysis after pull down assay of AKAP7-GST and caldendrin detected using antibody against CDD. Control experiments (empty GST in combination with CDD) were without signal.

5. Discussion

In the present study, we provided for the first time evidence for the negative feedback of intracellular Ca^{2+} release on CDI of HVA Ca^{2+} channels and for the modulation of this negative feedback mechanism by β-AR signalling in central neurons. Moreover, we observed a new interaction between caldendrin and AKAPs which may be of potential interest for the regulation of calcium channels physiology. The results of the present study can be summarized as follows: (i) Classical double pulse protocols reveal the occurrence of CDI in TC neurons in the slice preparation. (ii) Activators and inhibitors of CICR increase and decrease the degree of CDI, respectively. (iii) Inhibition of store-operated Ca^{2+} influx reduces the degree of CDI. (iv) Trains of action potential-like stimuli induce an ER-dependent reduction in HVA Ca^{2+} current amplitude. (v) $Ca_V1.2$ and RyR2 channels are in close proximity near the plasma membrane of identified TC neurons. (vi) β_2-ARs mediate the adrenergic modulation of CDI in TC neurons. (vii) Blocking of PKA completely suppresses the occurrence of CDI in TC neurons**.** (viii) AKAPs play a crucial role in CDI modulation and in translocation of PKA to sites close to $Ca_V1.2$. Moreover, blocking of the interaction between AKAPs and PKA significantly reduces CDI and translocation of PKA. (ix) Phosphorylation - dephosphorylation processes strongly interfere with CDI in TC neurons. (x) Disrupters and modulators of the cytoskeleton significantly reduce the abilities of the cell to modulate CDI. (xi) Calcium binding proteins have a great potential to specifically modulate CDI in TC neurons after β-AR signalling.

5.1 CDI in TC neurons

Previous studies have demonstrated the existence of CDI of HVA Ca^{2+} currents in TC neurons using the acutely isolated cell preparation *(Meuth et al., 2001; Meuth et al., 2002; Meuth et al., 2005)*. Based on these findings, the basic features of CDI in TC neurons can be defined as follows: (i) The degree of inactivation is 35 - 40% under control conditions; (ii) Both, L-type and Q-type Ca^{2+} channels are governed by CDI; (iii) CDI is influenced by a number of cellular mechanisms including repetitive neuronal activity, phosphorylation and dephosphorylation, Ca^{2+}-binding proteins, and the cytoskeleton. The present study adds to these findings by demonstrating an influence of intracellular Ca^{2+} release on the degree of CDI. While an advantage of the acutely isolated cell preparation is that HVA Ca^{2+} currents show little run down *(Budde et al., 1998)*, cells are devoid of most of their dendritic tree and synaptic connections. Therefore, in this study we used the thalamic slice preparation and confirmed the occurrence of CDI in TC neurons by using classical double pulse

protocols *(Eckert & Tillotson, 1981)*. Similar to our previous findings, we found a degree of CDI between 35 - 40% under control conditions. Quantification of the degree of CDI may be corrupted by the occurrence of run-down of HVA Ca^{2+} currents and a partial U-shape of the test pulse *I-V*. However, since a reduction of the driving force of Ca^{2+} currents has no influence on the degree of CDI in TC neurons in slices (this study) and after acute isolation *(Meuth et al., 2001)*, an influence of run-down on the inactivation process seems unlikely. The partial U-shape of the inactivation curve may be explained by two different mechanisms: (i) Incomplete removal of Ca^{2+} from the cytoplasm between voltage steps would be in agreement with the slow Ca^{2+} transients found with the low affinity and high capacity Ca^{2+} binding conditions (1.1 mM EGTA, 10 mM citrate) used in the present study *(Meuth et al., 2002)*. (ii) The partially U-shaped curve is consistent with the dominance of VDI over CDI at strongly depolarized potentials *(Hadley & Hume, 1987)*. However, the shift in hysteresis from the most depolarized potentials to the most hyperpolarized potentials of the inactivation curve with a reversed order of the conditioning pulses votes against the latter alternative.

5.1.1 Interaction between CICR and CDI

The release of Ca^{2+} from intracellular stores, based on the activation of RyR by Ca^{2+} influx through closely connected L-type Ca^{2+} channels, is a prototypical feature of Ca^{2+} signalling in cardiac cells and neurons *(Berridge et al., 2000)*. In ventricular myocytes a significant fraction of CDI depends on CICR, and is therefore termed CICR-dependent CDI *(Grantham & Cannell, 1996; Takamatsu et al., 2003)*. The negative feedback of intracellular Ca^{2+} release on CDI in TC neurons that we have demonstrated in this study is therefore in good agreement with the detection of RyR2 and $Ca_V1.2$ in TC neurons and dLGN tissue by specific fluorescent blockers *(Budde et al., 1998)* and antibodies *(Budde et al., 2000; Meuth et al., 2001)*.

In a previous study on isolated TC neurons it was assumed that 10 mM of the low affinity Ca^{2+} buffer citrate interfered with intracellular signalling in a way that Ca^{2+} entry via the plasma membrane and subsequently via the ER were separated in time *(Meuth et al., 2002)*. While this may be indeed true for fluorescence measurements of bulk intracellular Ca^{2+} levels *(Budde et al., 2000)*, the results of the present study demonstrate a clear contribution of CICR to CDI. These findings point to a very close spatial arrangement of HVA channels and RyRs that allows Ca^{2+} released from the ER to exert a feedback inhibition of Ca^{2+} entry via the plasma membrane very locally even in the presence of moderate exogenous Ca^{2+} buffering. Furthermore, in addition to the clustering of L-type Ca^{2+} channels on the plasma membrane of TC neurons *(Budde et al., 1998)*, spatial spread of CICR across the ER may contribute to the fact that signs of a shell mechanism for CDI have been found in TC neurons *(Meuth et al., 2001)*.

5.1.1.1 Possible functional relevance of HVA Ca^{2+} channels and CICR-dependent CDI

It has been suggested earlier that HVA Ca^{2+} channels and their inherent CDI process are most relevant for neuronal activity of dLGN TC neurons seen during depolarized membrane states, including tonic firing of action potentials, plateau-like depolarizations evoked by optic tract stimulation during early development, and fast high-threshold oscillations *(Pedroarena & Linas, 1997; Lo et al., 2002; Pape et al., 2004)*. Indeed, tonic action potential firing *(Budde et al., 2000)* as well as repetitive activation of HVA Ca^{2+} currents *(Meuth et al., 2002)* induces an increase in the intracellular Ca^{2+} concentration which follows a saturating hyperbolic function, thereby pointing to the Ca^{2+} limiting influence of CDI (in combination with VDI). The present findings add to this notion by demonstrating that tonic stimulation with action potential-like voltage steps induces a decrease in HVA Ca^{2+} current amplitude which is partially depending on CICR. Therefore, the close functional (and spatial) coupling between Ca^{2+} entry via HVA Ca^{2+} channels, CICR, CDI, and refilling of intracellular Ca^{2+} stores tightly controls intracellular Ca^{2+} levels and thus Ca^{2+}-dependent processes. It is interesting to note that caffeine-induced oscillations of intracellular Ca^{2+} levels in sympathetic ganglia cells are based on a similar combination of Ca^{2+} signalling tools, namely CICR, Ca^{2+}-dependent inactivation of plasma membrane Ca^{2+} influx, and two types of Ca^{2+} pumps *(Cseresnyes et al., 1999)*.

In summary, our findings from this part of the present study indicate that CDI in TC neurons is partially under the control of CICR thereby pointing to a cross-signalling between L-type Ca^{2+} channels and RyRs which controls the amount of Ca^{2+} influx during neuronal activity.

5.1.2 β-AR stimulation and modulation of CDI of $Ca_V1.2$ via phosphorylation and dephosphorylation processes

In the present study, we demonstrated that stimulation of β-ARs which leads to phosphorylation of Ca^{2+} channels in cAMP-dependent manner via PKA activation, significantly reduced degree of inactivation of L-type Ca^{2+} channels. The same results were obtained when channel dephosphorylation was inhibited. This indicates that phosphorylation keeps L-type Ca^{2+} channels in a state of high open probability, willing to open during depolarization *(You et al., 1995)*. The modulation of L-type Ca^{2+} channels through phosphorylation via different second messenger systems is well established, and includes phosphorylation by PKA and CaM kinase II *(for review, see Catterall, 1997; Rossie, 1999)*. Both types of modulation result in an increase in peak current amplitude *(Sculptoreanu et al., 1993; Xiao et al., 1994)*. Furthermore, CDI has been shown to be reduced by activation of cAMP-dependent phosphorylation *(Kalman et al., 1988; You et al., 1995; Meuth et al., 2002)*. Therefore, both the increment in HVA Ca^{2+} current amplitude and the reduction

of CDI after β-AR stimulation observed in the present study are consistent with a phosphorylation of L-type Ca^{2+} channels by PKA.

Ser1928 of the α1C L-type Ca^{2+} channel $Ca_V1.2$ is an important possible target of PKA activity in heart and brain *(Hulme et al., 2006; Hall et al., 2006; Davare et al., 2000)*. However, it has been recently shown that mutation of Ser1928 of cardiac L-type of Ca^{2+} channels has no effect on phosphorylation after β-AR stimulation *(Lemke et al., 2008)*, meaning that additional phosphorylation sites most probably exist *(Ganesan et al., 2006; Lemke et al., 2008)*. On the other hand, meaningful regulation of channel activity by PKA phosphorylation requires a proper balance with dephosphorylation processes. Several studies have shown in hippocampal neurons that protein phosphatases like PP2A, PP1 and calcineurin directly and stable bind to the C-terminal region of $Ca_V1.2$ *(Davare et al 2000; Hall et al., 2006; Oliveria et al., 2007)*. Moreover, the whole signalling pathway from β-AR to the $Ca_V1.2$ channel, including G-proteins, adenylate cyclase, PKA and the counterbalancing protein phosphatases, forms a closely associated protein complex in the forebrain *(Davare et al., 2001)*. However, the role of this complex in context of CDI modulation has not been addressed by this group yet. $Ca_V1.2$ channels are expressed in thalamocortical relay neurons *(Meuth et al., 2001)* and the existence of β-ARs coupled positively to adenylate cyclase in these neurons has been shown *(McCormick, 1992)*. Moreover, our group demonstrated previously an effect of calyculin A, which is a blocker of PP1 and PP2A *(Herzig & Neumann, 2000)* on CDI and Ca^{2+} current amplitude in TC neurons (*Meuth et al., 2002*). The present study confirmed the expression of $Ca_V1.2$ channels in thalamocortical relay neurons and obtained further evidence about the expression and involvement of a specific types of β-ARs, namely β_2-AR, in CDI modulation. Furthermore, this study adds to previous findings that Okadaic acid, which is known to block protein phosphatases, has a significant effect on CDI in TC neurons after β-AR stimulation. From our data, it is therefore reasonable to conclude that PKA and protein phosphatases antagonistically modulate CDI of $Ca_V1.2$ channels in TC neurons by phosphorylation and dephosphorylation processes.

Although our experiments with Okadaic acid demonstrated the role of dephosphorylation processes in modulation of CDI after β-AR stimulation in TC neurons, the specific type of phosphatase involved in TC neurons is still not clear. The original model of CDI in *Helix aspersa* included a dephosphorylation cycle by calcineurin (PP2B) as the fundamental step leading to channel closure *(Chad & Eckert, 1986)*. Later, evidence for and against an involvement of calcineurin was found *(Branchaw et al., 1997; Schuhmann et al., 1997; Victor et al., 1997; Lukyanetz et al., 1998; Burley & Sihra, 2000; Zeilhofer et al., 2000; Oliveria et al., 2007)*. In TC neurons, dephosphorylation by calcineurin boosts CDI, a conclusion that is corroborated by the effect of ascomycin, an inhibitor of calcineurin *(Kawai et al., 1993; Meuth et al., 2002)*, and the finding that calcineurin is expressed in dLGN *(Meuth et al., 2002)*. Although these observations clearly indicate a modulation of CDI by calcineurin in TC neurons, the inactivation process itself is probably not a dephosphorylation reaction.

In addition, the role of calcineurin on CDI after β-AR stimulation in TC neurons remains elusive, leaving some space for future studies.

5.1.2.1 Scaffold proteins like AKAPs specifically bind to the $Ca_V1.2$ and modulate channel after β-AR stimulation

$Ca_V1.2$ L-type Ca^{2+} channels can physically associate with either AKAP79/150 (AKAP5) or AKAP15/18 (AKAP 7) through a modified leucine zipper interaction *(Oliveria et al., 2007; Hulme et al., 2003)*. Both, the modulation of channels and its downstream signalling depend upon the identity of the associated AKAPs. Although both of these AKAPs target PKA to the channel, AKAP79/150 also targets calcineurin and thereby confers unique characteristics upon AKAP79/150-complexed L-type channels in neurons *(Oliveria et al., 2007)*. AKAP79/150 is the major AKAP protein in neurons, where it is widely distributed and has been shown to anchor protein kinases and other signaling proteins to multiple receptors and ion channels *(Bauman et al., 2004)*. For example, AKAP79/150 recruits PKA and calcineurin to the AMPA receptor *(Colledge et al., 2000)*, it associates with $Ca_V1.2$ *(Hall et al., 2007)* in neurons, it recruits PKA and calcineurin to the channel and is necessary for the β-AR stimulation of L-type calcium currents *(Davare et al., 2001; Bauman et al., 2004; Hall et al., 2007)* as well as for the L-type calcium current-mediated activation of the transcriptional regulator NFATc4 *(Oliveria et al., 2007)*. Moreover, colocalization with $Ca_V1.2$ and PSD (postsynaptic density) proteins in dendritic spines of hippocampal neurons *(Di Biase et al., 2008)* has been shown. Three different binding sites for AKAP79/150 were described in the N terminus, the cytoplasmic loop connecting repeats I and II, and in the C terminus of $Ca_V1.2$ *(Hall et al., 2007)*. The C-terminal leucine zipper was shown to be essential for AKAP binding and for β-AR stimulation and reversible phosphorylation of $Ca_V1.2$ in heart muscle and in neurons *(Hulme et al., 2003; Oliveria et al., 2007)*. Mutation of the three basic residues of this motif blocked AKAP79/150 and PKA binding and phosphorylation of the Ca^{2+} channel in response to β-AR stimulation *(Oliveria et al., 2007)*. Moreover, mutation of known binding sites on $Ca_V1.2$ for scaffold proteins AKAPs and PSD proteins did not change membrane expression of the $Ca_V1.2$ channel subunit *(Di Biase et al., 2008)*. This means that binding of these proteins is necessary for the regulation of $Ca_V1.2$ after β-AR stimulation but on the other hand does not have influence on membrane localization of $Ca_V1.2$.

Based on these previous findings, we hypothesized that AKAPs might also have an important function in regulation of CDI after β-AR stimulation in TC neurons. According to our model, after stimulation of β-AR adenylate cyclase gets activated via G proteins and produces cAMP which then activates PKA. With support of AKAPs, PKA targets its final effector, the $Ca_V1.2$ channels and phosphorylates them (see Figure 5 & 11). In the present study we demonstrated that blocking the binding of AKAPs to PKA significantly reduces CDI. Moreover, under similar conditions we showed

for the first time that PKA phosphorylation of $Ca_V1.2$ and translocation of this enzyme close to the channel depends on binding of PKA and AKAPs in hippocampal neurons. We believe that very similar processes occur in TC neurons. Moreover, our study directly confirmed an interaction between AKAPs and PKA in pull down assay and demonstrated that after stimulation of the β-AR signalling cascade a ternary complex is formed between PKA, AKAP, and Ca^{2+} channel $Ca_V1.2$ and that the formation of this complex is important for CDI modulation in TC neurons. Moreover, as mentioned before, AKAP79/150 also targets calcineurin which is able to activate protein phosphatase PP1 *(Guerini, 1997)* and therefore might have multiple function in regulation of CDI by influencing both phosphorylation by PKA and dephosphorylation processes.

5.1.2.2 Cytoskeleton, calcium binding proteins, and CDI upon activation of the β-AR signalling cascade

The cytoskeleton is a filamentous network of F-actin, microtubules and intermediate filaments and regulation of transmembrane ion flux is one of its important roles in cell signalling *(Janmey, 1998)*. Results obtained from experiments in molluscan neurons *(Johnson & Byerly, 1993)*, hippocampal pyramidal neurons *(Johnson & Byerly, 1994)* and TC neurons *(Meuth et al., 2005)* have suggested that the cytoskeleton is involved in CDI. Although the transduction mechanism coupling the cytoskeleton to CDI is not fully understood and seems to differ between different cell types, Ca^{2+}-dependent destabilization of cytoskeletal elements that have a structural relationship to the channel protein has been suggested *(Beck et al., 1999)*. Cytoskeletal stabilizers reduced CDI in TC neurons. The microtubule stabilizer taxol was more effective than the microfilament stabilizer phalloidin, indicating that both cytoskeletal components are not involved equally in CDI *(Meuth et al., 2005)*. These data are in agreement with a model in which microtubules stabilize a microfilament lattice, with the latter probably binding directly to the Ca^{2+} channel complex *(Johnson & Byerly, 1993; 1994)*. In this model the Ca^{2+} sensitivity of Ca^{2+} channels could be mediated by cytoskeletal depolymerization, since both, microtubule and microfilament components of the cytoskeleton, are disrupted by increases in the $[Ca^{2+}]_i$. It is interesting to note that a similar mechanism has been suggested for the Ca^{2+}-dependent reduction of NMDA receptor activity *(Rosenmund et al., 1993)*.

The present study adds to this scenario by demonstrating an important role for the correct organization of the cytoskeleton in terms of regulation and modulation of CDI in TC neurons after β-AR stimulation. The cytoskeleton is supposed to be an organizer of a complex intracellular network and its disruption results in reduction of phosphorylation and finally in reduction of CDI of the $Ca_V1.2$. Moreover, disruption of cytoskeleton most probably alters the normal ability of PKA to bind to the AKAPs and therefore results in significant decrease in translocation of PKA after β-AR stimulation. However, more experiments are needed in order to clarify the uncoupling of CDI from

Ca^{2+} entry during the presence of cytoskeletal stabilizers and corroborate the above model in TC neurons.

It has been shown previously that the introduction of exogenous synthetic Ca^{2+} chelators into relay neurons reduces CDI in TC neurons *(Meuth et al., 2001)*. Moreover, the purified Ca^{2+}-binding proteins like parvalbumin (PV), calbindin (CB) and calretinin (CR) affected CDI differently in these cells *(Meuth et al., 2005)*. While PV and CB reduced CDI significantly, CR had no effect. It is interesting to note that PV, the expression of which was demonstrated in relay neurons, exerts the strongest effect on CDI. The action of PV is most likely based on Ca^{2+} buffering, as PV is generally seen as a pure Ca^{2+} buffer *(Eberhard & Erne, 1994)*. Since CB and CR are believed to function also as Ca^{2+} signalling proteins *(Gander et al., 1996; Hubbard & McHugh, 1995; Maglocky & Freund, 1995)*, the mode of action of CB may be different. Other EF-hand Ca^{2+}-binding proteins (calmodulin (CaM), sorcin) have been shown to associate tightly with Ca^{2+} and K^+ channels *(Meyers et al., 1998; Levitan, 1999; Erickson et al., 2003)*. Furthermore, the finding that rather small amounts of Ca^{2+}-binding proteins are sufficient to disrupt CDI effectively has been described before in hippocampal granule cells, where a low concentration of exogenous CB substantially reduces this type of feedback coupling *(Naraghi & Neher, 1997)*.

There is a longstanding notion that the limiting action of CDI on Ca^{2+} entry through HVA channels depends on CaM. $Ca_V1.2$ channels locally generate large increases in $[Ca^{2+}]_i$, and they also harbor a CaM molecule at an IQ motif near the modified leucine zipper that supports the interaction with AKAP79/150. CaM has been shown to function as the Ca^{2+} sensor for L-type Ca^{2+} channel inactivation, facilitation, and signaling to the nucleus *(Dolmetsch et al., 2001; Erickson et al., 2003; Tillotson, 1979; Zühlke et al., 1999)*. Because of its proximity and established role in L-type Ca^{2+} channel signalling, CaM docked at the IQ motif is an appealing candidate as an activator of anchored calcineurin, although alternatively, other channel associated CaM molecules *(Mori et al., 2004)* may serve this function.

In the present study, the role of another Ca^{2+}-binding protein Caldendrin (CDD) as new candidate for the modulation of CDI after β-AR stimulation in TC neurons was investigated. CDD is a Ca^{2+}-binding protein similar to CaM that is localized in neuroendocrine cells *(Landwehr et al., 2003)* and subpopulations of neurons in the brain and retina *(Seidenbecher et al., 1998; Laube et al., 2002; Shultz et al., 2004)*. Several studies suggested a role of CDD in regulating postsynaptic signal transduction, perhaps in response to neuronal activity *(Seidenbecher et al., 1998; Seidenbecher et al., 2004; Smalla et al., 2003)*. Like CaM, CDD possesses EF-hand Ca^{2+} binding motifs and may regulate the activity of effector molecules in a Ca^{2+}-dependent manner *(Seidenbecher et al., 1998; Haeseleer et al., 2002)*. Although CaM interacts with and modulates numerous ion channels and neurotransmitter receptors *(Jurado et al., 1999; Hoeflich et al., 2002)*, the molecular targets of CDD are largely unknown. CDD is a splice variant of calcium binding protein type 1 (CaBP1) *(Haeseleer et al., 2000)*,

a Ca^{2+}-binding protein that directly regulates voltage-gated Ca^{2+} channels. Like CaM, CaBP1 alters the properties of $Ca_V2.1$ (P/Q-type) and $Ca_V1.2$ (L-type) voltage-gated Ca^{2+} channels *(Lee et al., 2002., Zhou et al., 2005)*. CaBP1 and CaM bind to similar sites in the main α1C-subunit of $Ca_V2.1$ and $Ca_V1.2$, but the functional consequences of these interactions are different. For $Ca_V1.2$, CaM mediates CDI *(Zühlke et al., 1999; Qin et al., 1999)*, while CaBP1 stabilizes channel opening *(Zhou et al., 2004; 2005)*. In a more recent study it was suggested that CDD provides moderate inhibition of CDI and that results from its interactions strictly with the C-terminal IQ-domain of α1C subunit of $Ca_V1.2$ *(Tippens & Lee, 2007)*. The competitive binding of CaM and CDD to the IQ-domain suggest that CDD inhibits CDI by displacing CaM from the IQ-site. Previous reports also indicated a cytoskeletal interaction of CDD, but not CaM, with microtubule-associated proteins, like MAP2b which is a member of AKAP family *(Seidenbecher et al., 2004*). Given that disruption of the cytoskeleton significantly affects CDI of L-type Ca^{2+} channels *(Johnson & Byerly, 1993; Galli & DeFelice, 1994; Meuth et al., 2005)*, CDD could destabilize interactions of $Ca_V1.2$ with cytoskeleton or scaffolding proteins like AKAPs resulting in a decrease of CDI. A potential link of $Ca_V1.2$ with the cytoskeleton or with scaffolding proteins AKAPs through CDD may further distinguish modulation of $Ca_V1.2$ channels by CDD, CaBP1, and CaM.

We have shown in the present study a direct interaction between AKAPs and CDD by using pull down assays. These data gave the basis for a model where CDD interacts with AKAPs (AKAP79/150 and AKAP7) and additionally supports the modulation of CDI via PKA and AKAPs in TC neurons after β-AR stimulation. Moreover, CDD associates with $Ca_V1.2$ in the brain and colocalizes with $Ca_V1.2$ in somatodendritic compartments of isolated hippocampal neurons *(Tippens & Lee, 2007)* and TC neurons (this study). Our results suggest a novel role for the neuron-specific Ca^{2+}-binding proteins in regulating CDI of TC neurons via specific binding with AKAPs and $Ca_V1.2$ Ca^{2+} channels. Namely, CDD is sitting between AKAPs and $Ca_V1.2$ and by binding to both molecules supports AKAPs in translocation of PKA. However, diverse effects of CDD and other calcium binding proteins as modulators of VGCCs, defining their significance in regulating neuronal Ca^{2+} signals remain an important challenge for future studies.

5.2 Functional significance of Ca^{2+} channel phosphorylation after β-AR stimulation

Release of transmitters from a number of brainstem terminals modulates the behavioural states of an individual by depolarizing thalamocortical relay neurons *(McCormick, 1992)*. During states of slow-wave sleep, thalamic relay neurons are hyperpolarized and display rhythmic burst activity *(Steriade et al., 1997)*. During states of wakefulness, these cells are depolarized and display tonic single spike activity, resulting in the faithful transmission of sensory signals through the dorsal thalamus. The shift from burst activity to tonic activity is mediated by increased activity of ascending

brainstem fibres that are thought to increasingly release acetylcholine (ACh), noradrenaline (NA) and serotonin (5-HT) during wakefulness. Both NA via β-receptors and 5-HT via an unknown 5-HT receptor subtype, activate adenylate cyclase *(McCormick, 1992)* in thalamocortical relay neurons and are thus able to positively modulate HVA Ca^{2+} currents.

When attempting to integrate the findings of the present study into the known framework of thalamic physiology it should be taken into account that the recording conditions are not completely physiological with Cs^{+} included in the recording solutions. In addition, the trains of short depolarisations only roughly mimic tonic activity of thalamocortical relay neurons *(Meuth et al., 2002)*. Nevertheless, the tonic activity mode can be assumed to strongly activate HVA Ca^{2+} currents. Furthermore, following release of NA, HVA Ca^{2+} current amplitudes will be increased while CDI is decreased. In addition, tonic sequences of action potentials are coupled to CICR from intracellular stores, further increasing Ca^{2+} entry into TC neurons during wakefulness *(Budde et al., 2000)*. These data indicate a fine-tuned interplay between activity dependent Ca^{2+} influx, intracellular Ca^{2+} pools, and the mode of activity, possibly to enable faithful signal integration and transfer during wakefulness.

Future studies will have to unravel the different modulatory pathways that act upstream from the multiple CDI mechanisms thereby pointing to additional functions of CDI and unraveling further the elusive role of HVA Ca^{2+} channels in thalamic physiology.

6. References:

A

Angelo R., Rubin C.S. Molecular characterization of an anchor protein (AKAPCE) that binds the RI subunit (RCE) of type I protein kinase A from Caenorhabditis elegans. *J. Biol. Chem.*, **273**, 14633–14643 (1998).

Armstrong DL. Calcium channel regulation by calcineurin, a Ca^{2+}-activated phosphatase in mammalian brain. *Trends Neurosci.*, **12**, 117–122 (1989).

B

Bauman A.L., Goehring A.S., Scott J.D. Orchestration of synaptic plasticity through AKAP signaling complexes. *Neuropharmacology*, **46**, 299 –310 (2004).

Beck H., Steffens R., Heinemann U., Elger C.E. Ca^{2+} - dependent inactivation of high-threshold Ca^{2+} currents in hippocampal granule cells of patients with chronic temporal lobe epilepsy. *J Neurophysiol.*, **82**, 946-954 (1999).

Berridge M.J. Neuronal calcium signaling. *Neuron*, **21**, 13–26 (1998).

Berridge M.J., Lipp P., Bootman M.D. The versatility and universality of calcium signalling. *Nature Reviews Molecular Cell Biology*, **1**, 11-21 (2000).

Berridge M.J., Bootman M.D., Roderick H.L. Calcium Signalling: Dynamics, homeostasis and remodelling. *Nature Rev. Mol. Cell. Bio.*, **4**, 517-29 (2003).

Branchaw J.L., Banks M.I., Jackson M.B. Ca^{2+}- and voltagedependent inactivation of Ca^{2+} channels in nerve terminals of the neurohypophysis. *J. Neurosci.*, **17**, 5772-5781 (1997).

Brehm P., Eckert R. Calcium entry leads to inactivation of calcium channel in *Paramecium*. *Science*, **202**, 1203–1206 (1978).

Broicher T., Kanyshkova T., Landgraf P., Rankovic V., Meuth P., Meuth S.G., Pape H.-C., Budde T. Specific expression of low-voltage-activated calcium channel isoforms and splice variants in thalamic local circuit interneurons. *Mol Cell Neurosci.*, **36**, 132-45 (2007).

Budde T., Munsch T., Pape H.-C. Distribution of L-type calcium channels in rat thalamic neurons. *Europ. J. Neurosci.*, **10**, 586-597 (1998).

Budde T., Sieg F., Braunewell K.H., Gundelfinger E.D., Pape H.-C. Ca^{2+}-induced Ca^{2+} release supports the relay mode of activity in thalamocortical cells. *Neuron*, **26**, 483-492 (2000).

Budde T., Meuth S.G., Pape H.-C. Calcium-dependent inactivation of neuronal calcium channels. *Nat. Rev. Neurosci.*, **3**, 873-83 (2002).

Budde T., Caputi L., Kanyshkova T., Staak R., Abrahamczik C., Munsch T., Pape H.-C. Impaired regulation of thalamic pacemaker channels through an imbalance of subunit expression in absence epilepsy. *J Neurosci.*, **25**, 9871-82 (2005).

Burley J.R., Sihra T.S. A modulatory role for protein phosphatase 2B (calcineurin) in the regulation of Ca^{2+} entry. *Eur. J. Neurosci.*, **12**, 2881- 2891 (2000).

C

Catterall W.A. Modulation of sodium and calcium channels by protein phosphorylation and G-proteins. *Adv. Second Messenger Phosphoprotein Res.,* **31**, 159-181 (1997).

Catterall W.A., Striessnig J., Snutch T.P., Perez-Reyes E. International Union of Pharmacology. XL. Compendium of voltage-gated ion channels: calcium channels. *Pharmacol Rev.*, **55**, 579-81. (2003).

Catteral W.A., Perez-Reyes E., Snutch T.P., Striessnig J. International Union of Pharmacology. XLVIII. Nomenclature and Structure-Function Relationships of Voltage-Gated Calcium Channels. *Pharmacol. Rev.*, **57**, 411–25 (2005).

Chad J.E., Eckert R. An enzymatic mechanism for calcium current inactivation in dialysed Helix neurones. *J. Physiol. (Lond.).*, **378**, 31-51 (1986).

Chavis P., Fagni L., Lansman J.B., Bockaert J. Functional coupling between ryanodine receptors and L-type calcium channels in neurons. *Nature*, **382**, 719–722 (1996).

Colledge M., Dean R.A., Scott G.K., Langeberg L.K., Huganir R.L., Scott J.D. Targeting of PKA to glutamate receptors through a MAGUK-AKAP complex. *Neuron*, **27**, 107–119 (2000).

Cseresnyes Z., Bustamante A.I., Schneider M.F. Caffeine-induced [Ca^{2+}] oscillations in neurones of frog sympathetic ganglia. *J Physiol.*, **514 (Pt 1)**, 83-99 (1999).

D

Davare M.A., Horne M.C., Hell J.W. Protein phosphatase 2A is associated with class C L-type calcium channels ($Ca_V1.2$) and antagonizes channel phosphorylation by cAMP- dependent protein kinase. *J. Biol. Chem.*, **275**, 39710-39717 (2000).

Davare M.A., Avdonin V., Hall D.D., Peden E.M., Burette A., Weinberg R.J., Horne M.C., Hoshi T., Hell J.W. A β_2 adrenergic receptor signalling complex assembled with the Ca^{2+} channel $Ca_V1.2$. *Science*, **293**, 62-3 (2001).

Dell'Acqua M.L., Scott J.D. Protein kinase A anchoring. *J. Biol. Chem.*, **272**, 12881–12884 (1997).

DeMaria C.D., Soong T.W., Alseikhan B.A., Alvania R.S., Yue D.T. Calmodulin bifurcates the local Ca^{2+} signal that modulates P/Q-type Ca^{2+} channels. *Nature*, **411**, 484-489 (2001).

Di Biase V., Obermair G.J., Szabo Z., Altier C., Sanguesa J., Bourinet E., Flucher B.E. Stable Membrane Expression of Postsynaptic $Ca_V1.2$ Calcium Channel Clusters Is Independent of Interactions with AKAP79/150 and PDZ Proteins. *J. Neurosci.*, **28**, 3845–13855 (2008).

Dolmetsch R.E., Pajvani U., Fife K., Spotts J.M., and Greenberg M.E. Signaling to the nucleus by an L-type calcium channel calmodulin complex through the MAP kinase pathway. *Science*, **294**, 333–339 (2001).

E

Eberhard M., Erne P. Calcium and magnesium binding to rat parvalbumin. *Eur J Biochem.*, **222**, 21–26 (1994).

Eckert R., Tillotson D.L. Calcium-mediated inactivation of the calcium conductance in caesium-loaded giant neurones of Aplysia californica. *J Physiol*, **314**, 265-280 (1981).

Erickson M.G., Liang H., Mori M.X., Yue D.T. FRET two hybrid mapping reveals function and location of L-type Ca^{2+} channel CaM preassociation. *Neuron*, **39**, 97–107 (2003).

F

Fabiato A. Calcium-induced release of calcium from the cardiac sarcoplasmic reticulum. *Am. J. Physiol.*, **245**, C1–C14 (1983).

Findlay I. Physiological modulation of inactivation in L-type Ca^{2+} channels: one switch. *J. Physiol.*, **554**, 275-83 (2003).

G

Galli A., DeFelicia L.J. Inactivation of L-type Ca channels in embryonic chick ventricle cells: dependence on the cytoskeletal agents colchicine and taxol. *Biophys J.*, **67**, 2296-304 (1994).

Gander J.C., Gotzos V., Fellay B., Schwaller B. Inhibition of the proliferative cycle and apoptotic events in WiDr cells after down-regulation of the calcium-binding protein calretinin using antisense oligodeoxynucleotides. *Exp Cell Res.*, **225**, 399–410 (1996).

Ganesan A.N., Maack C., Johns D.C., Sidor A., O'Rourke B. Beta-adrenergic stimulation of L-type Ca^{2+} channels in cardiac myocytes requires the distal carboxyl terminus of alpha1C but not serine 1928. *Circ Res.*, **98**, 11-8 (2006).

Gera S., Byerly L. Voltage- and calcium-dependent inactivation of calcium channels in Lymnaea neurons. *J. Gen. Physiol.*, **114**, 535-550 (1999).

Grantham C.J., Cannell M.B. Ca^{2+} influx during the cardiac action potential in guinea pig ventricular myocytes. *Circ Res*., **79**, 194-200 (1996).

Guerini D. Calcineurin: not just a simple protein phosphatase. *Biochem. Biophys. Res. Commun.*, **235**, 271-275 (1997).

H

Hadley R.W.,Hume J.R. An intrinsic potential-dependent inactivation mechanism associated with calcium channels in guinea-pig myocytes. *J Physiol.*, **389**, 205-222 (1987).

Haeseleer F., Sokal I., Verlinde C.L., Erdjument-Bromage H., Tempst P., Pronin A.N., Benovic J.L., Fariss R.N., Palczewski K. Five members of a novel $Ca(^{2+})$-binding protein (CABP) subfamily with similarity to calmodulin. *J. Biol. Chem.*, **275**, 1247–12460 (2000).

Haeseleer F., Imanishi Y., Sokal I., Filipek S., Palczewski K. Calcium-binding proteins: intracellular sensors from the calmodulin superfamily. *Biochem. Biophys. Res. Commun.*, **290**, 615–623 (2002).

Hall D.D., Feekes J.A., Arachchige Don A.S., Shi M., Hamid J., Chen L., Strack S., Zamponi G.W., Horne M.C., Hell J.W. Binding of protein phosphatase 2A to the L-type calcium channel $Ca_V1.2$ next to Ser1928, its main PKA site, is critical for Ser1928 dephosphorylation. *Biochemistry*, **45**, 3448-59 (2006).

Hall D.D., Davare M.A., Shi M., Allen M.L., Weisenhaus M., McKnight G.S., Hell J.W. Critical role of cAMP-dependent protein kinase anchoring to the L-type calcium channel $Ca_V1.2$ via A-kinase anchor protein 150 in neurons. *Biochemistry,* **46**,1635–1646 (2007).

Hell J.W., Yokoyama C.T., Wong S.T., Warner C., Snutch T.P., Catterall W.A. Differential phosphorylation of two size forms of the neuronal class C L-type calcium channel $\alpha 1$ subunit. *J. Biol. Chem.*, **268**, 19451–19457 (1993).

Hering S., Berjukow S., Sokolov S., Marksteiner R., Weiss R.G., Kraus R., Timin E.N. Molecular determinants of inactivation in voltage-gated Ca^{2+} channels. *J. Physiol. (Lond.)*., **528**, 237–249 (2000).

Herzig S., Neumann J. Effects of serine/threonine protein phosphatases on ion channels in excitable membranes. *Physiol. Rev.*, **80**, 173-210 (2000).

Hoeflich K.P., Ikura M. Calmodulin in action: diversity in target recognition and activation mechanisms. *Cell*, **108**, 739–742 (2002).

Huang L.J., Durick K., Weiner J.A., Chun J., Taylor S.S. Identification of a novel dual specificity protein kinase A anchoring protein, D-AKAP1. *J. Biol. Chem.*, **272**, 8057–8064 (1997).

Hubbard M.J., McHugh N.J. Calbindin28 kDa and calbindin30 kDa (calretinin) are substantially localised in the particulate fraction of rat brain. *FEBS Lett.*, **374**, 333–337 (1995).

Hulme J.T., Lin T.W., Westenbroek R.E., Scheuer T., Catterall W.A. β-adrenergic regulation requires direct anchoring of PKA to cardiac $Ca_V1.2$ channels via leucin zipper interaction with A kinase-anchoring protein 15. *Proc. Natl. Acad. Sci. USA.*, **100**, 13093-8 (2003).

Hulme J.T., Westenbroek R.E., Scheuer T., Catterall W.A. Phosphorylation of serine 1928 in the distal C-terminal domain of cardiac $Ca_V1.2$ channels during beta1-adrenergic regulation. *Proc. Natl. Acad. Sci. USA.*, **103**, 16574-9 (2006).

I

Iwasaki H., Mori Y., Hara Y., Uchida K., Zhou H., Mikoshiba K. 2-Aminoethoxydiphenyl borate (2-APB) inhibits capacitative calcium entry independently of the function of inositol 1,4,5-trisphosphate receptors. *Receptors Channels*, **7**, 429-39 (2001).

J

Janmey P.A. The cytoskeleton and cell signaling: component localization and mechanical coupling. *Physiol Rev*., **78**, 763–781 (1998).

Johnson B.D., Byerly L. A cytoskeletal mechanism for Ca^{2+} channel metabolic dependence and inactivation by intracellular Ca^{2+}. *Neuron*, **10**, 797-804 (1993).

Johnson B.D., Byerly L. Ca^{2+} channel Ca^{2+}-dependent inactivation in a mammalian central neuron involves the cytoskeleton. *Pflügers Arch.*, **429**, 14-21. 7-13 (1994).

Jones S.W. Calcium Channels: Unanswered Questions. *Journal of Bioenergetics and Biomembranes*, 35, 461-475 (2003).

Jurado L.A., Chockalingam P.S., Jarrett H.W. Apocalmodulin. *Physiol. Rev.*, **79**, 661–682 (1999).

K

Kalman D., O'Lague P.H., Erxleben C., Armstrong D.L. Calcium dependent inactivation of the dihydropyridine sensitive calcium channels in GH3 cells. *J. Gen. Physiol.*, **92**, 531-548 (1988).

Kawai M., Lane B.C., Hsieh G.C., Mollison K.W., Carter G.W., Luly J.R. Structure-activity profiles of macrolactam immunosuppressant FK-506 analogues. *FEBS Lett.*, **316**, 107-113 (1993).

L

Lader A.S., Kwiatkowski D.J., Cantiello H.F. Role of gelsolin in the actin filament regulation of cardiac L-type calcium channels. *Am. J. Physiol.*, **277**, C1277-C1283 (1999).

Laemmli U. Cleavage of structural proteins during the assembly of the head of bacteriophage T4. *Nature*, **227**, 680-685 (1970).

Landwehr M., Redecker P., Dieterich D.C., Richter K., Bockers T.M., Gundelfinger E.D., Kreutz M.R. Association of Caldendrin splice isoforms with secretory vesicles in neurohypophyseal axons and the pituitary. *FEBS Lett.*, 547, 189–192 (2003).

Laube G., Seidenbecher C.I., Richter K., Dieterich D.C., Hoffmann B., Landwehr M., Smalla K.H., Winter C., Bockers T.M., Wolf G., Gundelfinger E.D., Kreutz M.R. The neuron-specific Ca2+-binding protein caldendrin: gene structure, splice isoforms, and expression in the rat central nervous system. *Mol. Cell Neurosci.*, **19**, 459 475 (2002).

Lee A., Wong S.T., Gallagher D., Li B., Storm D.R., Scheuer T., Catterall W.A. Ca^{2+}/calmodulin binds to and modulates P/Q-type calcium channels. *Nature*, **399**, 155-159 (1999).

Lee A., Scheuer T., Catterall W.A. Ca2+/calmodulin-dependent facilitation and inactivation of P/Q-type Ca2+ channels. *J. Neurosci.*, **20**, 6830–6838 (2000).

Lee A., Westenbroek R.E., Haeseleer F., Palczewski K., Scheuer T., Catterall W.A. Differential modulation of $Ca_{(V)}2.1$ channels by calmodulin and Ca^{2+}-binding protein 1. *Nat. Neurosci.*, **5**, 210–217 (2002).

Lemke T., Welling A., Christel C.J., Blaich A., Bernhard D., Lenhardt P., Hofmann F., Moosmang S. Unchanged beta-adrenergic stimulation of cardiac L-type calcium channels in $Ca_V1.2$ phosphorylation site S1928A mutant mice. *J Biol Chem.*, **283**, 34738-44 (2008).

Levitan I.B. It is calmodulin after all! Mediator of the calcium modulation of multiple ion channels. *Neuron*, **22**, 645– 648 (1999).

Liang H., DeMaria C.D., Erickson M.G., Mori M.X., Alseikhan B.A., Yue D.T. Unified mechanisms of Ca^{2+} regulation across the Ca^{2+} channel family. *Neuron*, **39**, 951-60 (2003).

Lo F.S., Ziburkus J., Guido W. Synaptic mechanisms regulating the activation of a Ca^{2+}-mediated plateau potential in developing relay cells of the LGN. *J Neurophysiol.*, **87**, 1175-1185 (2002).

Lukyanetz E.A., Piper T.P., Sihra T.S. Calcineurin involvement in the regulation of high-threshold Ca^{2+} channels in NG108-15 (rodent neuroblastoma x glioma hybrid) cells. *J. Physiol. (Lond.)*, **510**, 371-385 (1998).

M

Magloczky Z., Freund T.F. Delayed cell death in the contralateral hippocampus following kainate injection into the CA3 subfield. *Neuroscience*, **66**, 847–860 (1995).

McCormick D.A. Neurotransmitter actions in the thalamus and cerebral cortex and their role in neuromodulation of thalamocortical activity. *Prog. Neurobiol.*, **39**, 337-388 (1992).

Meuth S.G., Budde T., Pape H.-C. Differential control of high-voltage acitivated Ca^{2+} current components by a Ca^{2+}-dependent inactivation mechanism in thalamic relay neurons. *Thalamus & Related Systems*, **1**, 31-38 (2001).

Meuth S., Pape H.-C., Budde T. Modulation of Ca^{2+} currents in rat thalamocortical relay neurons by activity and phosphorylation. *Europ. J. Neurosci.*, **15**, 1603-1614 (2002).

Meuth S.G., Kanyshkova T., Landgraf P., Pape H.-C., Budde T. Influence of Ca^{2+}-binding proteins and the cytoskeleton on Ca^{2+}-dependent inactivation of high-voltage activated Ca^{2+} currents in thalamocortical relay neurons. *Pflügers Arch.*, **450**, 111-22 (2005).

Meyers M.B., Puri T.S., Chien A.J., Gao T., Hsu P.H., Hosey M.M., Fishman G.I. Sorcin associates with the pore-forming subunit of voltage-dependent L-type Ca^{2+} channels. *J Biol Chem.*, **273**, 18930–18935 (1998).

Mori M.X., Erickson M.G., Yue D.T. Functional stoichiometry and local enrichment of calmodulin interacting with Ca^{2+} channels. *Science*, **304**, 432–435 (2004).

Munsch T., Budde T., Pape H.-C. Voltage-activated intracellular calcium transients in thalamic relay cells and interneurons. *Neuroreport*, **8**,2411-8. (1997).

N

Naraghi M., Neher E. Linearized buffered Ca^{2+} diffusion in microdomains and its implications for calculation of $[Ca^{2+}]$ at the mouth of a calcium channel. *J Neurosci*., **17**, 6961–6973 (1997).

Newlon M.G., Roy M., Morikis D., Carr D.W., Westphal R., Scott J.D., Jennings P.A. A novel mechanism of PKA anchoring revealed by solution structures of anchoring complexes. *EMBO J.*, **20**, 1651–1662 (2001).

O

Oliveria S.F., Dell'Acqua M.L., Sather W.A. AKAP79/150 anchoring of calcineurin controls neuronal L-type Ca^{2+} channel activity and nuclear signalling. *Neuron*, **55**, 261-75 (2007).

P

Pape H.-C., McCormick D.A. Noradrenaline and serotonin selectively modulate thalamic burst firing by enhancing a hyperpolarization-activated cation current. *Nature*, **340**, 715-8 (1989).

Pape H.-C., Budde T., Mager R., Kisvárday Z.F. Prevention of Ca(2+)-mediated action potentials in GABAergic local circuit neurones of rat thalamus by a transient K+ current. *J Physiol.*, **478**, **Pt 3**, 403-22 (1994).

Pape H.-C., Munsch T., Budde T. Novel vistas of calcium-mediated signalling in the thalamus. *Pflügers Arch.*, **448**, 131-38 (2004).

Pedroarena C., Llinas R. Dendritic calcium conductances generate high-frequency oscillation in thalamocortical neurons. *Proc. Natl. Acad. Sci. USA.*, **94**, 724-728 (1997).

Peterson B.Z., DeMaria C.D., Adelman J.P., Yue D.T. Calmodulin is the Ca^{2+} sensor for Ca^{2+} -dependent inactivation of L- type calcium channels. *Neuron*, **22**, 549-558 (1999).

Q

Qin N., Olcese R., Bransby M., Lin T., Birnbaumer L. Ca^{2+}- induced inhibition of the cardiac Ca^{2+} channel depends on calmodulin. *Proc. Natl Acad. Sci. USA.*, **96**, 2435-2438 (1999).

R

Rosenmund C., Clements J.D., Westbrook G.L. Nonuniform probability of glutamate release at a hippocampal synapse. *Science*, **262**, 754–757 (1993).

Rossie S. Regulation of voltage-sensitive sodium and calcium channels by phosphorylation. *Adv. Second Messenger Phosphoprotein Res.,* **33**, 23-48 (1999).

Rousset M., Cens T., Gavarini S., Jeromin A., Charnet P. Down-regulation of voltage-gated Ca2+ channels by neuronal calcium sensor-1 is beta subunit-specific. *J Biol Chem.*, **278**, 7019-26 (2003).

S

Sculptoreanu A., Rotman E., Takahashi M., Scheuer T., Catterall W.A. Voltage-dependent potentiation of the activity of cardiac L-type calcium channel alpha 1 subunits due to phosphorylation by cAMPdependent protein kinase. *Proc. Natl Acad. Sci. USA.*, **90**, 10135-10139 (1993).

Schuhmann K., Romanin C., Baumgartner W., Groschner K. Intracellular Ca^{2+} inhibits smooth muscle L-type Ca^{2+} channels by activation of protein phosphatase type 2B and by direct interaction with the channel. *J. Gen. Physiol.*, **110**, 503-513 (1997).

Schultz K., Janssen-Bienhold U., Gundelfinger E.D., Kreutz M.R., Weiler R. Calcium-binding protein Caldendrin and CaMKII are localized in spinules of the carp retina. *J. Comp. Neurol.*, **479**, 84–93 (2004)

Seidenbecher C.I., Langnaese K., Sanmarti-Vila L., Boeckers T.M., Smalla K.H., Sabel B.A., Garner C.C., Gundelfinger E.D., Kreutz M.R. Caldendrin, a novel neuronal calcium-binding protein confined to the somato-dendritic compartment. *J. Biol. Chem.*, **273**, 21324–21331 (1998).

Seidenbecher C.I., Landwehr M., Smalla K.H., Kreutz M., Dieterich D.C., Zuschratter W., Reissner C., Hammarback J.A., Böckers T.M., Gundelfinger E.D., Kreutz M.R. Caldendrin but not calmodulin binds to light chain 3 of MAP1A/B: an association with the microtubule cytoskeleton highlighting exclusive binding partners for neuronal Ca ($^{2+}$)-sensor proteins. *J Mol Biol.*, **336**, 957-70 (2004).

Sham J.S., Cleemann L., Morad M. Functional coupling of Ca^{2+} channels and ryanodine receptors in cardiac myocytes. *Proc. Natl Acad. Sci. USA.*, **92**, 121–125 (1995).

Smalla K.H., Seidenbecher C.I., Tischmeyer W., Schicknick H., Wyneken U., Bockers T.M., Gundelfinger E.D., Kreutz M.R. Kainate-induced epileptic seizures induce a recruitment of caldendrin to the postsynaptic density in rat brain. *Brain Res. Mol. Brain Res.,* **116**, 159–162 (2003).

Steriade M., Jones E.G., McCormick D.A. *Thalamus*. Elsevier, Amsterdam. (1997).

Stotz S.C., Zamponi G.W. Structural determinants of fast inactivation of high voltage-activated Ca^{2+} channels. *Trends Neurosci.,* **24**, 176-81 (2001).

Sun H., Leblanc N., Nattel S. Mechanisms of inactivation of L-type calcium channels in human atrial myocytes. *Am. J. Physiol.*, **272**, H1625–H1635 (1997).

T

Takamatsu H., Nagao T., Ichijo H., Adachi-Akahane S. L-type Ca^{2+} channels serve as a sensor of the SR Ca^{2+} for tuning the efficacy of Ca^{2+}-induced Ca^{2+} release in rat ventricular myocytes. *J. Physiol.*, **552**, 415-424 (2003).

Tasken K., Aandahl E.M. Localized effects of cAMP mediated by distinct routes of protein kinase A. *Physiol. Rev.*, **84**, 137–167 (2004).

Tillotson D. Inactivation of Ca conductance dependent on entry of Ca ions in molluscan neurons. *Proc. Natl. Acad. Sci. USA.*, **77**, 1497–1500 (1979).

Tippens A.L., Lee A. Caldendrin, a neuron-specific modulator of Ca_V/1.2 (L-type) Ca^{2+} channels. *J Biol Chem.*, **282**, 8464-73 (2007).

Trotter K.W., Fraser I.D., Scott G.K., Stutts M.J., Scott J.D., Milgram S.L. Alternative splicing regulates the subcellular localization of A-kinase anchoring protein 18 isoforms. *J. Cell Biol.*, **147**, 1481–1492 (1999).

V

Victor R.G., Rusnak F., Sikkink R., Marban E., O'Rourke, B. Mechanism of Ca^{2+}-dependent inactivation of L-type Ca^{2+} channels in GH3 cells: direct evidence against dephosphorylation by calcineurin. *J. Membr. Biol.*, **156**, 53-61 (1997).

X

Xiao R.P., Cheng H., Lederer W.J., Suzuki T., Lakatta E.G. Dual regulation of Ca^{2+}/calmodulin-dependent kinase II activity by membrane voltage and by calcium influx. *Proc. Natl Acad. Sci. USA.*, **91**, 9659-9663 (1994).

Y

You Y., Pelzer D.J., Pelzer S. Trypsin and forskolin decrease the sensitivity of L-type calcium current to inhibition by cytoplasmic free calcium in guinea pig heart muscle cells. *Biophys. J.*, **69**, 1838-1846 (1995).

Z

Zeilhofer H.U., Blank N.M., Neuhuber W.L., Swandulla D. Calcium-dependent inactivation of neuronal calcium channel currents is independent of calcineurin. *Neuroscience*, **95**, 235-241 (2000).

Zhou J., Olcese R., Qin N., Noceti F., Birnbaumer L., Stefani E. Feedback inhibition of Ca^{2+} channels by Ca^{2+} depends on a short sequence of the C terminus that does not include the Ca^{2+}-binding function of a motif with similarity to Ca^{2+}-binding domains. *Proc. Natl Acad. Sci. USA.*, **94**, 2301–2305 (1997).

Zhou H., Kim S.A., Kirk E.A., Tippens A.L., Sun H., Haeseleer F., Lee A. Ca^{2+}-binding protein-1 facilitates and forms a postsynaptic complex with $Ca_V1.2$ (L-type) Ca^{2+} channels. *J. Neurosci.*, **24**, 4698–4708 (2004).

Zhou H., Yu K., McCoy K.L., Lee A. Molecular mechanism for divergent regulation of $Ca_V1.2$ Ca^{2+} channels by calmodulin and Ca^{2+}-binding protein-1. *J. Biol. Chem.*, **280**, 29612–29619 (2005).

Zühlke R.D., Pitt G.S., Deisseroth K., Tsien R.W., Reuter H. Calmodulin supports both inactivation and facilitation of L-type calcium channels. *Nature*, **399**, 159-162 (1999).

W

Wang L., Sunahara R.K., Krumins A., Perkins G., Crochiere M.L., Mackey M., Bell S., Ellisman M.H., Taylor S.S. Cloning and mitochondrial localization of fulllength D-AKAP2, a protein kinase A anchoring protein. *Proc. Natl Acad. Sci. USA.*, **98**, 3220-3225 (2001).

Wong W., Scott J.D. AKAP signaling complexes: Focal points in space and time. *Nat. Rev. Mol. Cell Bio.*, **5**, 959-70 (2004).

7. Abbreviations

A

AC	Adenylate Cyclase
ACSF	Artificial Cerebro-Spinal Fluid
AKAP	A kinase anchoring protein
2-APB	2-aminoethoxydiphenyl borate
4 -AP	4-aminopyridine
AR	Adrenergic receptor

B

BAPTA	1,2-bis(o-aminophenoxy)ethane-N,N,N',N'-tetraacetic acid
BSA	Bovine serum albumin

C

cAMP	Cyclic adenosine monophosphate
CaBP1	Ca^{2+}-binding protein 1
CaM	Calmodulin
CaN	Calcineurin
cDNA	Complementary DNA
CDD	Caldendrin
CDI	Calcium dependent inactivation
CICR	Calcium induce calcium release
$[Ca^{2+}]_i$	Intercellular calcium concentration
COS-7	African green monkey cell line

D

dLGN	dorsal Lateral Geniculate Nucleus
DMEM	Dulbecco's Modified Eagle Medium
DMSO	Dimethylsulfoxid
DNA	Deoxyribonucleic acid
Dnase	Desoxyribonuclease

E

E.Coli	*Escherichia coli*
ER	Endoplasmic reticulum
EDTA	Ethylenediaminetetraacetic acid
EGTA	Ethylene Glycol Tetraacetic Acid

F

Fig.	Figure

FRET	Fluorescence Resonance Energy Transfer
G	
GABA	γ Amino butyric acid
GAPDH	Glyceraldehyde 3-phosphate dehydrogenase
GAD	Glutamate decarboxylase
GST	Glutathione S-transferase
GFP	Green Flourescent Protein
Gnas	Stimulatory subunit of G-proteins
GPCR	G-protein coupled receptors
H	
HBSS	Hank´s balanced salt solution
HEPES	4-(2-hydroxyethyl)-1-piperazineethanesulfonic acid
HVA	High voltage activated calcium channels
Hz	Hertz
I	
IF	Immunoflourescency
IgG	Immunoglobulin G
IN	Interneurons
InsP3	Inositol 1,4,5-trisphosphate
IP	Immunoprecipitation
IPTG	Isopropyl-f-D-l-thiogalactopyranoside
K	
kDa	kilo Dalton
L	
LVA	Low voltage activated calcium channels
M	
MAP2	Microtubule associated protein 2
MBP	Maltose binding protein
mRNA	Messenger RNA
N	
NA	Noradrenaline
NCS 1	Neuronal Ca^{2+} sensor protein 1
NIH	National Institute of Health
NRT	Nucleus Reticularis Thalami
P	
PAGE	Polyacrylamide Gel Electrophoresis

PIPES Piperazine-N,N'-bis(ethanesulfonic acid); 1,4-piperazinediethanesulfonic acid

PBS Phosphate Buffered Saline

PCR Polymerase Chain Reaction

PFA Parafolmaldehyde

PKA Protein kinase A

PKARIIβ Regulatory subunit β of protein kinase A

PKAcsβ Catalytic subunit β of protein kinase A

PKI Protein kinase A inhibitor

PP2A Protein phosphatase 2A

PP2B Protein phosphatase 2B

PP1 Protein phosphatase 1

Q

qRT-PCR Quantitative Real - Time Polymerase chain reaction

R

rpm Rotations per minute

RNA Ribonucleic acid

RT Room temperature

RT-PCR Reverse Transcriptase Polymerase Chain Reaction

RyR Ryanodine receptor

S

SDS Sodium Dodecyl Sulfate

SEM Standard Error Mean

SR Sarcoplasmic Reticulum

SSC Somato Sensory Cortex

T

TAE Tris-Acetat-EDTA

TBS Tris Buffered Saline

TC Thalamocortical relay neuron

TEMED Tetramethylethylenediamine

TRP Transient receptor potential

Tris Tris(hydorxymethyl)-aminomethane

V

VGCC Voltage gated calcium channel

VDI Voltage dependent inactivation

8. Curriculum Vitae

Name:	**Vladan**
Family name:	**Ranković**
Date of the birth:	**July 5th 1975**
Place of the birth:	**Smederevska Palanka, Serbia**
Nationality:	**Serbian**
Parents:	**Slobodan Ranković**
	Vojislavka Ranković
Education:	
1982-1990:	**Primary School "Milan Kršljanin" Krnjevo, Serbia.**
1990-1994:	**Medical high school "Dr Vojislav Dulić", Požarevac, Serbia.**
1994:	**University enrance examination.**
1995-2004:	**Faculty of Biology, University of Belgrade, Serbia.**
2002-2004:	**Diploma thesis, PCR Centre, Faculty of Biology, Belgrade, Serbia.**
2004:	**Diploma degree (Dipl.-Biol).**
June-Sept. 2005:	**Practical training at the Leibniz Institute for Neurobiology, Magdeburg, Germany.**
2005-2009:	**Doctoral thesis, Otto von Guericke University, Institute of Physiology, Magdeburg, Germany.**

June 22nd 2009, Magdeburg

9. Scientific publications:

Ivkovic M., **Rankovic V**., Tarasjev A., Orolicki S., Damjanovic A., Paunovic V.R., Romac S. Schizophrenia and polymorphic CAG repeats array of calcium-activated potassium channel (KCNN3) gene in Serbian population. *Int J Neurosci.*, **116**, 157-64 (2006).

Broicher T., Kanyshkova T., Landgraf P., **Rankovic V**., Meuth P., Meuth S.G., Pape H.-C., Budde T. Specific expression of low-voltage-activated calcium channel isoforms and splice variants in thalamic local circuit interneurons. *Mol Cell Neurosci.*, **36**, 132-45 (2007).

Rankovic V., Landgraf P., Ehling P., Kreutz M.R., Munsch T., Budde T. Intracellular Ca^{2+} release - dependent inactivation of Ca^{2+} currents in thalamocortical relay neurons. *Europ. J. Neurosci.*, (in revision) (2009).

Rankovic M., Jacob L., **Rankovic V**., Brandenburg L.O., Schroeder H., Höllt V., Koch T. ADP-ribosylation factor 6 regulates μ-opioid receptor trafficking and signalling via activation of phospholipase D2. *Cell Signal.*, (in revision) (2009).

Abstracts:

Rankovic V., Landgraf P., Kanyshkova T., Kreutz M.R., Budde T., Munsch T. β adrenergic signaling via PKA and AKAPs modulate CDI of L-type Ca^{2+} channels in thalamocortical relay neurons. *6th FENS (Forum of European Neuroscience) meeting, abstract*, Geneva, (2008).

Rankovic V., Landgraf P., Kanyshkova T., Budde T., Munsch T. Calcium dependent inactivation of L-type Ca^{2+} channels is modulated via β adrenergic signalling cascade in thalamocortical relay neurons. *38th annual meeting of Society for Neuroscience* (*SfN), abstract*, Washington DC, USA, (2008).

10. Erklärung

Ich erkläre, dass ich die der Naturwissenschaftlichen Fakultät der Otto-von-Guericke- Universität zur Promotion eingereichte Dissertation mit dem Titel

"Modulation of Ca^{2+} dependent inactivation of Ca^{2+} channels by intracellular signalling"

im Institut für Physiologie der Otto-von-Guericke-Universität Magdeburg mit Betreuung durch Prof. Dr. rer. nat. Oliver Stork ohne sonstige Hilfe durchgeführt und bei der Abfassung der Dissertation keine anderen als die dort aufgeführten Hilfsmittel benutzt habe. Bei der Abfassung der Dissertation sind Rechte Dritter nicht verletzt worden. Ich habe diese Dissertation bisher an keiner in- oder ausländischen Hochschule zur Promotion eingereicht. Ich übertrage der Naturwissenschaftlichen Fakultät das Recht, weitere Kopien meiner Dissertation herzustellen und zu vertreiben.

Magdeburg, Juni 2009

(Dipl.-Biol. Vladan Rankovic)